WATERBORNE PARASITIC PROTOZOA REMOVAL CAPACITIES OF WASTEWATER TREATMENT PLANTS WITH VARYING PROCESSES

A THESIS SUBMITTED TO
THE GRADUATE SCHOOL OF NATURAL AND APPLIED SCIENCES
OF
MIDDLE EAST TECHNICAL UNIVERSITY

BY

ASLI ONURSAL

IN PARTIAL FULFILLMENT OF THE REQUIREMENTS
FOR
THE DEGREE OF MASTER OF SCIENCE
IN
ENVIRONMENTAL ENGINEERING

AUGUST 2022

Approval of the thesis:

WATERBORNE PARASITIC PROTOZOA REMOVAL CAPACITIES OF WASTEWATER TREATMENT PLANTS WITH VARYING PROCESSES

submitted by **ASLI ONURSAL** in partial fulfillment of the requirements for the degree of **Master of Science** i**n Environmental Engineering, Middle East Technical University** by,

Prof. Dr. Halil Kalıpçılar
Dean, Graduate School of **Natural and Applied Sciences** _____

Prof. Dr. Bülent İçgen
Head of the Department, **Environmental Engineering** _____

Prof. Dr. Bülent İçgen
Supervisor, **Environmental Engineering, METU** _____

Examining Committee Members:

Prof. Dr. Filiz Bengü Dilek
Environmental Engineering, METU _____

Prof. Dr. Bülent İçgen
Environmental Engineering, METU _____

Prof. Dr. Gülay Aral Akarsu
Medical Parasitology, Ankara University _____

Assoc. Prof. Dr. Çağdaş Devrim Son
Biology, METU _____

Assist. Prof. Dr. Sema Sevinç Şengör
Environmental Engineering, METU _____

Date: 26.08.2022

I hereby declare that all information in this document has been obtained and presented in accordance with academic rules and ethical conduct. I also declare that, as required by these rules and conduct, I have fully cited and referenced all material and results that are not original to this work.

Name Last name : Aslı Onursal

Signature :

ABSTRACT

WATERBORNE PARASITIC PROTOZOA REMOVAL CAPACITIES OF WASTEWATER TREATMENT PLANTS WITH VARYING PROCESSES

Onursal, Aslı
Master of Science, Environmental Engineering
Supervisor: Prof. Dr. Bülent İçgen

August 2022, 148 pages

The parasitic protozoa *Giardia intestinalis, Entamoeba histolytica, Blastocystis hominis, and Cryptosporidium parvum* are causative agents for human giardiasis, amebiasis, blastocytosis (formerly known as hominis infection) and cryptosporidiosis, respectively. These infections are mostly associated with waterborne diseases. Due to the lack of regulations for monitoring these protozoa in the discharge point of wastewater treatment plants (WWTPs), the discharges that reach to surface waters lead to waterborne transmission. This highlights the importance of WWTPs' removal capacities for improving water safety sanitation and hygiene to minimize the spread of infectious parasitic agents. For this reason, in this study, five different types of WWTPs from Ankara-Turkey including conventional activated sludge (CAS), biological nutrient removal (BNR), sequencing batch reactor (SBR), membrane bioreactor (MBR), and WWTP with coagulation-flocculation and UV disinfection (CoFlUV) units were investigated over a year, seasonally in terms of their parasitic protozoa removal capacities. Seasonal abundances of these protozoa-specific genes in both influents and effluents of each WWTP were determined by quantitative polymerase chain reaction. The reduction

of protozoan rDNA copies in the effluent wastewater samples compared to the influent wastewater samples was assessed as removal capacity in $\log_{10}$ reduction values (LRVs). LRVs 1 and 2 were reachable for *G. intestinalis* in CAS, SBR, CoFlUV and MBR, for *B. hominis* in CAS, BNR and CoFlUV and for *C. parvum* and *E. histolytica* in all types of WWTPs tested. LRVs > 3 were reachable for *E. histolytica* in CoFlUV and MBR, for *B. hominis* in CAS, BNR, SBR and MBR and for *C. parvum* in all types of WWTPs tested. However, for *G. intestinalis* none of the WWTPs tested were able to reach LRV > 3. Significant seasonal variations were observed in SBR for *G. intestinalis*, in CAS, SBR, and CoFlUV for *E. histolytica*, in all types of WWTPs tested for *B. hominis,* and in CAS for *C. parvum* ($p<0.05$). The results elucidated that the removal of protozoa in WWTPs was highly affected by the process used and the discharges of these WWTPs could need further monitoring and surveillance to minimize the potential risk to public health.

Keywords: Gastrointestinal diseases, WWTP, protozoa removal, qPCR

ÖZ

FARKLI PROSESLERE SAHİP ATIK SU ARITMA TESİSLERİNDE SU KAYNAKLI PARAZİTİK PROTOZOALARIN GİDERİM KAPASİTESİNİN BELİRLENMESİ

Onursal, Aslı
Yüksek Lisans, Çevre Mühendisliği
Tez Yöneticisi: Prof. Dr. Bülent İçgen

Ağustos 2022, 148 sayfa

Giardia intestinalis, Entamoeba histolytica, Blastocystis hominis ve *Cryptosporidium parvum*, sırasıyla giardiasis, amebiasis, blastocytosis ve cryptosporidiosis'e sebep olan protozoon parazitlerdir. Bu enfeksiyonlar oldukça yaygındır ve çoğunlukla su kaynaklıdır. Bu protozoonların atıksu arıtma tesislerinin (AAT'ler) deşarj noktalarında izlenmesine yönelik düzenlemelerin olmaması nedeniyle, yüzey sularına ulaşan deşarjlar su yoluyla bulaşmalarına yol açmaktadır. Bu durum, su güvenliği sanitasyonu ve hijyeni açısından AAT'lerin parazitleri uzaklaştırma kapasitelerinin önemini ortaya çıkarmaktadır. Bu nedenle, bu çalışmada Ankara-Türkiye'de bulunan konvansiyonel aktif çamur (CAS), biyolojik besin giderimi (BNR), ardışık kesikli reaktör (SBR), membran biyoreaktör (MBR) ve koagülasyon-flokülasyon ve UV dezenfeksiyon ünitelerini içeren bir AAT (CoFlUV) olmak üzere beş farklı AAT türü, seçilen protozoonların giderim kapasiteleri açısından bir yıl süresince mevsimsel olarak incelenmiştir. Her bir AAT'nin hem giriş hem de çıkış suyunda bu protozoonlara özgü genler kantitatif polimeraz zincir reaksiyonu ile belirlenmiştir. Çıkış suyu numunelerindeki protozoan rDNA kopyalarının giriş suyu numunelerine kıyasla azalması, $\log_{10}$

giderim değeri (LRV) şeklinde belirlenmiştir. LRV 1 ve 2'ye *G. intestinalis* için CAS, SBR, CoFlUV ve MBR'de, *B. hominis* için CAS, BNR ve CoFlUV'de ve *C. parvum* ve *E. histolytica* için test edilen tüm AAT'lerde ulaşılmıştır. LRV > 3 değerlerine *E. histolytica* için CoFlUV ve MBR'de, *B. hominis* için CAS, BNR, SBR ve MBR'de ve *C. parvum* için test edilen tüm AAT'lerde ulaşılmıştır. Ancak, *G. intestinalis* için test edilen hiçbir AAT LRV 3'e ulaşamamıştır. Mevsimsel farklılıklar *G. intestinalis* için SBR'de, *E. histolytica* için CAS, SBR ve CoFlUV'de, *B. hominis* için test edilen tüm AAT'lerde ve *C. parvum* için CAS'ta gözlenmiştir ($p<0.05$). Sonuçlar, AAT'lerde protozoaların gideriminin kullanılan proseslerden büyük ölçüde etkilendiğini ve bu AAT'lerin deşarjlarının halk sağlığı açısından potansiyel riski en aza indirmek için daha fazla izleme ve gözetim gerektirebileceğini ortaya koymuştur.

Anahtar Kelimeler: Gastrointestinal hastalıklar, AAT, protozoa giderimi, qPCR

To all the books in the world

ACKNOWLEDGMENTS

First and foremost, I would like to express my deepest gratitude to my supervisor Prof. Dr. Bülent İçgen for his guidance, patience, encouragement, and most importantly for his continuous support throughout my research.

I wish to thank my examining committee members; Prof. Dr. Filiz Bengü Dilek, Prof. Dr. Gülay Aral Akarsu, Assoc. Prof. Dr. Çağdaş Devrim Son and Assist. Prof. Dr. Sema Sevinç Şengör for their comments and contributions.

I would like to thank both the old and the new members of ICGEN Team, Serkan Küçükünsal, Osman Kayalı, Merve Akçakaya, Sera Tuncay and Cansu Gülcan for their help and friendship.

I am grateful for my Z-30 friends Berivan Tunca and Ertan Hoşafcı, as they are the best office friends always helping me through every scientific or personal problem and supplying me with endless coffee.

I would like to thank my friends Mert "hocam " Erkanlı, Bahar Evren, Cansu Polat, Gülçin Balcı, and Sinan Özhan Kaya for their help, encouragement, moral support and being my family in METU.

I am deeply thankful to my big sister Burcu Yeni for being the best role model and helping me shape my life without realizing it. Thank you for guiding me to come to METU, for guiding me to be a tough girl, and for introducing me to Supernatural and some good music.

I would like to thank my dear friend Naz Zeynep Şimşek (my sister from another mother) for her unlimited support throughout my last four years at METU and her encouragement and moral support through all my problems. Thank you for always being there for me even when you do not agree with my actions. You are the best in always talking some sense into me, I am grateful.

I am thankful for my best friend Enes Körükoğlu, for never leaving my side since the day we met and facing the good and bad days together with me, for always guiding me through my problems, and for being my senpai, I love having you in my life.

I am thankful for my furry children Luna and Yon, for making my days brighter and filling them with joy. Adopting you was the best choice I made.

Last but not least, I am deeply thankful to my mother Nesrin and father Erdal for being the best parents a girl could ask for and my dear brother Deniz Ali for being an incredible little brother, I love you the most.

TABLE OF CONTENTS

ABSTRACT v

ÖZ vii

ACKNOWLEDGMENTS x

TABLE OF CONTENTS xii

LIST OF TABLES xv

LIST OF FIGURES xvii

LIST OF ABBREVIATIONS xxiii

CHAPTERS

1 INTRODUCTION 1

2 LITERATURE REVIEW 3

2.1 Importance of protozoa 3

2.1.1 *Giardia intestinalis* 5

2.1.2 *Entamoeba histolytica* 7

2.1.3 *Blastocystis hominis* 9

2.1.4 *Cryptosporidium parvum* 11

2.2 Dissemination routes of parasitic protozoa in the environment 13

2.3 Common types of WWTPs and their importance in the dissemination of protozoan parasites 15

2.3.1 Conventional Activated Sludge (CAS) 15

2.3.2 Biological Nutrient Removal (BNR) 17

2.3.3 Sequencing Batch Reactor (SBR) 18

2.3.4 WWTP with coagulation-flocculation and UV disinfection unit (CoFlUV) 19

2.3.5 Membrane bioreactor (MBR) 20

2.4 Methods for parasitic protozoan detection in the environmental samples 21

2.4.1 Polymerase chain reactions (PCR) 24

2.4.2 Quantitative polymerase chain reactions (qPCR) 25

3 MATERIALS AND METHODS 27
3.1 Types of WWTPs tested in the study 27
3.2 Collection of samples 29
3.2.1 Water samples 29
3.2.2 Sludge samples 29
3.3 Total DNA extractions 31
3.4 Qualitative analyses of protozoan DNA 34
3.5 Quantitative analyses of protozoan DNA 37
3.6 Data analyses and statistics 38
4 RESULTS AND DISCUSSION 41
4.1 Qualitative analyses of protozoan parasites 41
4.1.1 Optimization of the PCR conditions and construction of standard curves 41
4.2 Quantitative analyses and removal of protozoan parasites 45
4.2.1 Quantitative analyses for *G. intestinalis* 45
4.2.2 Quantitative analyses of *E. histolytica* 54
4.2.3 Quantitative analyses of *B. hominis* 63
4.2.4 Quantitative analyses of *C. parvum* 72
4.3 Parasitic protozoa removal capacities of WWTPs 81
4.3.1 in CAS 81
4.3.2 in BNR 88
4.3.3 in SBR 91
4.3.4 in CoFlUV 95
4.3.5 in MBR 98
4.4 Removal of protozoa in literature 102
5 CONCLUSION AND RECOMMENDATIONS 103
5.1 Conclusion 103
5.2 Future prospects and recommendations 105
REFERENCES 107

APPENDICES

A. Raw data obtained from the qPCR analyses of protozoan parasites 117

B. Statistical analyses of the qPCR results 125

LIST OF TABLES

TABLES

Table 2.1. The advantages and drawbacks of MBR systems 21
Table 2.2. Benefits and limitations of some molecular techniques used in protozoa detection 23
Table 3.1. Average influent and effluent water qualities of selected WWTPs 30
Table 3.2. Average operational parameters of selected WWTPs 30
Table 3.3. Chemicals used in the extraction process 31
Table 3.4. Primers used in the study 36
Table 4.1. Seasonal LRVs in CAS 84
Table 4.2. Seasonal LRVs in CAS sludge 85
Table 4.3. Seasonal LRVs in BNR 90
Table 4.4. Seasonal LRVs in SBR 94
Table 4.5. Seasonal LRVs in CoFlUV 98
Table 4.6. Seasonal LRVs in MBR 100
Table 4.7. Removal of studied protozoa in literature 102
Table 5.1. LRV for protozoan parasites 103
Table A.1. qPCR analyses of protozoan parasites of CAS 118
Table A.2. qPCR analyses of protozoan parasites of CAS Sludge 119
Table A.3. qPCR analyses of protozoan parasites of BNR 120
Table A.4. qPCR analyses of protozoan parasites of SBR 121
Table A.5. qPCR analyses of protozoan parasites of CoFlUV 122
Table A.6. qPCR analyses of protozoan parasites of MBR 123
Table B.1. Seasonal variations for the removal of *G. intestinalis* in CAS 125
Table B.2. Seasonal variations for the removal of *G. intestinalis* in CAS Sludge 126
Table B.3. Seasonal variations for the removal of *G. intestinalis* in BNR 127
Table B.4. Seasonal variations for the removal of *G. intestinalis* in SBR 128
Table B.5. Seasonal variations for the removal of *G. intestinalis* in CoFlUV 129
Table B.6. Seasonal variations for the removal of *G. intestinalis* in MBR 130
Table B.7. Seasonal variations for the removal of *E. histolytica* in CAS 131
Table B.8. Seasonal variations for the removal of *E. histolytica* in CAS Sludge 132
Table B.9. Seasonal variations for the removal of *E. histolytica* in BNR 133
Table B.10. Seasonal variations for the removal of *E. histolytica* in SBR 134
Table B.11. Seasonal variations for the removal of *E. histolytica* in CoFlUV 135

Table B.12. Seasonal variations for the removal of *E. histolytica* in MBR 136
Table B.13. Seasonal variations for the removal of *B. hominis* in CAS 137
Table B.14. Seasonal variations for the removal of *B. hominis* in CAS Sludge 138
Table B.15. Seasonal variations for the removal of *B. hominis* in BNR 139
Table B.16. Seasonal variations for the removal of *B. hominis* in SBR 140
Table B.17. Seasonal variations for the removal of *B. hominis* in CoFlUV 141
Table B.18. Seasonal variations for the removal of *B. hominis* in MBR 142
Table B.19. Seasonal variations for the removal of *C. parvum* in CAS 143
Table B.20. Seasonal variations for the removal of *C. parvum* in CAS Sludge 144
Table B.21. Seasonal variations for the removal of *C. parvum* in BNR 145
Table B.22. Seasonal variations for the removal of *C. parvum* in SBR 146
Table B.23. Seasonal variations for the removal of *C. parvum* in CoFlUV 147
Table B.24. Seasonal variations for the removal of *C. parvum* in MBR 148

LIST OF FIGURES

FIGURES

Figure 2.1. Main groups of protozoa 4
Figure 2.2. Image of *G. intestinalis* trophozoite and cyst stages and fecal-oral life cycle 5
Figure 2.3. Life cycle and transmission of *G. intestinalis* 6
Figure 2.4. Microscopies of *E. histolytica* A) typical cyst with four nuclei, B) trophozoite form, C) trophozoite showing phagocytic mouths (arrows) 8
Figure 2.5. Life cycle and transmission of *E. histolytica* 9
Figure 2.6. Morphological forms of *Blastocystis* sp. subtype 4 by phase-contrast microscopy. a) Vacuolar and fecal cyst forms displaying extensive size variation (arrowheads). Note the refractile appearance and loose outer coat of cyst (arrows). b) Granular form (arrowhead). c) Amoebid form (arrow) 10
Figure 2.7. Life cycle and transmission of *B. hominis* 11
Figure 2.8. SEM image of oocysts of *C. parvum* in the intestinal mucosa 12
Figure 2.9. Life cycle and transmission of *C. parvum* 13
Figure 2.10. Dissemination routes of protozoan parasites 15
Figure 2.11. Typical conventional WWTP diagram 16
Figure 2.12. Typical BNR system diagram (A^2O) 17
Figure 2.13. Typical SBR system diagram 18
Figure 2.14. Typical coagulation flocculation system diagram 19
Figure 2.15. Typical UV disinfection system diagram (a) and thymine dimer formation (b) 20
Figure 2.16. Typical MBR system diagram 21
Figure 2.17. Schematic diagram of PCR 24
Figure 2.18. SYBR Green detection and melting curve example of qPCR 26
Figure 3.1. Picture of CAS system sampled in this study. 27
Figure 3.2. Picture of BNR system sampled in this study. 27
Figure 3.3. Picture of SBR system sampled in this study. 28
Figure 3.4. Picture of CoFlUV system sampled in this study. 28
Figure 3.5. Picture of MBR system sampled in this study. 28
Figure 3.7. Experimental flow of protozoan DNA extraction 33
Figure 3.8. Experimental flow of PCR method used in the study 35
Figure 3.9. Experimental flow of qPCR method used in the study 38

Figure 4.1. PCR optimization of the primer for *G. intestinalis* with different annealing temperatures. M, 50 bp DNA ladder from top to bottom 500, 400, 250, 100, and 50 bp, respectively (a). Standard curve of agarose gel for molecular weight estimation (b)..... 42
Figure 4.2. PCR optimization of the primer for *E. histolytica* with different annealing temperatures. M, 50 bp DNA ladder from top to bottom 500, 400, 250, 100, and 50 bp, respectively (a). Standard curve of agarose gel for molecular weight estimation (b)..... 43
Figure 4.3. PCR optimization of the primer for *B. hominis* with different annealing temperatures. M, 50 bp DNA ladder from top to bottom 500, 400, 250, 100, and 50 bp, respectively (a). Standard curve of agarose gel for molecular weight estimation (b). 44
Figure 4.4. PCR optimization of the primer for *C. parvum* with different annealing temperatures. M, 50 bp DNA ladder from top to bottom 500, 400, 250, 100, and 50 bp, respectively (a). Standard curve of agarose gel for molecular weight estimation (b). 45
Figure 4.5. Amplification (top), standard (middle) and melting (bottom) curves of the qPCR analyses of *G. intestinalis* for summer influents in CAS (a), BNR (b), SBR (c), CoFlUV (d) and MBR (e). Ct, threshold cycle; RFU, reporter signal; Normalized d(Fluorescence)/dT, differential of fluorescence over temperature. 46
Figure 4.6. Amplification (top), standard (middle) and melting (bottom) curves of the qPCR analyses of *G. intestinalis* in autumn influents in CAS (a), BNR (b), SBR (c), CoFlUV (d) and MBR (e). Ct, threshold cycle; RFU, reporter signal; Normalized d(Fluorescence)/dT, differential of fluorescence over temperature. 47
Figure 4.7. Amplification (top), standard (middle) and melting (bottom) curves of the qPCR analyses of *G. intestinalis* in winter influents in CAS (a), BNR (b), SBR (c), CoFlUV (d) and MBR (e). Ct, threshold cycle; RFU, reporter signal; Normalized d(Fluorescence)/dT, differential of fluorescence over temperature. 48
Figure 4.8. Amplification (top), standard (middle) and melting (bottom) curves of qPCR analyses of *G. intestinalis* in spring influents in CAS (a), BNR (b), SBR (c), CoFlUV (d) and MBR (e). Ct, threshold cycle; RFU, reporter signal; Normalized d(Fluorescence)/dT, differential of fluorescence over temperature. 49
Figure 4.9. Amplification (top), standard (middle) and melting (bottom) curves of the qPCR analyses of *G. intestinalis* in summer effluents in CAS (a), BNR (b), SBR (c), CoFlUV (d), MBR (e) and CAS sludge (f). Ct, threshold cycle; RFU, reporter signal; Normalized d(Fluorescence)/dT, differential of fluorescence over temperature. 50
Figure 4.10. Amplification (top), standard (middle) and melting (bottom) curves of the qPCR analyses of *G. intestinalis* in autumn effluents in CAS (a), BNR (b), SBR (c), CoFlUV (d), MBR (e) and CAS sludge (f). Ct, threshold cycle; RFU, reporter signal; Normalized d(Fluorescence)/dT, differential of fluorescence over temperature. 51

Figure 4.11. Amplification (top), standard (middle) and melting (bottom) curves of the qPCR analyses of *G. intestinalis* in winter effluents in CAS (a), BNR (b), SBR (c), CoFlUV (d), MBR (e) and CAS sludge (f). Ct, threshold cycle; RFU, reporter signal; Normalized d(Fluorescence)/dT, differential of fluorescence over temperature. 52
Figure 4.12. Amplification (top), standard (middle) and melting (bottom) curves of the qPCR analyses of *G. intestinalis* in spring effluents in CAS (a), BNR (b), SBR (c), CoFlUV (d), MBR (e) and CAS sludge (f). Ct, threshold cycle; RFU, reporter signal; Normalized d(Fluorescence)/dT, differential of fluorescence over temperature. 53
Figure 4.13. Amplification (top), standard (middle) and melting (bottom) curves of the qPCR analyses of *E. histolytica* in summer influents in CAS (a), BNR (b), SBR (c), CoFlUV (d) and MBR (e). Ct, threshold cycle; RFU, reporter signal; Normalized d(Fluorescence)/dT, differential of fluorescence over temperature. 55
Figure 4.14. Amplification (top), standard (middle) and melting (bottom) curves of the qPCR analyses of *E. histolytica* in autumn influents in CAS (a), BNR (b), SBR (c), CoFlUV (d) and MBR (e). Ct, threshold cycle; RFU, reporter signal; Normalized d(Fluorescence)/dT, differential of fluorescence over temperature. 56
Figure 4.15. Amplification (top), standard (middle) and melting (bottom) curves of the qPCR analyses of *E. histolytica* in winter influents CAS (a), BNR (b), SBR (c), CoFlUV (d) and MBR (e). Ct, threshold cycle; RFU, reporter signal; Normalized d(Fluorescence)/dT, differential of fluorescence over temperature. 57
Figure 4.16. Amplification (top), standard (middle) and melting (bottom) curves of the qPCR analyses of *E. histolytica* in spring influents in CAS (a), BNR (b), SBR (c), CoFlUV (d) and MBR (e). Ct, threshold cycle; RFU, reporter signal; Normalized d(Fluorescence)/dT, differential of fluorescence over temperature. 58
Figure 4.17. Amplification (top), standard (middle) and melting (bottom) curves of the qPCR analyses of *E. histolytica* in summer effluents in CAS (a), BNR (b), SBR (c), CoFlUV (d), MBR (e) and CAS sludge (f). Ct, threshold cycle; RFU, reporter signal; Normalized d(Fluorescence)/dT, differential of fluorescence over temperature. 59
Figure 4.18. Amplification (top), standard (middle) and melting (bottom) curves of the qPCR analyses of *E. histolytica* in autumn effluents in CAS (a), BNR (b), SBR (c), CoFlUV (d), MBR (e) and CAS sludge (f). Ct, threshold cycle; RFU, reporter signal; Normalized d(Fluorescence)/dT, differential of fluorescence over temperature. 60
Figure 4.19. Amplification (top), standard (middle) and melting (bottom) curves of the qPCR analyses of *E. histolytica* in winter effluents in CAS (a), BNR (b), SBR (c), CoFlUV (d), MBR (e) and CAS sludge case (f). Ct, threshold cycle; RFU, reporter signal; Normalized d(Fluorescence)/dT, differential of fluorescence over temperature. 61

Figure 4.20. Amplification (top), standard (middle) and melting (bottom) curves of the qPCR analyses of *E. histolytica* in spring effluents in CAS (a), BNR (b), SBR (c), OSB (d), MBR (e) and CAS sludge (f). Ct, threshold cycle; RFU, reporter signal; Normalized d(Fluorescence)/dT, differential of fluorescence over temperature. 62
Figure 4.21. Amplification (top), standard (middle) and melting (bottom) curves of the qPCR analyses of *B. hominis* in summer influents in CAS (a), BNR (b), SBR (c), CoFlUV (d) and MBR (e). Ct, threshold cycle; RFU, reporter signal; Normalized d(Fluorescence)/dT, differential of fluorescence over temperature. 64
Figure 4.22. Amplification (top), standard (middle) and melting (bottom) curves of the qPCR analyses of *B. hominis* in autumn influents in CAS (a), BNR (b), SBR (c), CoFlUV (d) and MBR (e). Ct, threshold cycle; RFU, reporter signal; Normalized d(Fluorescence)/dT, differential of fluorescence over temperature. 65
Figure 4.23. Amplification (top), standard (middle) and melting (bottom) curves of the qPCR analyses of *B. hominis* in winter influents in CAS (a), BNR (b), SBR (c), CoFlUV (d) and MBR (e). Ct, threshold cycle; RFU, reporter signal; Normalized d(Fluorescence)/dT, differential of fluorescence over temperature. 66
Figure 4.24. Amplification (top), standard (middle) and melting (bottom) curves of the qPCR analyses of *B. hominis* in spring influents in CAS (a), BNR (b), SBR (c), CoFlUV (d) and MBR (e). Ct, threshold cycle; RFU, reporter signal; Normalized d(Fluorescence)/dT, differential of fluorescence over temperature. 67
Figure 4.25. Amplification (top), standard (middle) and melting (bottom) curves of the qPCR analyses of *B. hominis* in summer effluents in CAS (a), BNR (b), SBR (c), CoFlUV (d), MBR (e) and CAS sludge (f). Ct, threshold cycle; RFU, reporter signal; Normalized d(Fluorescence)/dT, differential of fluorescence over temperature. 68
Figure 4.26. Amplification (top), standard (middle) and melting (bottom) curves of the qPCR analyses of *B. hominis* in autumn effluents in CAS (a), BNR (b), SBR (c), CoFlUV (d), MBR (e) and CAS sludge (f). Ct, threshold cycle; RFU, reporter signal; Normalized d(Fluorescence)/dT, differential of fluorescence over temperature. 69
Figure 4.27. Amplification (top), standard (middle) and melting (bottom) curves of the qPCR analyses of *B. hominis* in winter effluents in CAS (a), BNR (b), SBR (c), CoFlUV (d), MBR (e) and CAS sludge (f). Ct, threshold cycle; RFU, reporter signal; Normalized d(Fluorescence)/dT, differential of fluorescence over temperature. 70
Figure 4.28. Amplification (top), standard (middle) and melting (bottom) curves of the qPCR analyses of *B. hominis* in spring effluents in CAS (a), BNR (b), SBR (c), CoFlUV (d), MBR (e) and CAS sludge (f). Ct, threshold cycle; RFU, reporter signal; Normalized d(Fluorescence)/dT, differential of fluorescence over temperature. 71

Figure 4.29. Amplification (top), standard (middle) and melting (bottom) curves of the qPCR analyses of C. parvum in summer influents in CAS (a), BNR (b), SBR (c), CoFlUV (d) and MBR (e). Ct, threshold cycle; RFU, reporter signal; Normalized d(Fluorescence)/dT, differential of fluorescence over temperature. 73
Figure 4.30. Amplification (top), standard (middle) and melting (bottom) curves of the qPCR analyses of *C. parvum* in autumn influents in CAS (a), BNR (b), SBR (c), CoFlUV (d) and MBR (e). Ct, threshold cycle; RFU, reporter signal; Normalized d(Fluorescence)/dT, differential of fluorescence over temperature. 74
Figure 4.31. Amplification (top), standard (middle) and melting (bottom) curves of the qPCR analyses of *C. parvum* in winter influents in CAS (a), BNR (b), SBR (c), CoFlUV (d) and MBR (e). Ct, threshold cycle; RFU, reporter signal; Normalized d(Fluorescence)/dT, differential of fluorescence over temperature 75
Figure 4.32. Amplification (top), standard (middle) and melting (bottom) curves of the qPCR analyses of *C. parvum* in spring influents in CAS (a), BNR (b), SBR (c), CoFlUV (d) and MBR (e). Ct, threshold cycle; RFU, reporter signal; Normalized d(Fluorescence)/dT, dif 76
Figure 4.33. Amplification (top), standard (middle) and melting (bottom) curves of the qPCR analyses of *C. parvum* in summer effluents in CAS (a), BNR (b), SBR (c), CoFlUV (d) and MBR (e). Ct, threshold cycle; RFU, reporter signal; Normalized d(Fluorescence)/dT, differential of fluorescence over temperature. 77
Figure 4.34. Amplification (top), standard (middle) and melting (bottom) curves of the qPCR analyses of *C. parvum* in autumn effluents in CAS (a), BNR (b), SBR (c), CoFlUV (d) and MBR (e). Ct, threshold cycle; RFU, reporter signal; Normalized d(Fluorescence)/dT, differential of fluorescence over temperature. 78
Figure 4.35. Amplification (top), standard (middle) and melting (bottom) curves of the qPCR analyses of *C. parvum* in winter effluents in CAS (a), BNR (b), SBR (c), CoFlUV (d) and MBR (e). Ct, threshold cycle; RFU, reporter signal; Normalized d(Fluorescence)/dT, differential of fluorescence over temperature 79
Figure 4.36. Amplification (top), standard (middle) and melting (bottom) curves of the qPCR analyses of C. parvum in winter effluents in CAS (a), BNR (b), SBR (c), CoFlUV (d) and MBR (e). Ct, threshold cycle; RFU, reporter signal; Normalized d(Fluorescence)/dT, differential of fluorescence over temperature 80
Figure 4.37. Schematic diagram of the CAS system tested in the study. 82
Figure 4.38. Seasonal LRVs for *G. intestinalis*, *E. histolytica*, *B. hominis* and *C. parvum* in CAS. Error bars correspond to the standard deviation of mean values of the three measurements for three replicates. 83

Figure 4.39. Seasonal LRVs for *G. intestinalis*, *E. histolytica, B. hominis* and *C. parvum* in CAS Sludge. Error bars correspond to the standard deviation of mean values of the three measurements for three replicates. 85
Figure 4.40. Food web of protozoa in CAS systems..... 86
Figure 4.41. Major pathogen removal and inactivation mechanisms in CAS (Naughton 2017)..... 87
Figure 4.42. Schematic diagram of the BNR system tested in the study. 89
Figure 4.43.Seasonal LRVs for *G. intestinalis*, *E. histolytica, B. hominis* and *C. parvum* in BNR. Error bars correspond to the standard deviation of mean values of the three measurements for three replicates. 90
Figure 4.44 Schematic diagram of the SBR system tested in the study. 92
Figure 4.45. Seasonal LRVs for *G. intestinalis*, *E. histolytica, B. hominis* and *C. parvum* in SBR. Error bars correspond to the standard deviation of mean values of the three measurements for three replicates. 94
Figure 4.46. Schematic diagram of the CoFlUV system tested in the study. 96
Figure 4.47. Seasonal LRVs for *G. intestinalis*, *E. histolytica, B. hominis* and *C. parvum* in CoFlUV. Error bars correspond to the standard deviation of mean values of the three measurements for three replicates. 97
Figure 4.48. Schematic diagram of the MBR system tested in the study. 99
Figure 4.49. Seasonal LRVs for *B. hominis, E. histolytica*, and *G. intestinalis* in MBR. Error bars correspond to the standard deviation of mean values of the three measurements for three replicates. 100
Figure 4.50. Major factors affecting pathogen removal in membrane bioreactors. 101

LIST OF ABBREVIATIONS

ABBREVIATIONS

A^2O: Anaerobic-Anoxic-Oxic

BNR: Biological Nutrient Removal

BOD: Biochemical Oxygen Demand

CAS: Conventional Activated Sludge

COD: Chemical Oxygen Demand

CoFlUV: Coagulation Flocculation unit with UV disinfection

DGGE: Denaturing Gradient Gel Electrophoresis

EDTA: Ehtylenediaminetetraacetic Acid

$FeCl_3$: Iron Chloride

FISH: Fluorescent *in situ* Hybridization

HRT: Hydraulic Retention Time

LOD: Limit of Detection

LOQ: Limit of Quantification

LRV: Log Removal Value

MBR: Membrane Bioreactor

MF: Microfiltration

MLSS: Mixed Liquor Suspended Solids

NF: Nanofiltration

PAO: Phosphate Accumulating Organisms

PCR: Polymerase Chain Reaction

qPCR: Quantitative Polymerase Chain Reaction

RAS: Return Activated Sludge

RLB: Reverse Line Blotting

RO: Reverse Osmosis

RT: Retention Time

SBR: Sequencing Batch Reactor

SRT: Solids Retention Time

TBE: Tris-Boric acid-EDTA

TE: Tris-EDTA

t-RFLP: Terminal Restriction Fragment Length Polymorphism

TSS: Total Suspended Solids

UF: Ultrafiltration

UV: Ultra-violet

WAS: Waste Activated Sludge

WW: Wastewater

WWTP: Wastewater Treatment Plant

CHAPTER 1

INTRODUCTION

Protozoa are unicellular eukaryotes found in most habitats worldwide. Most protozoan species are free-living, however, some species live as parasites after infecting animals. The parasitic stage of protozoan species that actively feeds and proliferates is called the trophozoite stage, while cyst is the stage with a protective membrane or thickened wall. Infections caused by these parasites range from asymptomatic to life-threatening, depending on type of parasite and resistance of the host (Tortora et al. 2016).

One of the easiest means of transmission of these parasites is the consumption of water contaminated with protozoan cysts. Such waterborne parasitic protozoans are increasingly causing serious diseases in the world with symptoms such as nausea, abdominal pain, vomiting, diarrhea, and fever (Gallas-Lindemann et al. 2016). Moreover, since these protozoa form cysts, they are resistant to harsher environmental conditions and to disinfection (Kitajima et al. 2014). Therefore, these cysts are also responsible for the survival and transmission of parasites (Sukprasert et al. 2008). Cysts are transmitted to humans via a fecal-oral route through water and food contaminated with animal or human feces (Dungeni et al. 2010). According to the record of the World Health Organization (WHO), only diarrheal diseases are responsible for 1.7 billion cases each year. They are mostly caused by poor water sanitation and kill 525000 children under the age of 5 mostly in low-income countries (WHO 2022).

Dissemination of these parasitic protozoa increases humans' hospitalization and mortality rates, therefore, they are considered as a serious environmental problem (CDC 2022). These parasitic protozoa can spread to the environment, especially to

water bodies such as rivers, lakes, and wastewater treatment plants (WWTPs) from the fecal matter of humans and animals. As they are especially resistant to disinfection because of cysts they can go past wastewater treatment procedures in WWTPs and spread right to the receiving bodies. Water from these receiving water bodies like rivers is then used in animal husbandry, agricultural irrigation during which humas are exposed to risk (Aghalari et al. 2020). Therefore, assessing the capacity of WWTPs with different processes regarding protozoan parasites is of great importantance. For this reason, in this study, five common types of WWTPs with varying processes consisting of conventional activated sludge (CAS), sequencing batch reactor (SBR), biological nutrient removal (BNR), a WWTP with coagulation-flocculation and UV disinfection unit (CoFlUV) and membrane bioreactor (MBR) were assessed for their seasonal removal capacities of four protozoan parasites commonly seen in Turkey namely *Giardia intestinalis* (causative agent of giardiasis), *Cryptosporidium parvum* (causative agent of cryptosporidiosis), *Entamoeba histolytica* (causative agent of amebiasis) and *Blastocystis hominis* (causative agent of blastocytosis).

In Chapters 2, 3, 4, and 5 a literaure review of this study, materials and methods of the experiments conducted, results and discussion of the experimental results and conclusion and recommendations are given, respectively.

CHAPTER 2

LITERATURE REVIEW

2.1 Importance of protozoa

Protozoa belong to unicellular eukaryotes (Protists) along with algae and lower fungi. Protists are subdivided into three groups namely plant-like algae, fungi-like slime molds, and animal-like protozoa. However, these groups often overlap (Tortora et al. 2016). Although the word "protozoa" refers to the "first animals," which describe animal like nutrition, protozoa are quite distinct from animals. Trophozoites, which are in the feeding and growth stages, consume bacteria and small nutrients. Although some protozoa are a part of the normal microbiota of animals, a few of them causes serious damage to health and economy (Tortora et al. 2016b). Protozoa are divided into taxonomic groups according to their motility; *Sarcodina* (amoeba), *Mastigophora* (flagellates), *Ciliophora* (ciliates) (Figure 2.1). A non-motile group also exists called *Apicomplexa* that are all parasitic for higher animals (Madigan et al. 2006).

Protozoa usually reproduce asexually via budding, schizogony, or fission. However sexual reproduction via conjugation has been observed in some protozoa and some protozoa produce gametes to form diploid zygote during reproduction (Tortora et al. 2016b). Under unfavorable conditions some protozoa especially parasitic ones produce protective capsules called cysts. The cysts formed by the members of the phylum *Apicomplexa* are called oocysts (Tortora et al. 2016).

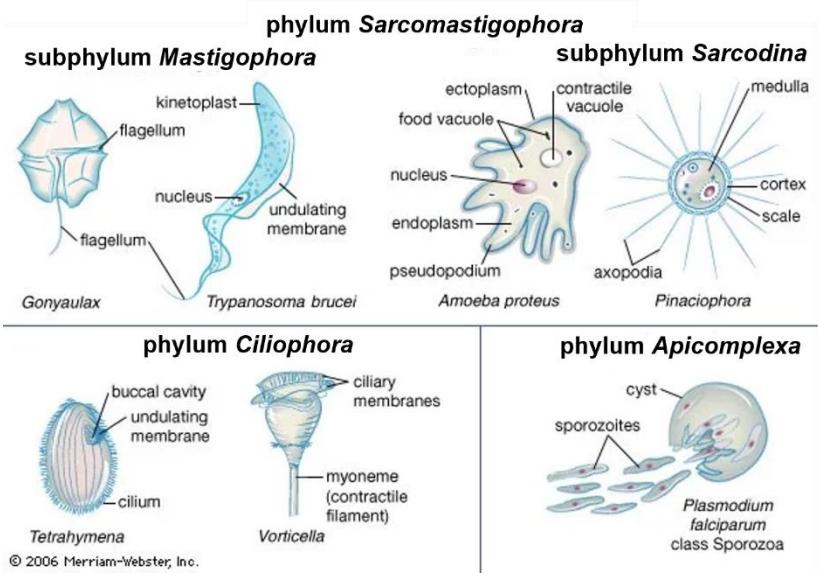

Figure 2.1. Main groups of protozoa(Pelczar 2020).

Enteric protozoa are common parasites that can be found in the intestines of humans and other mammals. They can be found in fecally contaminated water and transmitted to humans and other mammals (Guidelines for Canadian Drinking Water Quality Guideline Technical Document Enteric Protozoa: Giardia and Cryptosporidium 2019). Infections caused by such protozoa range from asymptomatic to life-threatening symptoms, depending on both the parasite and the host resistance. The common symptom of these parasitic protozoa infections is diarrhea. Diarrheal diseases seem to be one of the leading causes of death worldwide and, it was reported that, in 2017, 1.6 million people died due to diarrheal diseases. One-third of these deaths were children under the age of five and diarrheal diseases were the third leading cause of child mortality (Dadonaite et.al. 2019). The infections and outbreaks caused by these enteric protozoa are found to be underestimated and are increasingly causing serious diseases throughout the world (Gallas-Lindemann et al. 2016). Therefore, epidemics brought on by protozoan infections and diarrheal diseases pose a risk to the general public health and need to be addressed immediately.

In Turkey, commonly seen protozoan parasites causing gastrointestinal diseases are recorded as *Giardia intestinalis* (causative agents of giardiasis), *Cryptosporidium*

parvum (causative agents of cryptosporidiosis), *Entamoeba histolytica* (causative agents of amebiasis) and *Blastocystis hominis* (causative agents of blastocytosis) (Akpolat et al. 2022; Tanrıverdi Çaycı et al. 2017). Therefore, this study especially focused on the removal/reduction of these four parasites in WWTPs with varying processess.

2.1.1 Giardia intestinalis

Giardia intestinalis is a unicellular eukaryotic microorganism with eight flagella and two nuclei and is the causative agent of giardiasis, a common diarrheal disease (Nosala et al. 2015).

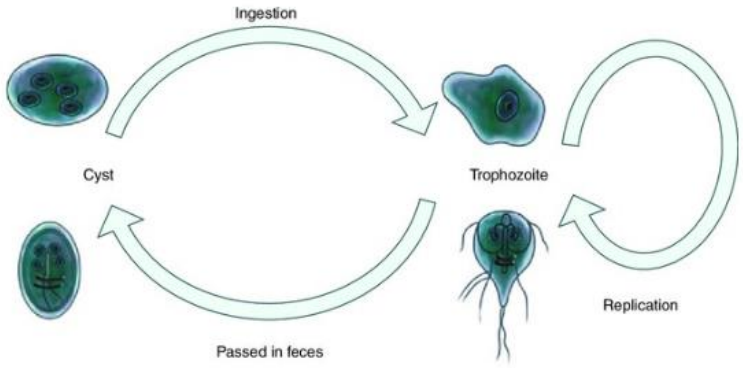

Figure 2.2. Image of *G. intestinalis* trophozoite and cyst stages and fecal-oral life cycle(Wiser 2021)

The life cycle of this parasite is very simple and consists of following stages; trophozoite as vegetative state and cyst as transmittable state (Figure 2.2). Transmission occurs either directly by contacting host or indirectly by consumption of contaminated food or water (CDC 2021). The life cycle and transmission are depicted in Figure 2.3. The cyst form is resistant to chlorination and UV disinfection and often received from contaminated water sources. While passing through the gastrointestinal tract, cysts can survive when they are exposed to pH changes and bile. After that, they reach the small intestine and excyst to become trophozoites which are motile and start cell divisions. These trophozoites can move through the

lumen of the small intestine with their flagella until they come across a suitable place for attachment to colonize. Finally, the trophozoites encyst and mature cysts are discarded into environment with feces (Nosala et al. 2015). The number of cysts excreted with feces can reach up to millions per day, therefore giardiasis poses a major public health concern in especially developing and even developed countries (Nikaeen et al. 2003).

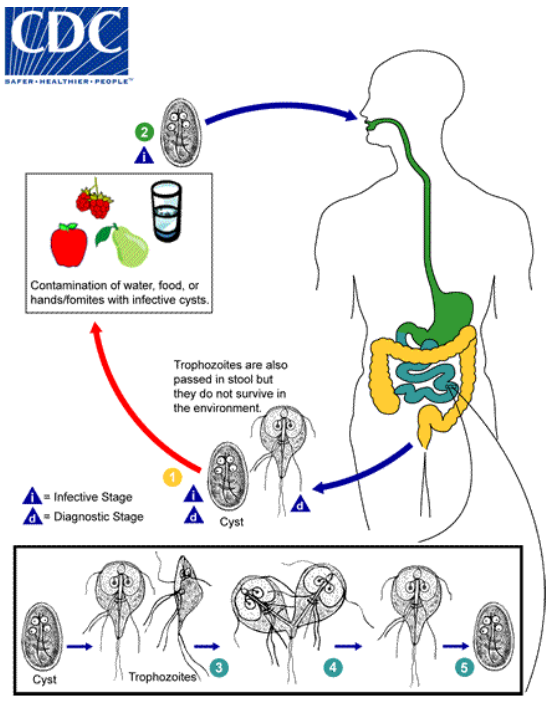

Figure 2.3. Life cycle and transmission of *G. intestinalis*(CDC 2017)

Symptoms of infections range from asymptomatic to acute watery diarrhea, nausea, epigastric symptoms, and weight loss. Worldwide, an average of 200 million cases of giardiasis are diagnosed annually (Hooshyar et al. 2019). *G. intestinalis* is one of the commonly seen parasitic protozoan species in Turkey. In the last ten years, this parasite was found to be the second commonly seen parasite being found in almost 32 % of 6% of diarrhea patients (Akpolat et al. 2022). In another study this parasite was found in 4.7% of 7.5% of diarrhea patients (Gülmez et al. 2013). Giardiasis epidemiology is impacted by a variety of factors, including the large number of cysts that are released into the environment through the feces of infected hosts, the low

infectious dose that allows even a single cyst to spread infection, and the cysts' high resistance to environmental stress, which allows them to survive in the environment for months while maintaining infectiousness (CDC 2021). Because of the large number of giardiasis cases around the world and the lack of research on the prevention of infection, *Giardia* was placed on the World Health Organization's (WHO) Neglected Tropical Diseases Initiative in 2004 (Nosala et al. 2015). Most of the treatment processes showed removals lower than 3 logarithmic reduction values (LRV). While chlorine disinfection is not effective for *Giardia,* with appropriate dosage UV disinfection exhibits promising removal values (CDC 2021).

2.1.2 Entamoeba histolytica

Entamoeba histolytica is a pseudopod-forming non-flagellate ameba that causes amebic dysentery and liver abscess. *E. dispar* is a non-pathogenic parasite morphologically identical to pathogenic *E. histolytica,* therefore, causing diagnostic confusion. Although there are at least eight different amebae that live in the human intestinal tract, these amebae are usually accepted as commensals except *E. histolytica* (Plutzer et al. 2016). The cysts of this parasite are typically 12-15 µm and have four nuclei and the dimensions of the trophozoite form range between 10-60 µm having a single nucleus (Figure 2.4) (CDC 2019).

The life cycle of *E. histolytica* consists of cyst which is the infective form and trophozoite which is the invasive form (Figure 2.5). (Peterson et al. 2011). Amebic dysentery is spread mostly through contaminated water or food. Although the stomach acid can kill trophozoites it is not effective on cysts. Therefore, cysts ingested with the contaminated food or water can reach the intestinal tract. Excystation occurs in the bowel lumen and the trophozoite form is released. Then the trophozoite form starts to multiply in the epithelial cells of large intestine resulting in severe dysentery (Tortora et al. 2016).

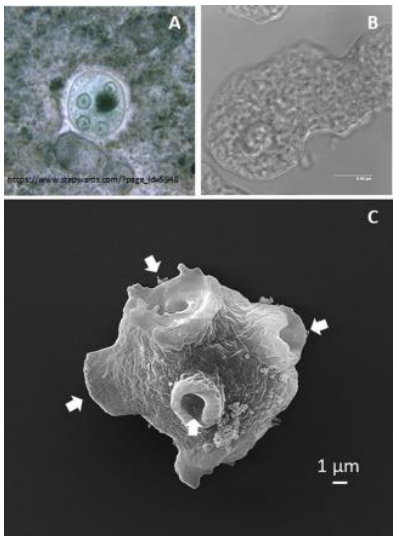

Figure 2.4. Microscopies of *E. histolytica* A) typical cyst with four nuclei, B) trophozoite form, C) trophozoite showing phagocytic mouths (arrows)(Carrero et al. 2020).

Worldwide, *E. histolytica* causes 50 million infections and over 100000 deaths annually (Hemmati et al. 2015). In Turkey, this parasite was the third most prevalent parasite in the last ten years being seen in 3.75% of the 6% of diarrhea patients (Akpolat et al. 2022). With the conventional wastewater treatment processes and secondary sedimentation, only 0.3 LRV of *E. histolytica* was observed. While chemical disinfectants such as chlorine showed 2 LRV reduction, UV disinfection showed more promising results (Ben Ayed et al. 2017).

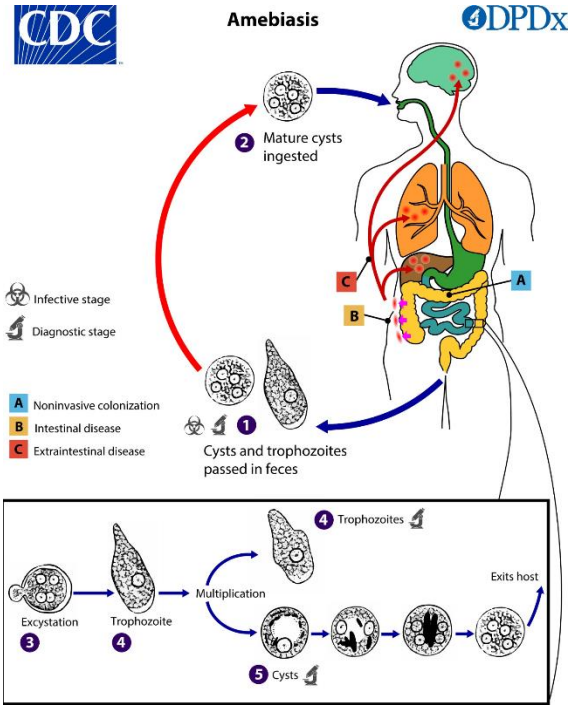

Figure 2.5. Life cycle and transmission of *E. histolytica*(CDC 2019)

2.1.3 Blastocystis hominis

Blastocystis hominis is an intestinal parasite in humans and a wide range of animals. This parasite belongs to the *Stramenopiles* (heterotrophic and photosynthetic protozoa) and it is the only known *Stramenopile* that causes infection in humans (Wawrzyniak et al. 2013). Other than the cyst form there are three major forms of these parasites namely, vacuolar, granular, and ameboid (Figure 2.6) (Stenzel et al. 1996).

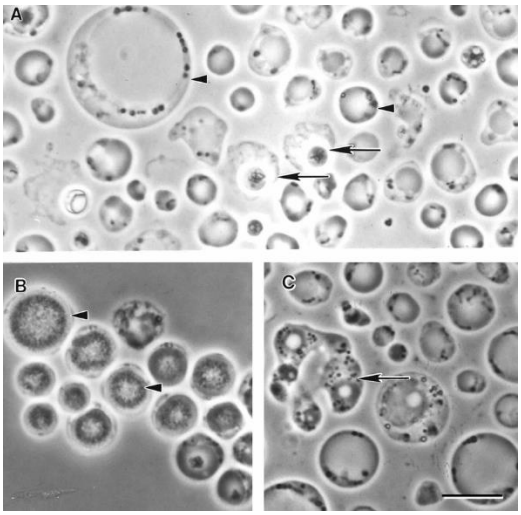

Figure 2.6. Morphological forms of *Blastocystis* sp. subtype 4 by phase-contrast microscopy. a) Vacuolar and fecal cyst forms displaying extensive size variation (arrowheads). Note the refractile appearance and loose outer coat of cyst (arrows). b) Granular form (arrowhead). c) Amoebid form (arrow)(Tan 2008)

In humans, transmission occurs with the ingestion of contaminated water or food. The transmissible stage is the cyst form and upon ingestion, the parasite excyst in the large intestine turns into the vacuolar form. This vacuolar form divides via binary fission and develops into either amoebid or granular form. Then, encystation occurs in the colon, and the formed cysts are discarded with the feces (Figure 2.7) (de la Cruz et al. 2017).

Symptoms caused by *Blastocystis* are often non-specific and can be confused with infections caused by viruses or bacteria (de la Cruz et al. 2017). *B. hominis* is found to be more prevalent in developing countries 50-60% than it is in developed countries 10% (Koloren et al. 2018). In Turkey, this species was the most frequently detected parasite causing diarrhea in the last ten years, being seen with 57.61% of 6% of diarrhea patients (Akpolat et al. 2022). In another study this parasite was found in 71.6% of 7.5% of diarrhea patients (Gülmez et al. 2013). *Blastocystis* is confirmed to be robust toward wastewater treatment techniques and should be included as a parameter when investigating parasites in wastewater (Suresh et al. 2005).

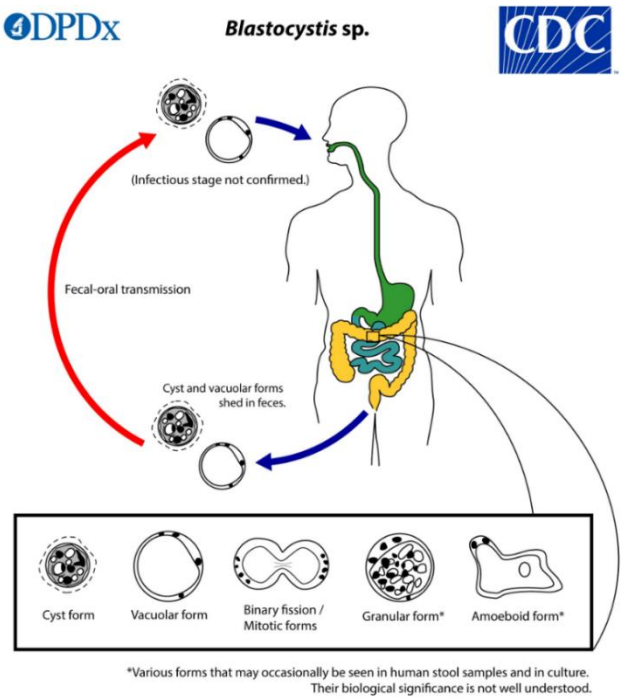

Figure 2.7. Life cycle and transmission of *B. hominis*(CDC 2019)

2.1.4 Cryptosporidium parvum

Cryptosporidium parvum is an animal-like protist perceived as one of the major causes of diarrheal diseases, contributing significantly to the global burden of gastroenteritis (Figure 2.8). This parasite is the causative agent of cryptosporidiosis (CDC 2019).

The life cycle of *C. parvum* begins with the ingestion of oocysts through contaminated water or food (Figure 2.9). After the excystation in the upper small intestine, the sporozoites are released to the mucus layer and turn into a trophozoite there. At this point, the parasite divides mitotically resulting in type I meront,(Leitch et al. 2011) and production of 6 to 8 merozoites occur. Merozoites are similar to the sporozoites. Then these merozoites attach to enterocytes and start an asexual infectious cycle or the merozoites can result in type II meront which produces 4

merozoites. Similarly to type I, type II merozoites attach to enterocytes and produce either a macrogamont (female) or a microgamont (male). These male cells then produce a diploid zygote which differentiates into oocysts. After the sexual cycle, 20% of the oocysts are formed with thin walls that are excyst within the host to cause autoinfection, and 80% of them are thick-walled that are released into the environment with the feces (Leitch et al. 2011).

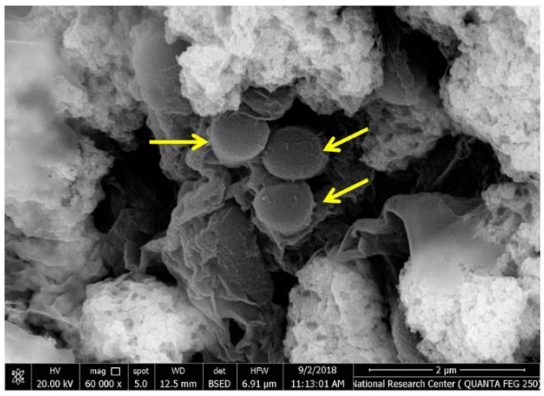

Figure 2.8. SEM image of oocysts of *C. parvum* in the intestinal mucosa(Aboelsoued et al. 2019)

Cryptosporidiosis is cholera-like diarrhea that can last up to 10-14 days and can become life-threatening in immunocompromised individuals including AIDS patients (Tortora et al. 2016). *C. parvum* was found to be one of the leading causes of moderate to severe diarrhea in toddlers ranking third after rotavirus and *Shigella* (Sow et al. 2016). In Turkey, this parasite was one of the most seen diarrhea-causing parasites with 0.52% of the 6% of diarrhea cases in the last ten years (Akpolat et al. 2022). Acknowledging the transmission links to poverty, and the effect of these diseases on children, malnourished and immunocompromised people, this parasite was added to WHO's Neglected Diseases Initiative in 2004 (CDC 2019). Oocysts of this parasite are resistant to chlorine and filtration must be used to remove them from water (Tortora et al. 2016).

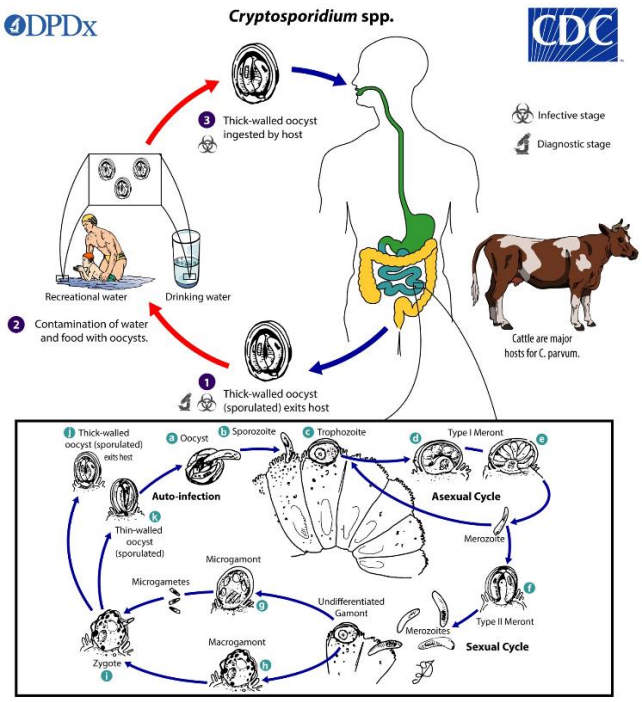

Figure 2.9. Life cycle and transmission of *C. parvum*(CDC 2019)

2.2 Dissemination routes of parasitic protozoa in the environment

The transmissible stage of parasitic protozoa, cysts, are excreted with feces therefore their presence in wastewater is expected however there are no regulations or guidelines concerning the occurrence of protozoa in treated wastewater that will be discharged to water bodies or used during the agricultural processes (ben Ayed et al. 2017). The cysts of these parasites are insensitive to the common disinfection processes employed in the WWTPs which makes it difficult to control the risk they pose to humans. They can survive in wastewater for up to 1 year in cold weather (Cacciò et al. 2003). Since they are highly resistant to disinfectants and environmental stress, and the conventional WWTPs are not designed to remove them, parasitic protozoa may be present in the effluent of the plant and therefore can be discharged into the receiving water bodies. Activated sludge systems showed average removal rate of 1.75 LRV for protozoan cysts which indicates the possibility of survival of protozoan cysts in the environment (Sroka et al. 2013). After the

dissemination, they can easily spread through the environment remaining viable for long periods of time and posing a potential health risk (Benito et al. 2020). Moreover, some of these pathogenic parasites require a low infective dose meaning humans can be infected with a dose as low as 10 cysts (Zacharia et al. 2018).

Cysts of protozoan parasites are removed from the wastewater by adsorbing onto the sludge particles and settling with the sludge. Because sludge, a byproduct of wastewater treatment, can be utilized as fertilizer or a soil conditioner, the techniques for treating wastewater should assure that these cysts are eliminated or rendered inactive (Benito et al. 2020).

The treatment procedures used determine the plant's efficiency and the quality of the final effluent. Therefore, despite the treatment the effluent wastewater can still contain parasitic protozoa (Domenech et al. 2018a). As mentioned before, protozoa cysts have been detected in the effluent wastewater and sludge of WWTPs, however only a little is known about wastewater treatment and how it may affect their removal (Sroka et al. 2013). The literature results show that testing different treatment processes to compare their capacities regarding the removal/reduction of parasitic protozoa would be informative towards, (1) achieving a better understanding on the survival capacity of protozoa, (2) enhancing parasitic infection risk studies, and (3) making necessary adaptions to WWTPs according to the need of the population (Benito et al. 2020). Figure 2.10 depicts a schematic illustration of the dissemination pathways for protozoan parasites.

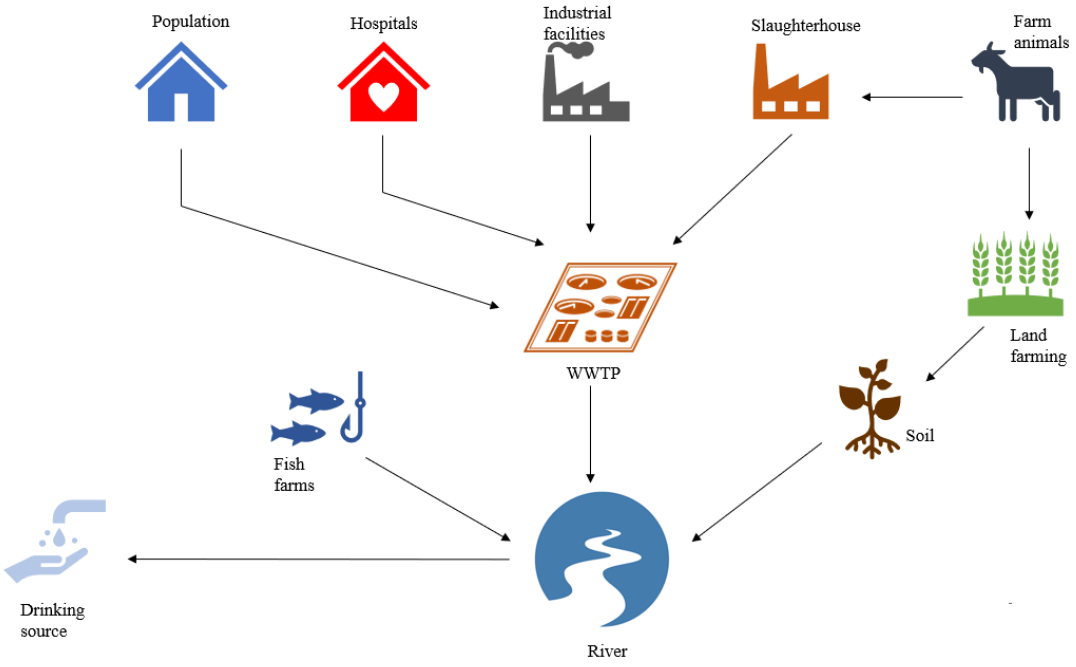

Figure 2.10. Dissemination routes of protozoan parasites(Stalder et al. 2012)

2.3 Common types of WWTPs and their importance in the dissemination of protozoan parasites

Common types of WWTPs include CAS, BNR, SBR, extended aeration unit with UV disinfection (also called WWTP with the coagulation-flocculation unit and UV disinfection throughout this study (CoFlUV)), and MBR. The processes that occur in these WWTPs and research on how it affects the spread of protozoan parasites is discussed in the sections below:

2.3.1 Conventional Activated Sludge (CAS)

The CAS process uses a large mass of aerobic microorganisms kept in suspension by mixing and aeration to convert organic waste and other ingredients to gases and cell tissue. This process often involves physical and chemical processes as well as biological processes. Conventional treatment systems generally consist of preliminary, primary, and secondary treatment processes. In some cases, however,

they can also include tertiary or even advanced treatment processes (Metcalf & Eddy 2014).

The preliminary treatment removes coarse solids from the wastewater and prepares the wastewater for further treatment. Primary treatment removes readily settleable solids and floating material from wastewater reducing the suspended solids content. Biodegradable organic materials and residual suspended particles are eliminated during secondary treatment. In this process, the removal of biodegradable organic matter occurs via aerobic microorganisms in aerated tanks. These microorganisms utilize biodegradable organics and produce inorganic end-product and new biomass. Secondary sedimentation tanks are used to eliminate microorganisms from the treated wastewater after this procedure. For sludge processing, the extracted biological solids are referred to as biological (activated) sludge and are frequently mixed with the primary sludge. Although they are not common, when the removal of secondary treatment is not enough tertiary and/or advanced treatment is used to further treat the wastewater (Metcalf & Eddy 2014). In Figure 2.11 a typical CAS process diagram is depicted.

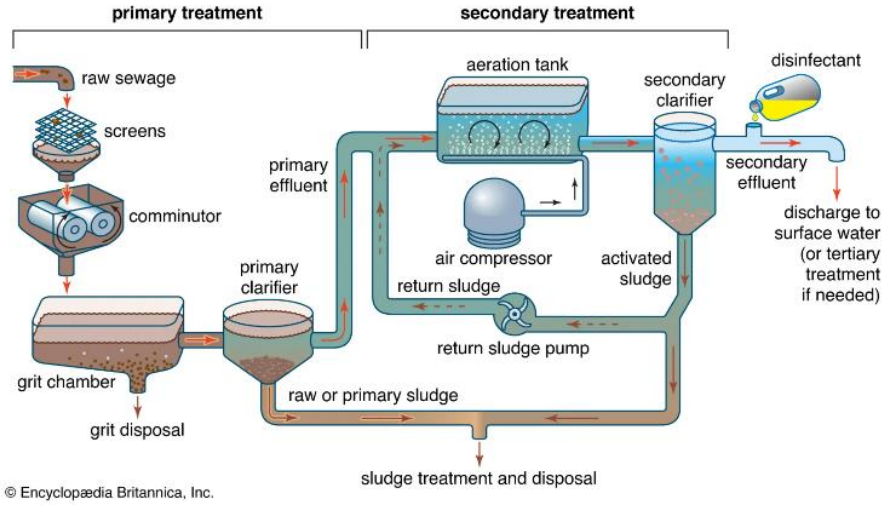

Figure 2.11. Typical conventional WWTP diagram(Nathanson 2022)

2.3.2 Biological Nutrient Removal (BNR)

Nutrients such as nitrogen and phosphorus are the primary causes of eutrophication in surface waters. Enrichment of nitrogen and phosphorus results in algal blooms, low dissolved oxygen, fish deaths, and depletion of desirable flora and fauna (EPA 2007). BNR systems were developed for the removal of nitrogen and phosphorus from the wastewater to prevent eutrophication in surface waters (Metcalf & Eddy 2014). BNR systems mainly include nitrification, denitrification, and phosphorus removal steps (Water Environment Federation 2007). In Figure 2.12, a BNR process diagram is depicted. The nitrification process is the biological oxidation of ammonium ions to produce nitrate and is done by nitrifying bacteria such as *Nitrosomonas* and *Nitrobacter*. Nitrification consists of two stages, the first is the stage where *Nitrosomonas* oxidizes ammonium to nitrite and the second is where *Nitrobacter* oxidizes nitrite to nitrate (Tortora et al. 2016). The denitrification process on the other hand is the process in which nitrate ions are converted to nitrogen gas via denitrifying bacteria such as *Pseudomonas* (Tortora et al. 2016). BNR processes also include enhanced biological phosphorus removal by using organisms called phosphorus accumulating organisms (PAOs). These organisms accumulate phosphorus and have been used to provide over 80% biological phosphorus removal under anaerobic conditions (Metcalf & Eddy 2014).

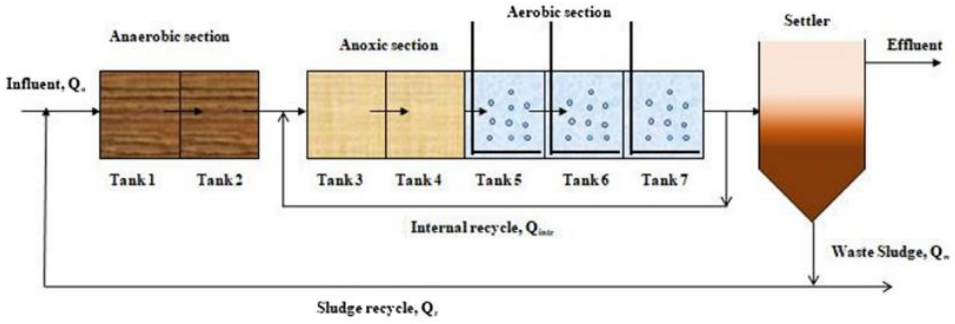

Figure 2.12. Typical BNR system diagram (A^2O)(Shiek et al. 2021).

2.3.3 Sequencing Batch Reactor (SBR)

SBR systems are used generally in small package plants since this system consists only of one reactor (Ghangrekar and Bengal 2014). Five different stages occur in the same tank and these stages are called fill, react, settle, decant, and idle (Metcalf & Eddy 2014). The reactor is filled, then aerated for a predetermined period of time. The wastewater in the reactor is allowed to settle after the aeration cycle is finished, and then the effluent is decanted (Ghangrekar and Bengal 2014). The idle stage is used only in a multi-task system (Metcalf & Eddy 2014). Using a single reactor for the processes gives an advantage to SBR process as there is no need for a return activated sludge (RAS) (Metcalf & Eddy 2014). These systems have a relatively small footprint and are often used when available land for a WWTP is limited (EPA 1999). An SBR process diagram is depicted in Figure 2.13.

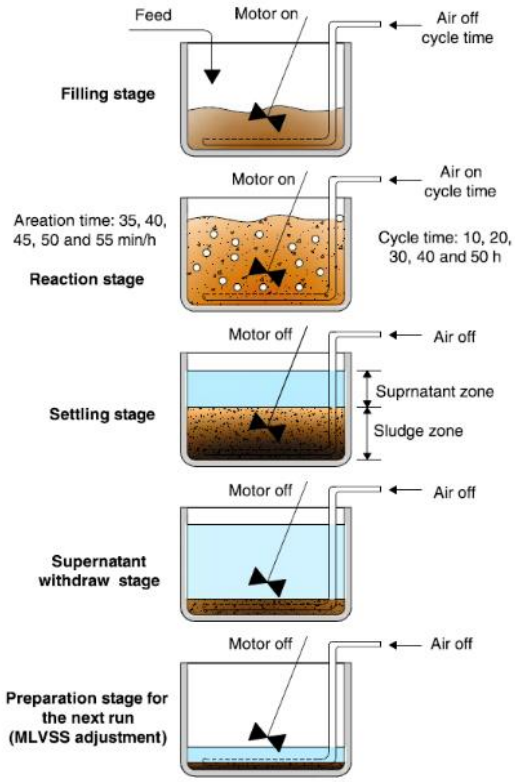

Figure 2.13. Typical SBR system diagram(Amini et al. 2016)

2.3.4 WWTP with coagulation-flocculation and UV disinfection unit (CoFlUV)

2.3.4.1 Coagulation-flocculation

Colloidal particles, typically having a net negative charge, are commonly found in wastewater. The size of these particles generally ranges from 0.001 to 1 μm which does not allow them to settle, and these particles follow the Brownian motion which keeps them in suspension. This process aims to make these small colloidal particles show particle growth via collision with the chemical coagulants (Metcalf & Eddy 2014). By using this process many contaminants that can be absorbed by the colloids such as metals, toxic organic matter, and even pathogens can be removed from wastewater (Shammas 2005). In the coagulation-flocculation process, generally, a chemical coagulant is added to first destabilize these negatively charged colloids. Then a flocculant is added so that the larger flocs can be formed, and these smaller colloids can be removed from wastewater by sedimentation (Metcalf & Eddy 2014). The typical diagram of a coagulation-flocculation unit is depicted in Figure 2.14.

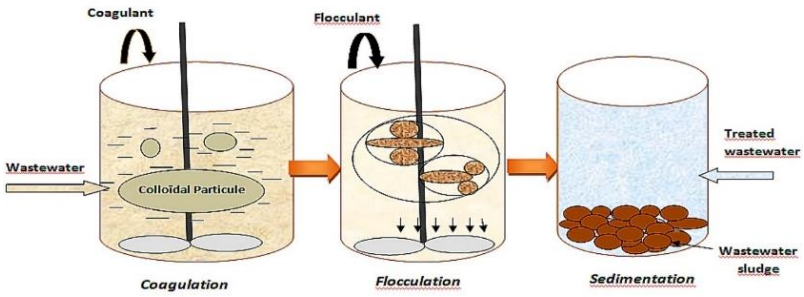

Figure 2.14. Typical coagulation flocculation system diagram(Ibrahim at.al. 2020).

2.3.4.2 UV disinfection

Ultra-violet light disinfection with the light being in photon form can inactivate microorganisms either by causing damage to the proteins or causing damage to the

nucleic acids (thymine dimerization) (Linden and Murphy 2017). UV light is considered non-ionizing radiation as it has a longer wavelength and lower energy. Therefore, the radiation is not very penetrating and UV light is considered a disinfectant but not a sterilizing agent. The UV radiation has a wavelength of 260 nm, and this specific wavelength is absorbed by the DNA. The DNA's regular base pairing is disrupted when this radiation absorbs by nearby thymine bases, which cross-link to generate thymine dimers. However, this effect is only a disinfection method as the organisms have either a light repair system or a nucleotide excision repair system to undo these thymine dimers when specific conditions are available (Tortora et al. 2016). The typical diagram of a UV disinfection unit and thymine dimer formation are depicted in Figure 2.15.

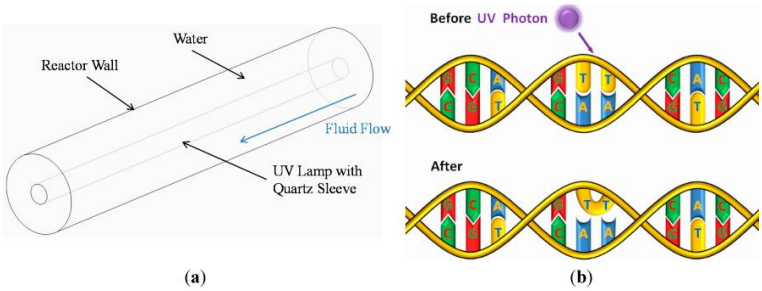

Figure 2.15. Typical UV disinfection system diagram (a) and thymine dimer formation (b)(Gross et al. 2015)

2.3.5 Membrane bioreactor (MBR)

MBR process is a combined process of the biological reactor and membrane filtration (Al-Asheh et.al. 2021). This is the process used for the removal of residual particulate and colloidal matter including microorganisms. In this process, wastewater is passed through porous material excluding the particles that have a size between 0.005 to 2.0 µm (Metcalf & Eddy 2014). Membrane processes include microfiltration (MF), ultrafiltration (UF), nanofiltration (NF), and reverse osmosis (RO). The membrane bioreactor process combines an activated sludge system with

usually MF or UF instead of a sedimentation tank (Metcalf & Eddy 2014). The typical diagram of an MBR unit is depicted in Figure 2.16.

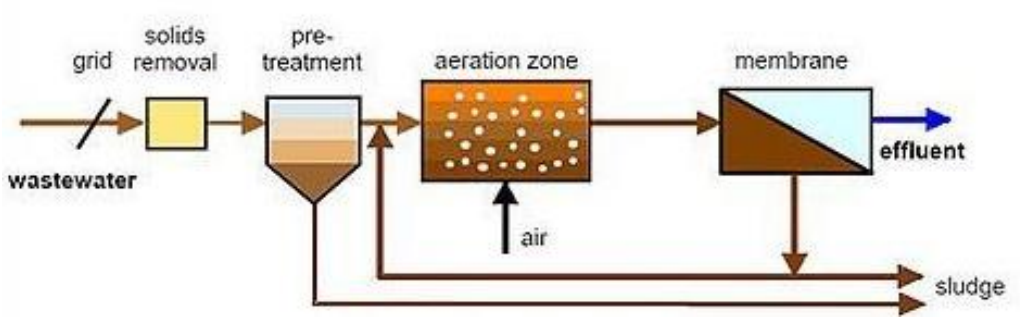

Figure 2.16. Typical MBR system diagram(Karim and Mark 2017)

The advantages and drawbacks of MBR systems are given in Table 2.1.

Table 2.1. The advantages and drawbacks of MBR systems (Saleh & Gupta 2016)

Advantages of MBR	**Disadvantages of MBR**
Continuous separation under mild condition	Low membrane lifetime
Membrane properties can be adjusted	Low selectivity and flux
Scaling up is easy	Scaling up is linear
Hybrid processing is possible	Concentration polarization membrane fouling

2.4 Methods for parasitic protozoan detection in the environmental samples

It is possible to evaluate the occurrence and prevalence of waterborne protozoa using both traditional and modern molecular approaches (Skotarczak 2009). Water and wastewater systems have been evaluated using a number of techniques based on the amplification and comparison of rRNA sequences. These methods consist of reverse line blotting, PCR, qPCR, terminal restriction fragment length polymorphism (t-RFLP), denaturing gradient gel electrophoresis (DGGE), fluorescent *in situ* hybridization (FISH) and reverse line blotting (RLB) (Adamska et al. 2015; Gilbride et al. 2006). Usually, the amount of information held by the genetic locus under study heavily influences the choice of an assay and molecular marker. When identifying the various species within a genus, certain tests can be used to discriminate between

isolates of the same species (genotypes), whereas others can be used for both purposes (Skotarczak 2009).

Among the aforementioned molecular methods, DGGE is used to differentiate amplified rRNA gene fragments, which are usually just 500 bp in length, based on sequence variations rather than size variations. Phylogenetic composition can be evaluated by removing and sequencing specific bands (Gilbride et al. 2006).On the other hand, the t-RFLP experiment uses one or both fluorescently labeled primers to tag the PCR result. Following restriction endonuclease digestion of the amplicons, the fragments are sorted by capillary electrophoresis. An electrophoretic profile is created as a distinctive hallmark for each microbial community after the tagged fragments are found (Gilbride et al. 2006). Another useful technique is FISH when analyzing samples of microbial communities. This technique can be used to assess the abundance of each microorganism in a population. FISH has been used to create a quantitative description of the microbial community structure in activated sludge and wastewater because of its capacity to count specific microbial cells (Gilbride et al. 2006). RLB technique is referred to as a reverse dot blot assay for the detection of pathogens. It is based on the hybridization of PCR products to certain probes immobilized on a membrane to detect variations in the amplified sequences (Adamska et al. 2015). PCR and qPCR are also potent molecular tools in which the gene sequence corresponding to the intended target can be amplified. qPCR has advantages over traditional PCR in terms of practicality and allows for the real-time monitoring of DNA amplification (Kralik et al. 2017). One other benefit of qPCR is the ability to quantify genetic targets throughout a broad dynamic range as opposed to the endpoint analysis of conventional PCR (Smith et al. 2009). Some benefits and limitations of the techniques are given in Table 2.2.

Table 2.2. Benefits and limitations of some molecular techniques used in protozoa detection (Adamska et al. 2015; Gilbride et al. 2006)

Technique	**Benefits**	**Limitations**
Denaturing gradient gel electrophoresis (DGGE)	Culture-independent Suitable for a wide range of pathogens	DNA extraction and PCR biases
Terminal-restriction fragment length polymorphism (t-RFLP)	Culture-independent Fast and semi-quantitative Suitable for a wide range of pathogens	DNA extraction and PCR biases
Fluorescent *in situ* Hybridization (FISH)	Quantitative	Inactive cells cannot be detected
Polymerase chain reactions (PCR)	Rapid detection of target pathogens	Target specific primers
Quantitative PCR	Quantitative	Target specific primers
Reverse line blotting (RLB)	Simultaneous detection of many microorganisms	Not repetitive Signals may be weak

For the genotyping of protozoan species, PCR and qPCR have been utilized widely and have several advantages over traditional techniques. For waterborne protozoans, numerous polymerase chain reaction assays have been described (Sánchez et al. 2018). The amount of information conveyed by the genetic marker being studied determines which test should be used in most cases. Some tests can only be used to distinguish between isolates of the same species (genotypes), whereas others can be used to identify species within a genus. qPCR also made it possible to study the infection's quantitative aspects with exceptional sensitivity. For instance, it is possible to identify carrier statuses, count the number of (oo)cysts in a sample, and study quantitative aspects of gene expression during the infection's any stages (Skotarczak 2009).

2.4.1 Polymerase chain reactions (PCR)

PCR is a simple and sensitive enzymatic assay that allows for the *in vitro* amplification of small samples of DNA (Garibyan and Avashia 2013). PCR makes use of the enzyme DNA polymerase that copies DNA molecules. High temperatures applied in the PCR reaction to denature the DNA, therefore an isolate of the DNA polymerase from a thermophilic hot spring bacterium (*Thermophilus aquaticus*) is used during the reaction (Madigan and Martinko 2006). After denaturation with high temperatures, each strand of DNA will serve as a template for new DNA synthesis. Four nucleotides (dNTPs), primers that are complementary to the ends of the target DNA strands and *Taq* polymerase are added to the template to start the reaction and synthesize new strands. A diagram of PCR reactions is given in Figure 2.17. Following agarose gel electrophoresis, the amplification products in a standard PCR assay are typically seen with ethidium bromide or alternative, less carcinogenic dyes. The estimated size of the PCR product determines the specificity of the assay. For the detection of protozoa in fecal samples, PCR has been demonstrated to be a sensitive and specific alternative (Verweij and van Lieshout 2011).

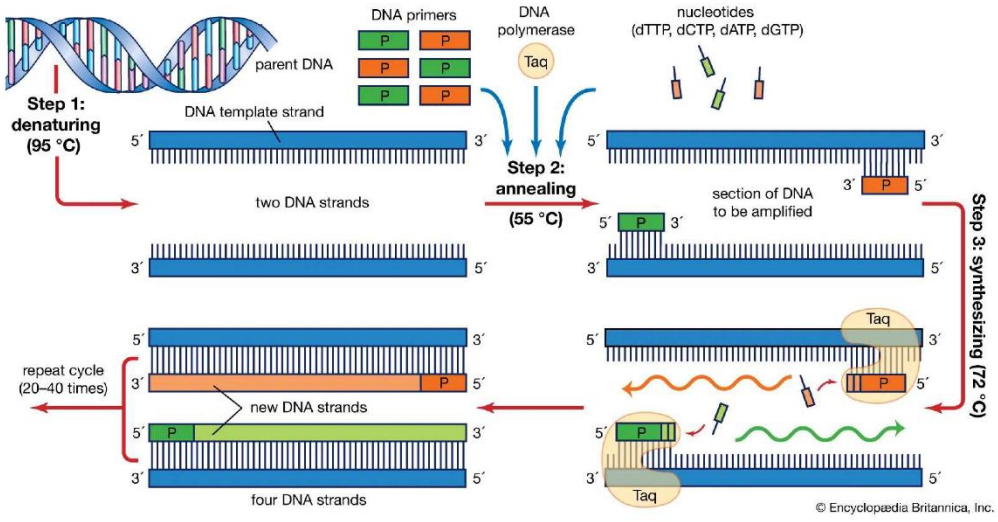

Figure 2.17. Schematic diagram of PCR(Brittanica 2021)

2.4.2 Quantitative polymerase chain reactions (qPCR)

qPCR, also known as real time PCR, allows for the monitoring of DNA amplification in real time through monitoring of fluorescence (Kralik et.al 2017). In this method, the newly made DNA is tagged with fluorescent dye (Tortora et al. 2016) and after each cycle, fluorescence is monitored, and the strength of the signal corresponds to the amount of DNA amplicons present in the sample at that particular instant. (Figure 2.18). qPCR allows for the determination of the absolute quantity of the target DNA in the sample (Kralik et.al 2017).

qPCR has been developed to allow for the detection and identification of multiple microorganisms at the species level (Bonilla et al. 2015). This method not only measures free DNA but also cellular DNA (Berglund et al. 2017).

The phase on which PCR is concentrated is the early exponential phase of the amplification process, when the number of amplified products is proportional to the concentration of template DNA. This phase is used for DNA quantification when employing qPCR. A fluorescent detecting device is used by a real-time PCR to track the results continuously throughout the procedure. (Fontaine and Guillot 2002). qPCR's closed-tube format not only cuts labor time in a busy diagnostic laboratory but also considerably lowers the possibility of contamination(s) (van Lieshout and Roestenberg 2015).

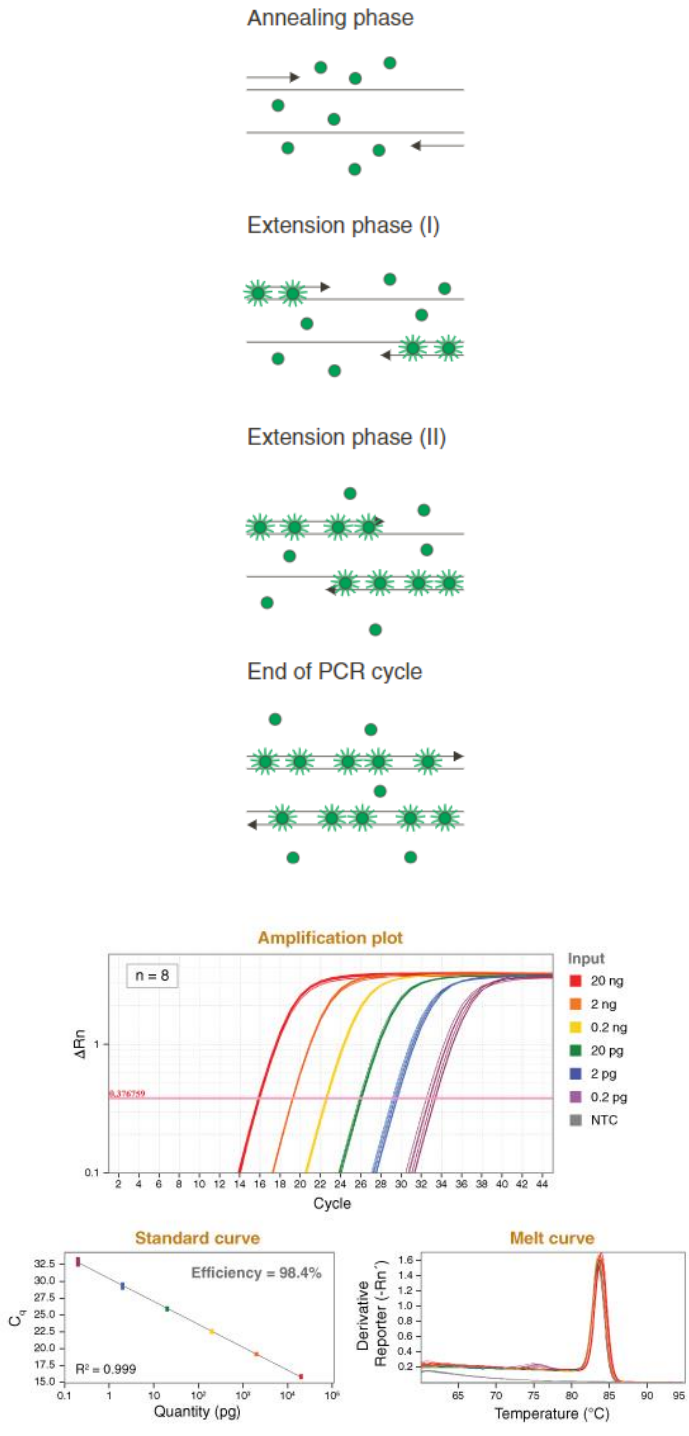

Figure 2.18. SYBR Green detection and melting curve example of qPCR (van der Velden et al. 2003)

CHAPTER 3

MATERIALS AND METHODS

3.1 Types of WWTPs tested in the study

Five WWTPs with varying processes including CAS (Figure 3.1), BNR (Figure 3.2), SBR (Figure 3.3), CoFlUV (Figure 3.4) and MBR (Figure 3.5) were used in this study.

Figure 3.1. Picture of CAS system sampled in this study.

Figure 3.2. Picture of BNR system sampled in this study.

Figure 3.3. Picture of SBR system sampled in this study.

Figure 3.4. Picture of CoFlUV system sampled in this study.

Figure 3.5. Picture of MBR system sampled in this study.

Average operational parameters and influent and effluent water qualities are presented in Table 3.1 and Table 3.2, respectively. During the study's sampling period, all WWTPS' effluent discharge requirements complied with Turkish

Regulation on Water Pollution Control (Republic of Turkey Environment and Urban Ministry 2004).

3.2 Collection of samples

An amount of 1 L of water and sludge samples were taken from each WWTP in triplicate and placed in sterilized bottles. For DNA extraction, the obtained samples are delivered to the lab in a portable cooling box within two hours. The samples were collected seasonally in between 2020-2021 to account for the seasonal variations regarding protozoan removal. DNA extractions were done within 24 h of sample collection.

3.2.1 Water samples

For the pre-treatment of water samples for later use, the method developed by Lemarchand et. al. (2005) was selected to be used. Prior to the subsequent DNA extraction, the samples were centrifuged at 1000 g for 16 min. and the pellets were kept at -20°C.

3.2.2 Sludge samples

The sludge samples not used in the extraction were centrifuged at 16000 g for 15 min and the pellets were stored at -20°C until DNA extraction (Lemarchand et al. 2005).

Table 3.1. Average influent and effluent water qualities of selected WWTPs

WWTP	Water quality											
	pH		TSS (mg/L)		COD (mg/L)		BOD (mg/L)		Total N (mg/L)		PO_4-P (mg/L)	
	Influent	Effluent	Influent	Effluent	Influent	Effluent	Influent	Effluent	Influent	Effluent	Influent	Effluent
CAS	7.7	8.0	297	24	402	52	240	19	56	39.0	5.0	1.2
BNR	7.7	8.0	207	18	334	27	183	15	28.8	9.0	5.8	2.0
SBR	8.0	7.6	177	24	352	49	201	19	na	na	na	na
CoFlUV	8.5	6.0	600	200	2500	400	800	100	na	na	na	na
MBR	7.3	7.7	na	na	426	19	250	nd	na	na	na	na

TSS, total suspended solids, COD, chemical oxygen demand, BOD, biochemical oxygen demand, coagulant, $FeCl_3$, UV dosage 15 mJ/cm^2, nd, non-detected, na, data not available.

Table 3.2. Average operational parameters of selected WWTPs

WWTP	Operating parameters					
	Flow rate (m^3/d)	MLSS (mg/L)	HRT (h)	SRT (d)	RAS (%)	WW source
CAS	765000	1730	12	3	60	Dom
BNR	41818	4125	28	16	85	Dom
SBR	3000	5216	8	na	-	Dom
CoFlUV	10000	400	27	27	100	30% Dom
MBR	15000	4180	18	na	na	Dom

MLSS, mixed liquor suspended solids; HRT, hydraulic retention time; SRT, solids retention time; RAS, return activated sludge; WW, wastewater; h, hour, Dom, domestic; na, data not available, nd, non-detected

3.3 Total DNA extractions

The methodology for total DNA extraction is given below and the chemicals used during the extraction method are listed in Table 3.3.

Table 3.3. Chemicals used in the extraction process

Chemicals	**Suppliers**
Phenol	Merck, Germany
Chloroform	>99%, Mercdk, Germany
Sodium acetate	Sigma-Aldrich, Germany
Isopropanol	Merck, Germany
Ethanol	Razı, Iran
Tris	BDH, UAE
EDTA	Sigma-Aldrich, Germany

DNA extractions were done within 24 h after sample collection by modifying the protocol developed by Stirling and Bartlett (1996) (Figure 3.6). 500 µL of water and sludge samples were transferred to Eppendorf tubes and were sonicated (Bandelin, Germany) with 35% amplitude for 1 min in picked ice. To the sonicated samples 1 volume of phenol-chloroform (1:1) was added and the samples were centrifuged at 19000 g for 10 min. After centrifugation (Thermo Scientific, USA), the upper phase was drawn and transferred to a new Eppendorf tube. The phenol-chloroform step was repeated two times to fully purify the samples from proteins. To this upper phase, 1/10 volume of sodium acetate and 6/10 volume of isopropanol is added, and the samples were kept at -20°C for 10 min. The cooled samples are then centrifuged at 19000 g for 10 min. After this 300 µL of 70% of ethanol was added to the pellets and the samples were centrifuged again at 19000 g for 10 min. After the last centrifugation, the ethanol was left to evaporate and the 50 µL of TE buffer was added to the samples for storage at -20°C until further analyses. The quality and concentration of extracted DNA were determined by nanodrop (Berthold, Germany) and 1.5% agarose gel electrophoresis (Bio-Rad, USA) (Lee et al. 2012). Before

analyses the spectrophotometer (Berthold, Germany) was blanked with the TE Buffer that was also used to store the extracted DNA. In the spectrophotometric analyses the purity of the extracted DNA was assessed using the 260/280 nm and 260/230 nm ratios. The ratio of absorbance at 260/280 nm should be around 1.8 for the DNA to be accepted as pure. This ratio was around 1.8 for all the samples measured. The 260/230 nm ratio should be in the range of 2.0-2.2, and for all the samples measured, this value was between 2.0 and 2.2. For the agarose gel electrophoresis analyses, to be used as an electrical conducting agent and to prepare the agarose gel, 10x TBE Buffer containing 108 g/L Tris (BDH, UAE), 55 g/L Boric acid (BioShop, Canada) and 40 mL/L EDTA (Sigma-Aldrich, Germany) (pH 8) was prepared and diluted to 1x. An amount of 15 g agarose /1 L 1x TBE Buffer was prepared, and 40 mL of this solution was used to make the agarose gel and 2.5 µL RedSafe™ dye (INtRON Biotechnology, South Korea) was used to dye the gel (Lee et al. 2012).

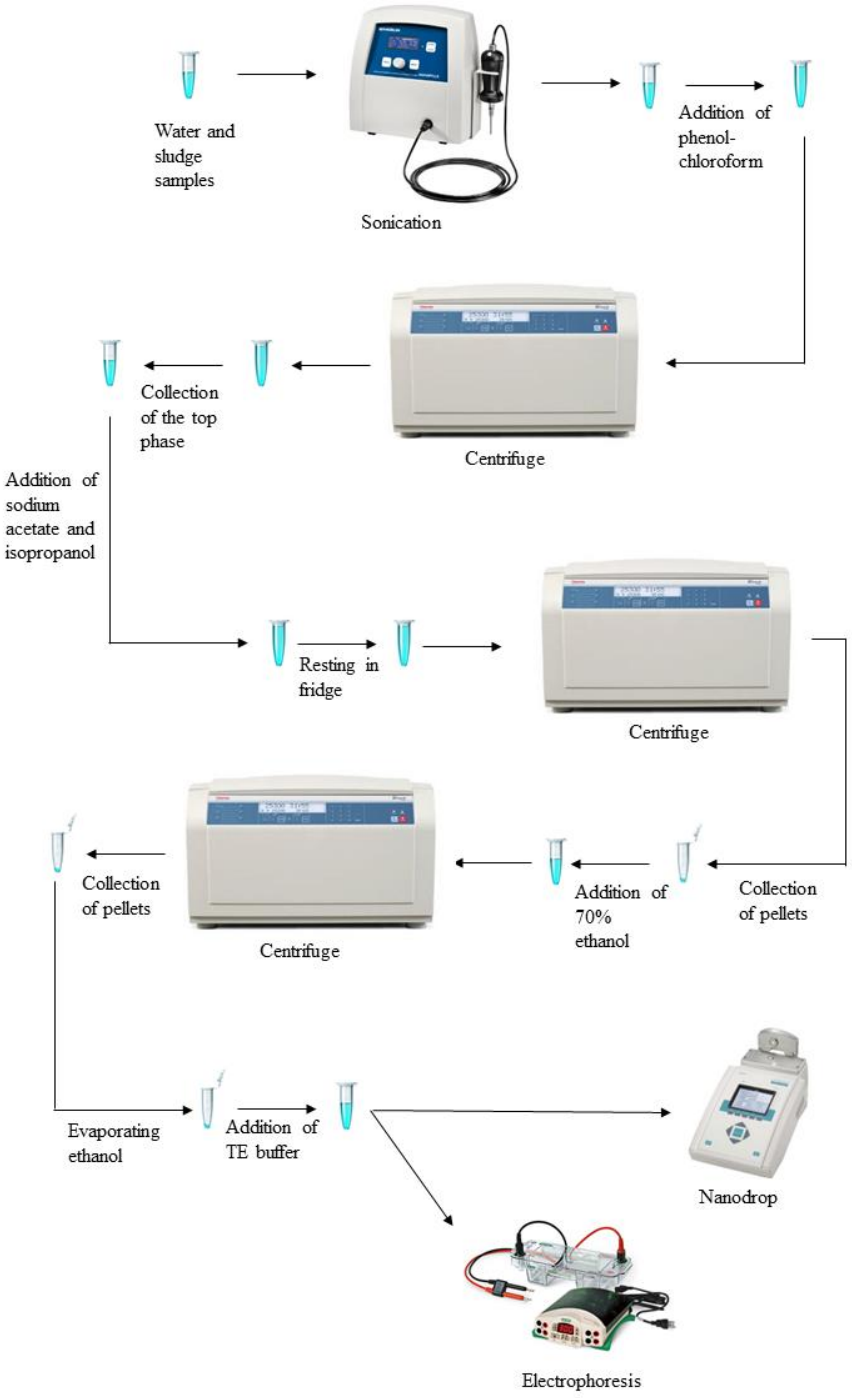

Figure 3.6. Experimental flow of protozoan DNA extraction

3.4 Qualitative analyses of protozoan DNA

For the qualitative analyses of protozoan parasites PCR was performed (Figure 3.8). Specifically selected primers selected for this study and their target protozoan parasites are depicted in Table 3.4.

PCR optimization was done for each protozoan parasite and primer by changing the reference temperature. PCR reactions were carried out in 25 µL reaction mixtures consisting of 2.5 µL 10x PCR buffer (Solis BioDyne, Estonia), 2.5 µL 10x $MgCl_2$ (Solis BioDyne, Estonia), 2mM dNTPs (New England Biolabs, USA), forward and reverse primers, 100 ng template DNA and 0.2 µL Taq DNA polymerase (Solis BioDyne, Estonia) using T100 Thermal Cycler (Bio-Rad, USA). The PCR program contained the following steps: initial denaturation at 95°C for 3 min, 35 cycles of denaturation at 95°C for 15 sec, annealing at annealing temperatures for 45 sec, elongation at 72°C for 45 sec and at the end of cycles final extension at 72°C for 7 min.

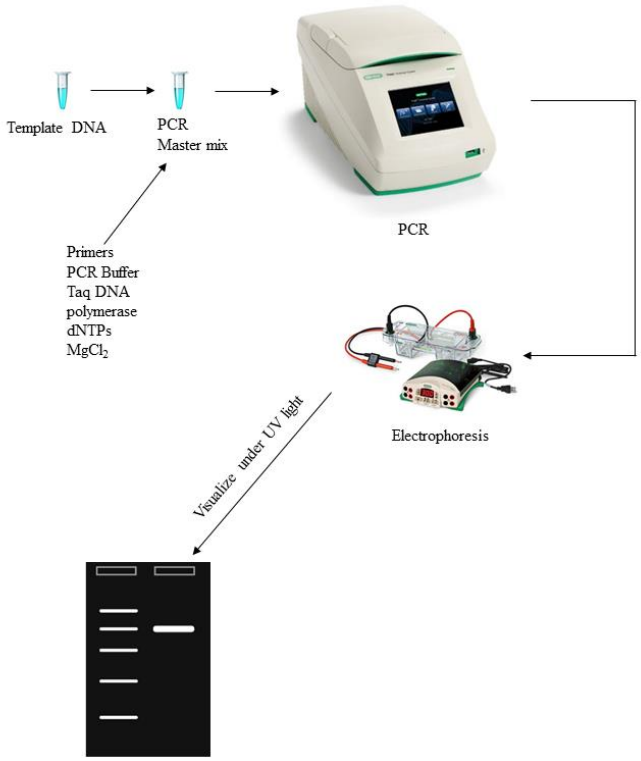

Figure 3.7. Experimental flow of PCR method used in the study

In each PCR reaction, negative controls were included. The reproducibility of the reactions was confirmed by performing duplicate PCR reactions. The amplicons were analyzed through 1.5% agarose gel which is stained with RedSafe (Intron, Korea) at 90 V (Moreno et al. 2018). To be able to calculate the PCR amplicons' molecular weight 50 bp DNA ladder (EUR X, Perfect Plus) was loaded into each agarose gel. Lastly, the agarose gel was visualized under UV light.

The copy numbers of protozoan DNA per µL were calculated according to Whelan et. al (2003) with the following equation (1):

$$\frac{\text{Copy number of DNA}}{\mu L} = \frac{b*c}{L*a*10^{12}} \quad (1)$$

In equation 1, the letters a, b, c and L represent the weight of kb DNA per pmol (1 kb DNA = 0.66 µg/pmol), Avogadro Number (6.022x1023/mol), the concentration of template in µg/µL and length of template containing the target gene, respectively.

Table 3.4. Primers used in the study

Primer name	Organism	Sequence (5'→ 3')	Amplicon size (bp)	Annealing temperature (°C)	References
Ehd-239F	*E. histolytica*	ATTGTCGTGGCATCCTAACTCA	174	59	(Verweij et al. 2004)
Ehd-88R	*E. histolytica*	GCGGACGGCTCATTATAACA	174	59	(Verweij et al. 2004)
Blasto FWD-F5	*B. hominis*	GGTCCGGTGAACACTTTGGATTT	119	60	(Moreno et al. 2018a)
Blasto R-F2	*B. hominis*	CCTACGGAAACCTTGTTACGACTTCA	119	60	(Moreno et al. 2018a)
P241-F	*G. intestinalis*	CATCCGCGAGGAGGTCAA	75	60	(Guy et al. 2003a)
P241-R	*G. intestinalis*	GCAGCCATGGTGTCGATCT	75	60	(Guy et al. 2003a)
CPrF3	*C. parvum*	CAG TTG GGG GCA TTT GTT TGT ATT	118	59	(Minarovi et al. 2007)
CPrR3	*C. parvum*	CCC CTA ACT TTC GTT CTT GAT T	118	59	(Minarovi et al. 2007)

F, forward; R, reverse

3.5 Quantitative analyses of protozoan DNA

qPCR analyses were performed for the quantitative analyses of protozoan parasites (Figure 3.8). Coyote Mini8 real-time PCR (Coyote Bio, Columbia) was used for the qPCR reactions. A 20 µL reaction mixture containing 1 µL template DNA, 4 µL 5x EvaGreen ® qPCR Master Mix, and forward and reverse primers were prepared for the qPCR analyses. Negative controls were included in each qPCR assay to evaluate non-specific amplifications. Lambda DNA (New England Biolabs, USA) was used to construct the standard curves for qPCR (Guy et al. 2003). Data obtained from the qPCR were analyzed using Mini8 Plus qPCR Software (v. 2.0.13; Coyote Bio, Columbia). The copy numbers of target protozoan DNA were calculated based on the standard curves constructed with Lambda DNA. The following steps were included in the qPCR assay: initial denaturation at 95ºC for 12 min, following 40 cycles of denaturation at 95ºC for 15 sec, annealing for 30 sec, elongation at 72ºC for 30 sec. To generate the melting curves at the end of the cycles, the tubes were gradually heated from 70ºC to 95ºC. The DNA samples were analyzed in triplicate. The specificity of the products was checked with R^2 values and melting curves. For all the standard curves R^2 values were higher than 0.99. The abundance of protozoan DNA was calculated by the normalization of DNA copies to the sample volume used (1L) to generate log DNA copies per L.

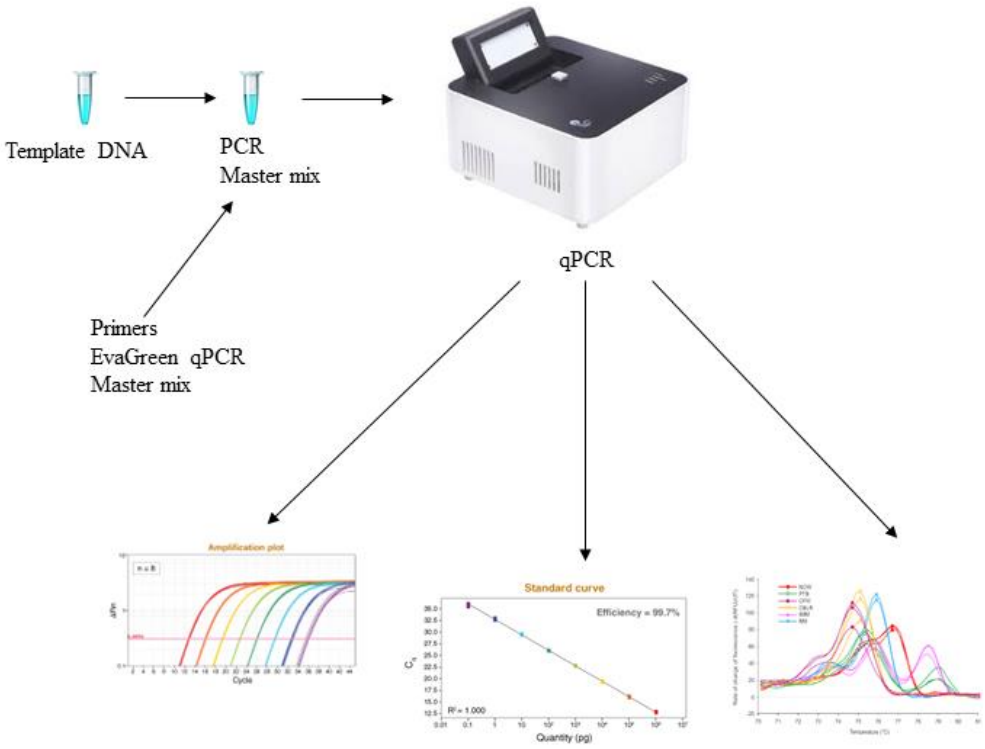

Figure 3.8. Experimental flow of qPCR method used in the study

3.6 Data analyses and statistics

Removal efficiencies for each WWTP regarding protozoan parasites were measured with logarithmic removal values (LRV) (Domenech et al. 2018). LRVs were calculated by taking the logarithm of the ratio of protozoan DNA concentrations in the influents and effluents of the WWTPs as shown in equation (2):

$$LRV = Log_{10} (C_{influent} / C_{effluent}) \quad (2)$$

LRV of 1 represents 90% removal efficiency of target protozoa, LRV of 2 represent 99% removal efficiency and LRV of 3 represents 99.9% removal efficiency. This pattern is followed as LRVs become greater. In their paper, Teel et.al. (2022) depicts

according to the Nevada Administrative Code, a treatment process may be credited with a maximum of 6- and a minimum of 1-log reduction. In addition, WHO recommends 4-log reduction for protozoan parasites for potential agricultural reuse (Oakley 2019). In Turkey, there are no current regulations regarding protozoan removal, therefore, LRV 3 was selected as a baseline for efficient removal in this study. WWTPs with LRVs lower than 3 were assumed to be not fully effective and release protozoan parasites in the discharge points. Seasonal removal variations of protozoan DNA were also assessed through One-way Analysis of Variance (ANOVA) and Tukey's Post-hoc Tests (SPSS Statics for Windows v.28,0; IBM Corp., Armonk, NY) at a significance level of $p < 0.05$. The limit of detection (LOD) value for each qPCR assay was determined as the lowest measurement and LRVs were calculated by setting samples below the LOD as 0. The limit of quantification (LOQ) value was also determined for each qPCR analysis as the highest measurement and the values which were below the limit of quantification but above the limit of detection were set to the mean of these limits (Berglund et al. 2017).

CHAPTER 4

RESULTS AND DISCUSSION

4.1 Qualitative analyses of protozoan parasites

4.1.1 Optimization of the PCR conditions and construction of standard curves

PCR analyses were used for the qualitative analyses of protozoan parasites. Optimization of PCR conditions was done by changing the annealing temperatures of the primers. Template DNA used for the PCR reactions was extracted from the samples taken. Standard curves for qPCR analyses were constructed by using Lambda DNA (Guy et al. 2003). After the qPCR analyses, product specificities were checked via R^2 values, and melting curves.

4.1.1.1 Optimization of *G. intestinalis* primer

Primer targeting the parasite *G. intestinalis* was chosen from the study of Guy et.al. (2003). In that study, Lambda DNA was used as a template DNA when constructing the standard curves in qPCR analyses. The reference annealing temperature for the selected primer was 60°C (Table 3.4). In the current study, Lambda DNA was also used for the construction of standard curves. The optimum PCR condition of the primer was investigated by varying the annealing temperature between 57°C and 60°C (Figure 4.1).

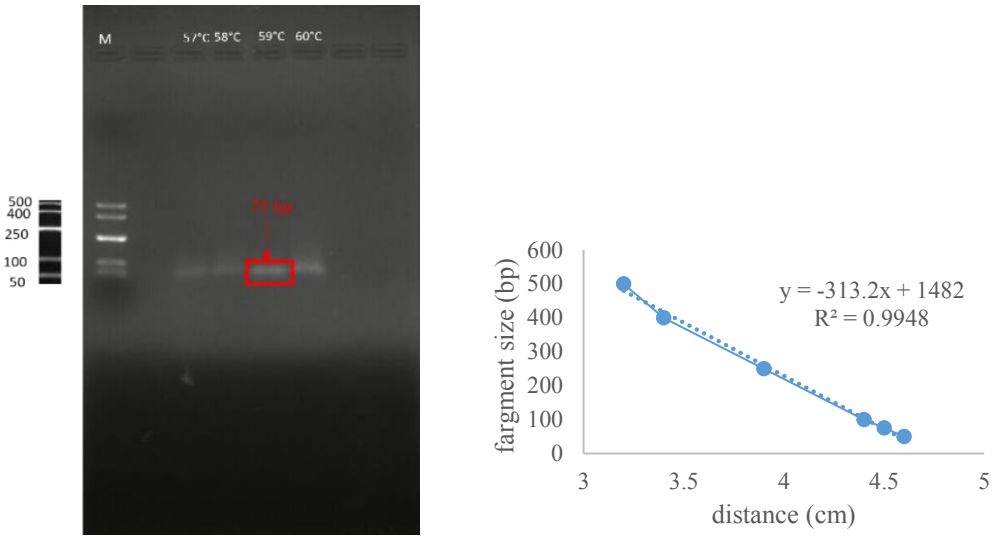

Figure 4.1. PCR optimization of the primer for *G. intestinalis* with different annealing temperatures. M, 50 bp DNA ladder from top to bottom 500, 400, 250, 100, and 50 bp, respectively (a). Standard curve of agarose gel for molecular weight estimation (b).

Electrophoresis analysis of the PCR amplicons showed that the optimum PCR results were obtained at 59°C (Figure 4.1). Optimized conditions for the primer were then used in the quantitative analyses for *G. intestinalis*.

4.1.1.2 Optimization of *E. histolytica* primer

Primer targeting *E. histolytica* was chosen from the study conducted by Verweij et.al. (2004). The reference annealing temperature for the selected primer was 59°C (Table 3.4). The optimum PCR condition of the primer was investigated by varying the annealing temperature between 57°C and 60°C (Figure 4.2).

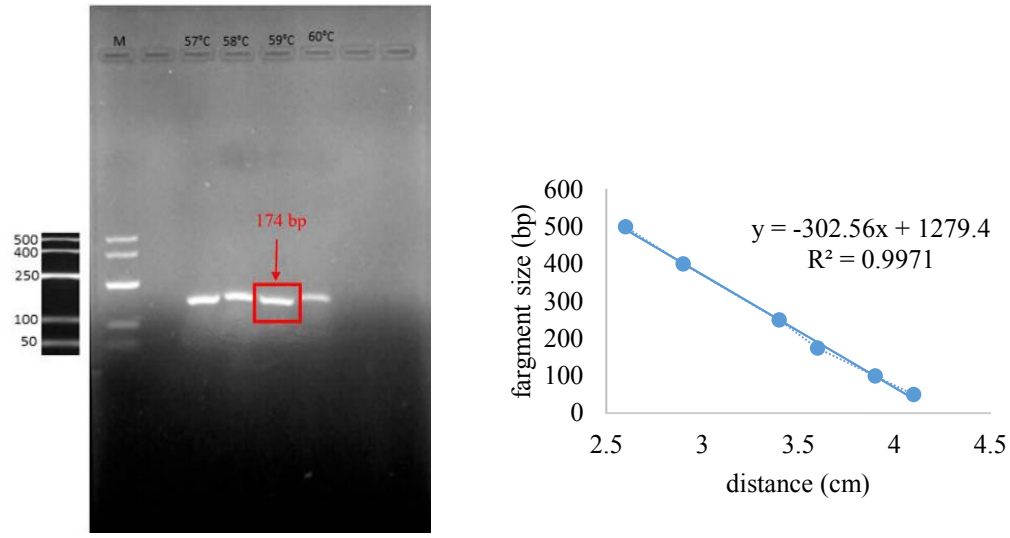

Figure 4.2. PCR optimization of the primer for *E. histolytica* with different annealing temperatures. M, 50 bp DNA ladder from top to bottom 500, 400, 250, 100, and 50 bp, respectively (a). Standard curve of agarose gel for molecular weight estimation (b).

Electrophoresis analysis of the PCR amplicons showed that the optimum PCR results were obtained at 59°C (Figure 4.2). Optimized conditions for the primer were then used in the quantitative analyses of *E. histolytica*.

4.1.1.3 Optimization of *B. hominis* primer

Primer that targets *B. hominis* parasite was chosen from the study of Moreno et.al. (2018). The reference annealing temperature for the selected primer was 60°C (Table 3.4). The optimum PCR condition of the primer was investigated by changing the annealing temperature from 57°C to 60°C (Figure 4.3).

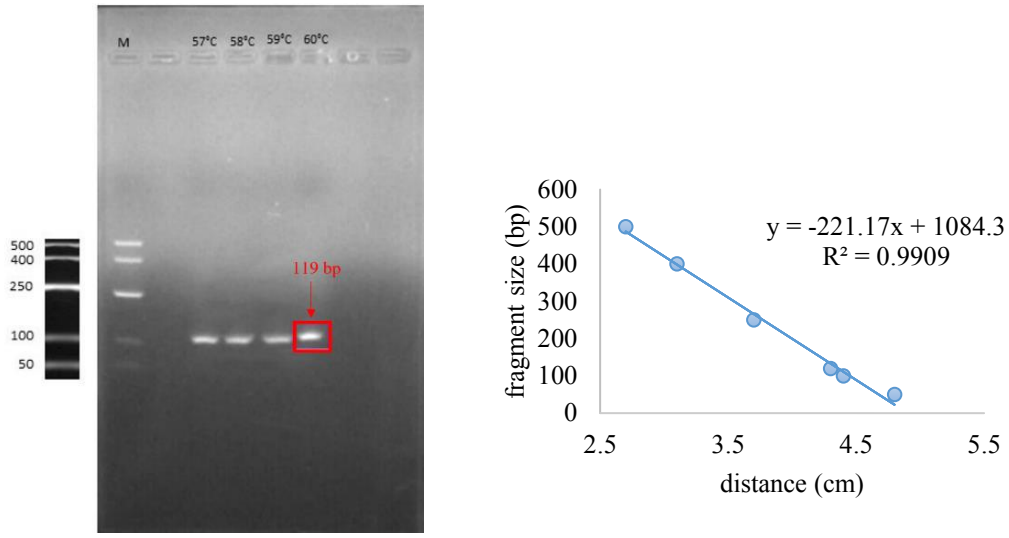

Figure 4.3. PCR optimization of the primer for *B. hominis* with different annealing temperatures. M, 50 bp DNA ladder from top to bottom 500, 400, 250, 100, and 50 bp, respectively (a). Standard curve of agarose gel for molecular weight estimation (b).

Electrophoresis analysis of the PCR amplicons showed that the optimum PCR results were obtained at 60°C (Figure 4.3). Optimized conditions for the primer were then used in the quantitative analyses of *B. hominis*.

4.1.1.4 Optimization of *C. parvum* primer

Primer that targets *C. parvum* parasite was chosen from the study of Minarovi et.al. (2007). The reference annealing temperature for the selected primer was 60°C (Table 3.4). The optimum PCR condition of the primer was investigated by changing the annealing temperature from 57°C to 60°C (Figure 4.3).

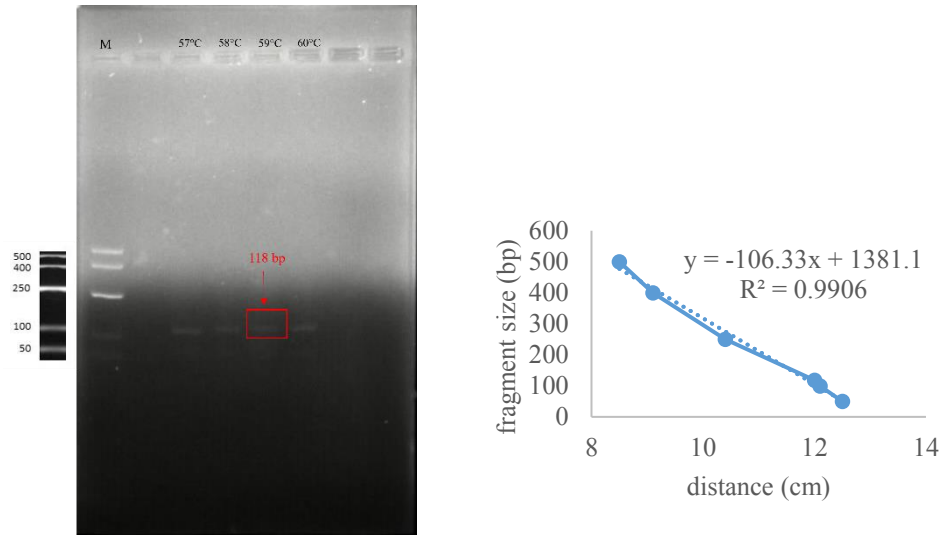

Figure 4.4. PCR optimization of the primer for *C. parvum* with different annealing temperatures. M, 50 bp DNA ladder from top to bottom 500, 400, 250, 100, and 50 bp, respectively (a). Standard curve of agarose gel for molecular weight estimation (b).

Electrophoresis analysis of the PCR amplicons showed that the optimum PCR results were obtained at 60°C (Figure 4.4). Optimized conditions for the primer were then used in the quantitative analyses of *C. parvum*.

4.2 Quantitative analyses and removal of protozoan parasites

4.2.1 Quantitative analyses for *G. intestinalis*

After the PCR optimization, standard curve was constructed by using Lambda DNA (Figure 4.5 to Figure 4.12). In all qPCR reactions, R^2 values were higher than 0.99. The LOQ for *G. intestinalis* was 10.96 log DNA copy number/L. The absolute abundances of *G. intestinalis* were calculated by the normalization of DNA copy numbers to the sample volume used to generate the DNA copies per L.

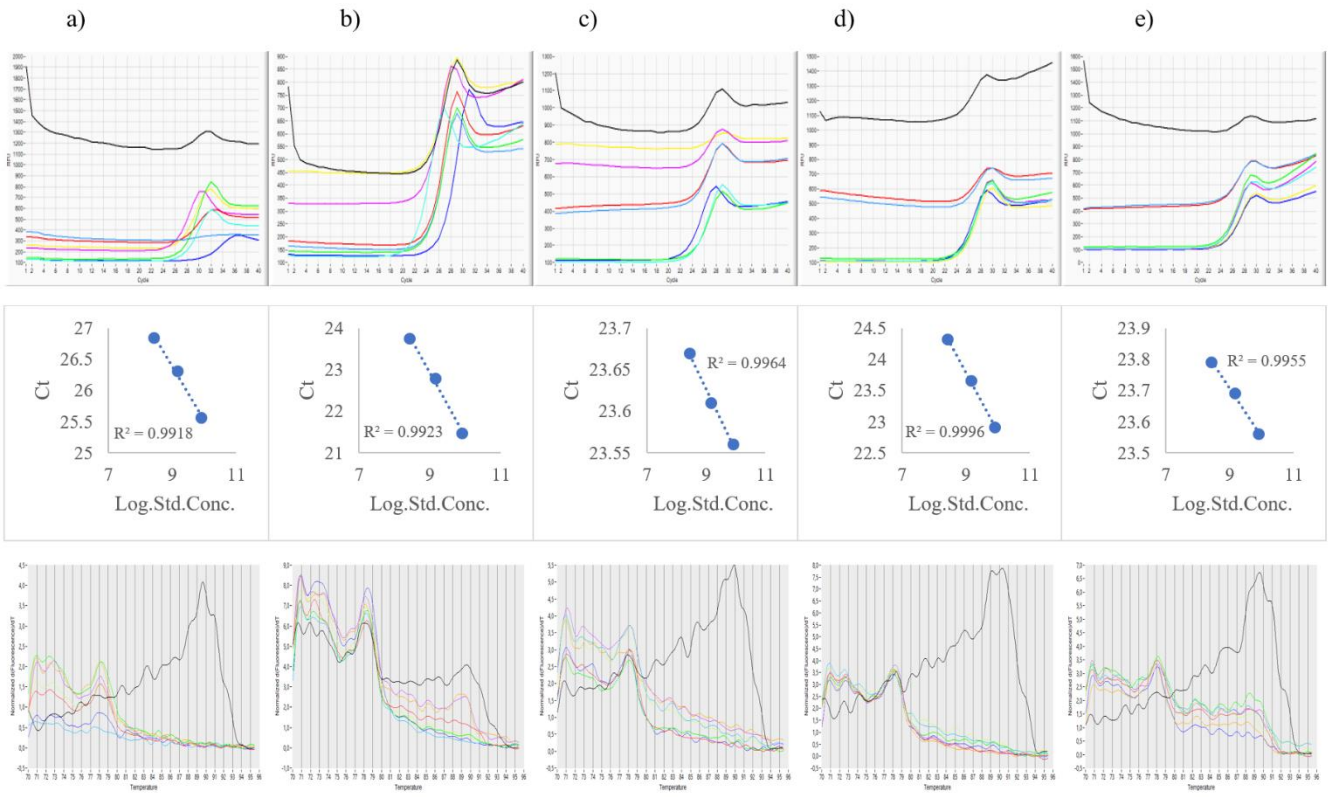

Figure 4.5. Amplification (top), standard (middle) and melting (bottom) curves of the qPCR analyses of *G. intestinalis* for summer influents in CAS (a), BNR (b), SBR (c), CoFlUV (d) and MBR (e). Ct, threshold cycle; RFU, reporter signal; Normalized d(Fluorescence)/dT, differential of fluorescence over temperature.

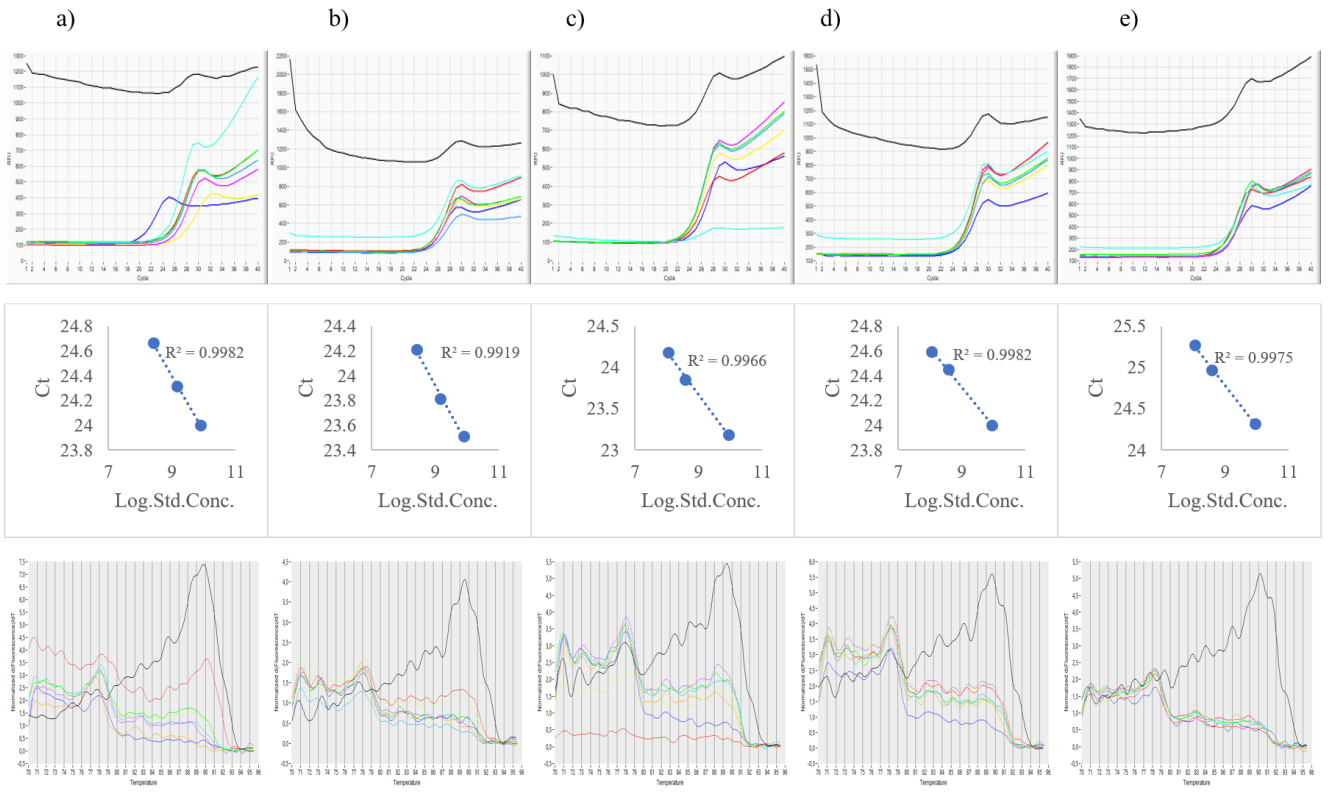

Figure 4.6. Amplification (top), standard (middle) and melting (bottom) curves of the qPCR analyses of *G. intestinalis* in autumn influents in CAS (a), BNR (b), SBR (c), CoFlUV (d) and MBR (e). Ct, threshold cycle; RFU, reporter signal; Normalized d(Fluorescence)/dT, differential of fluorescence over temperature.

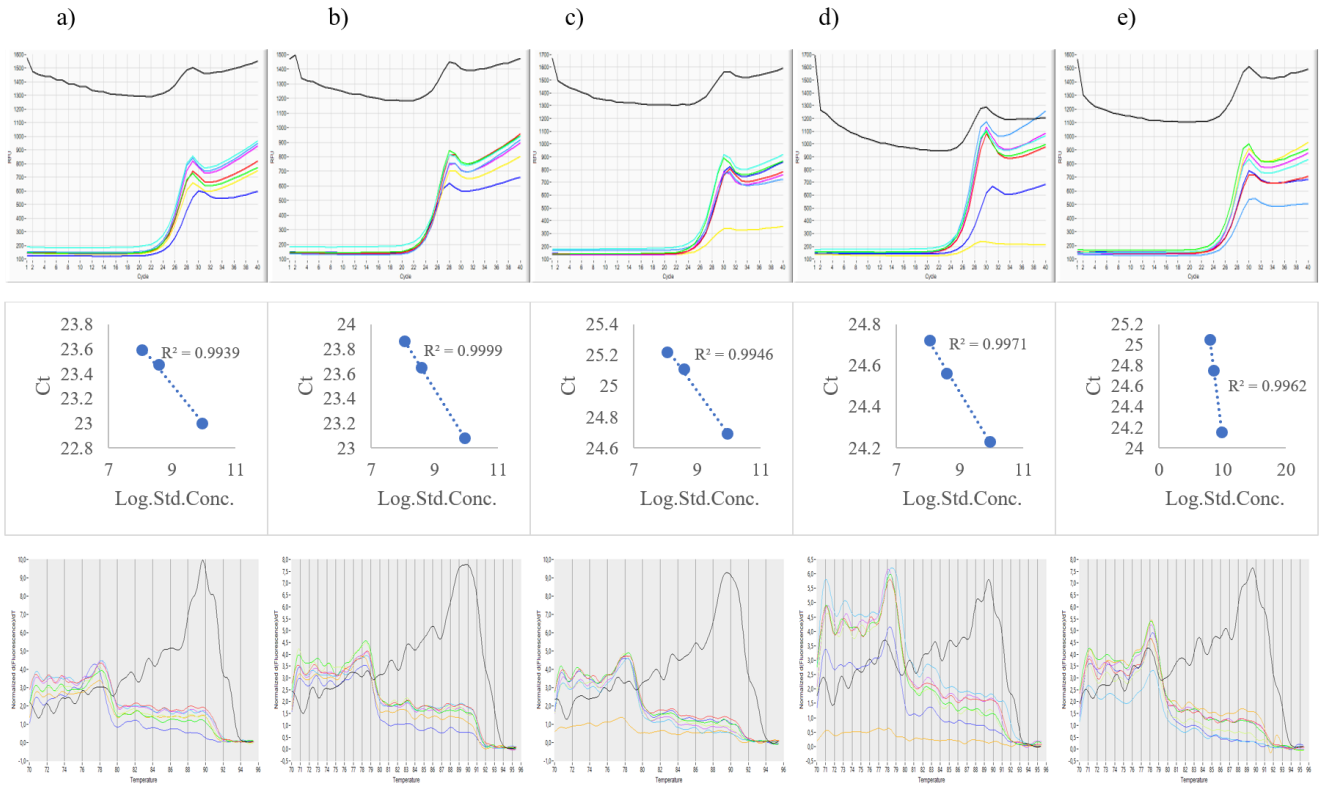

Figure 4.7. Amplification (top), standard (middle) and melting (bottom) curves of the qPCR analyses of *G. intestinalis* in winter influents in CAS (a), BNR (b), SBR (c), CoFlUV (d) and MBR (e). Ct, threshold cycle; RFU, reporter signal; Normalized d(Fluorescence)/dT, differential of fluorescence over temperature.

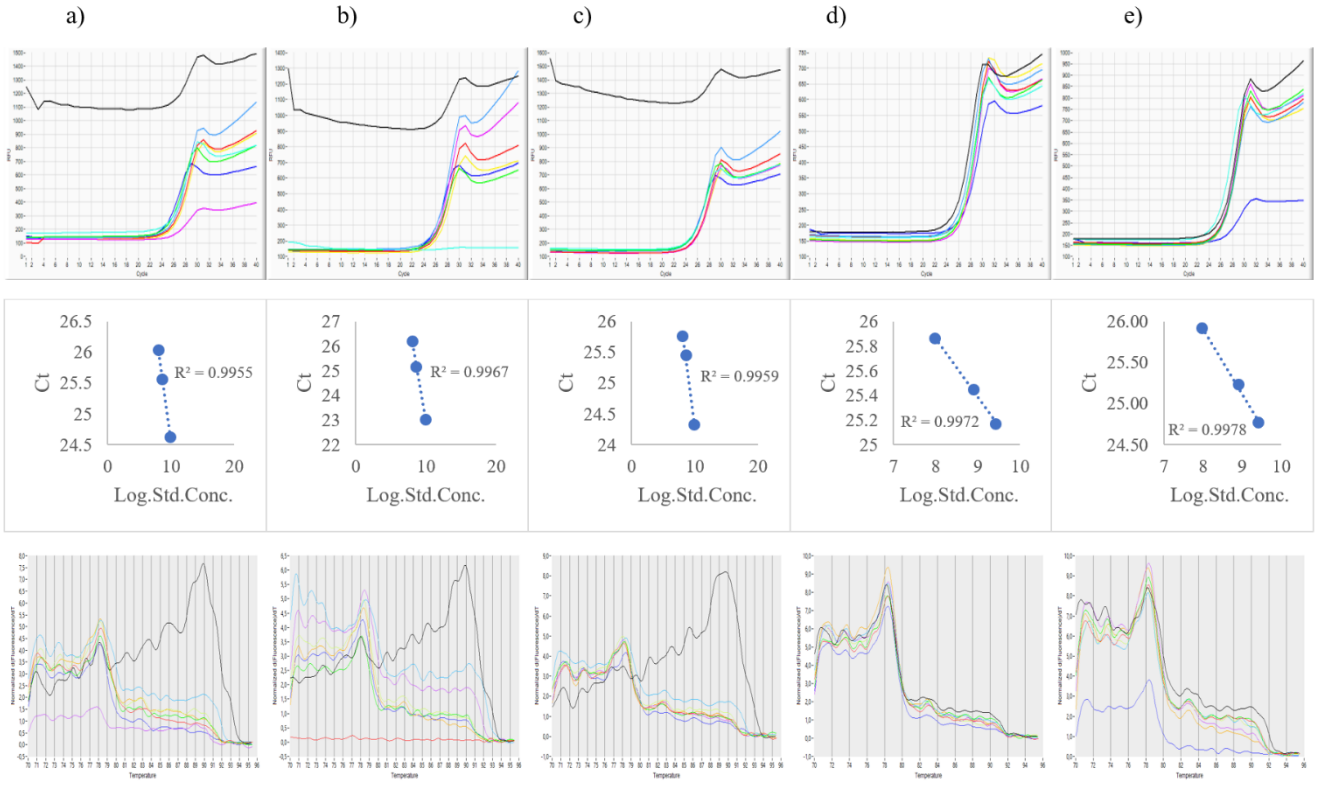

Figure 4.8. Amplification (top), standard (middle) and melting (bottom) curves of qPCR analyses of *G. intestinalis* in spring influents in CAS (a), BNR (b), SBR (c), CoFlUV (d) and MBR (e). Ct, threshold cycle; RFU, reporter signal; Normalized d(Fluorescence)/dT, differential of fluorescence over temperature.

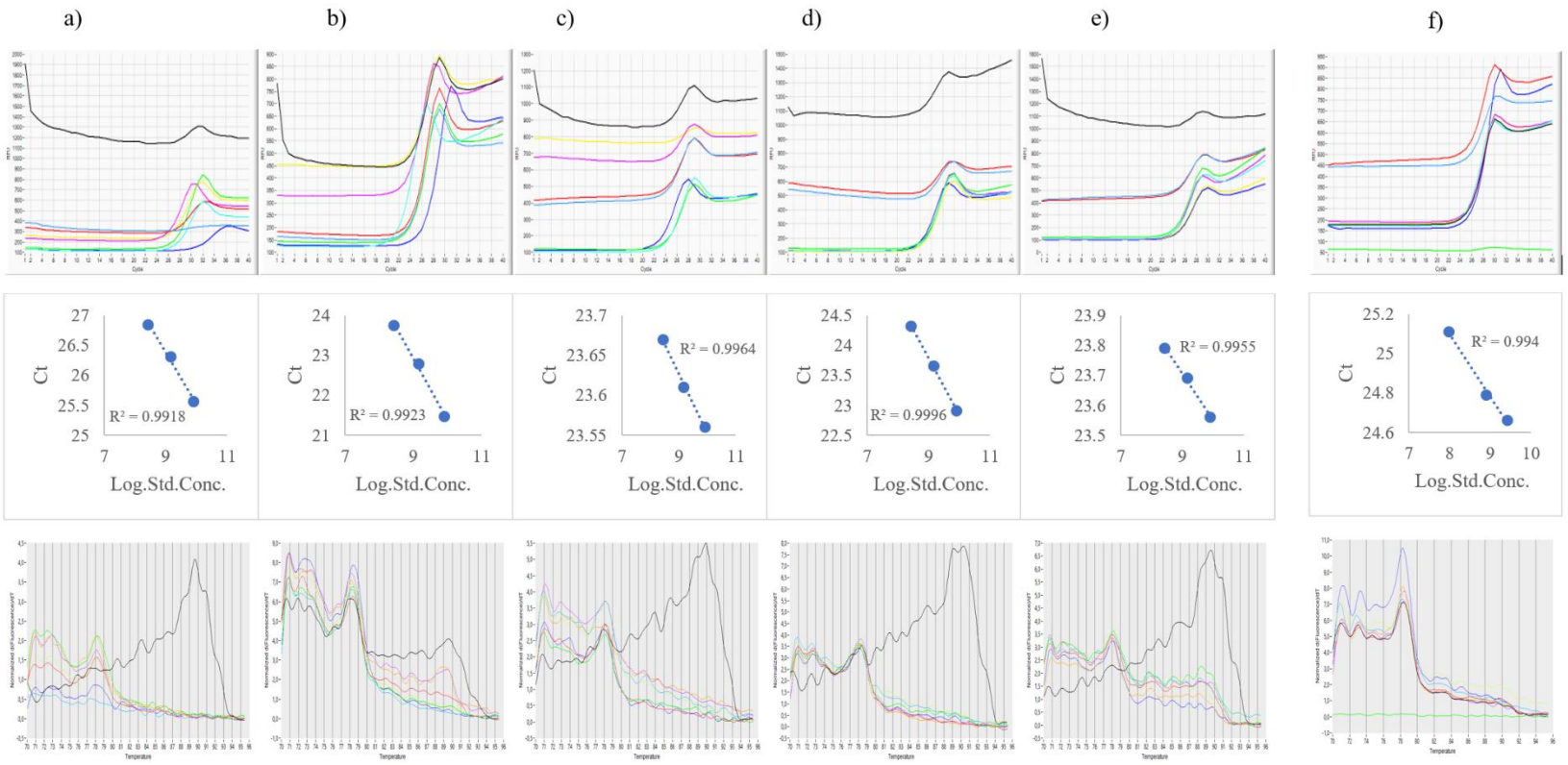

Figure 4.9. Amplification (top), standard (middle) and melting (bottom) curves of the qPCR analyses of *G. intestinalis* in summer effluents in CAS (a), BNR (b), SBR (c), CoFlUV (d), MBR (e) and CAS sludge (f). Ct, threshold cycle; RFU, reporter signal; Normalized d(Fluorescence)/dT, differential of fluorescence over temperature.

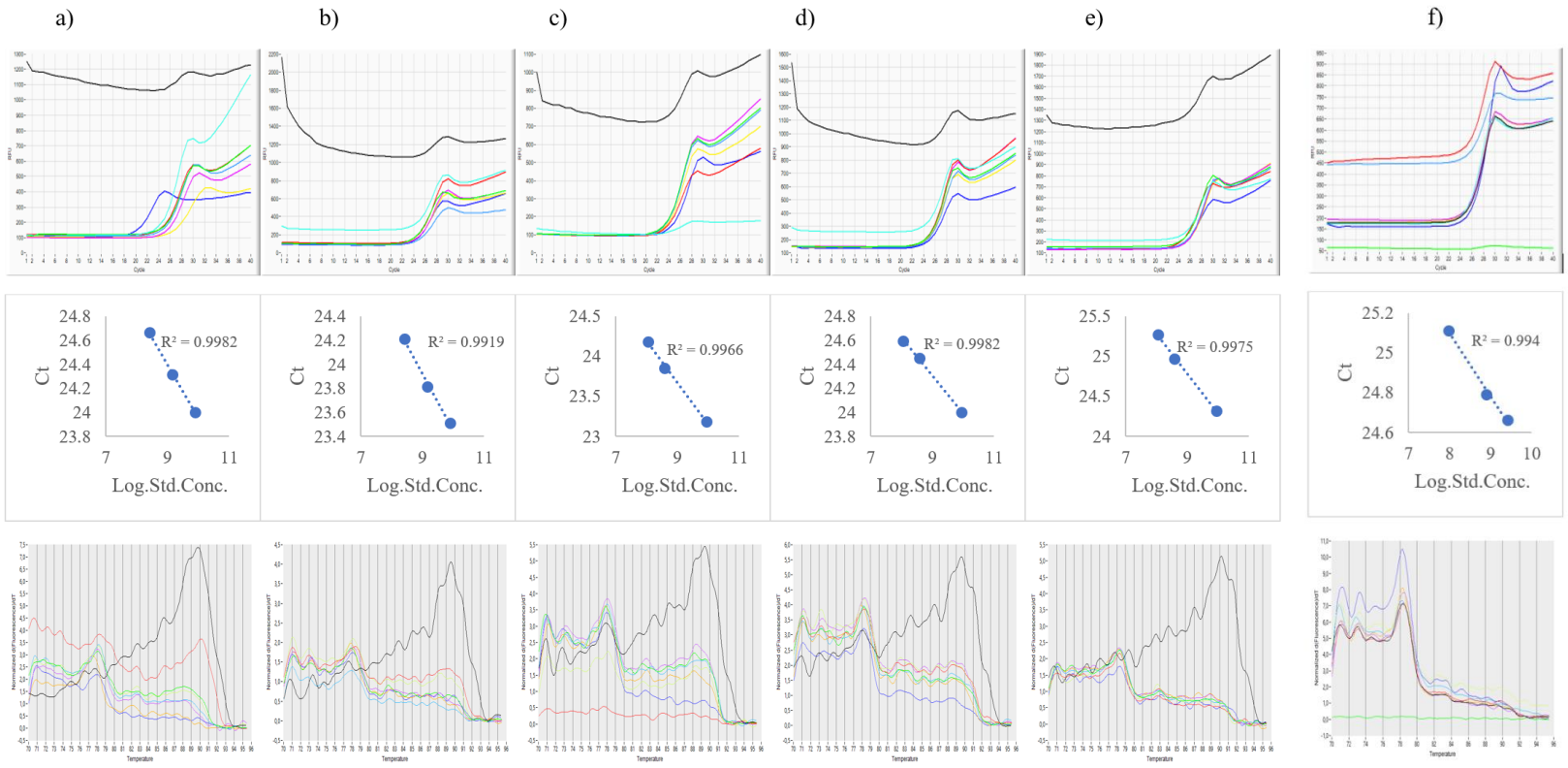

Figure 4.10. Amplification (top), standard (middle) and melting (bottom) curves of the qPCR analyses of *G. intestinalis* in autumn effluents in CAS (a), BNR (b), SBR (c), CoFlUV (d), MBR (e) and CAS sludge (f). Ct, threshold cycle; RFU, reporter signal; Normalized d(Fluorescence)/dT, differential of fluorescence over temperature.

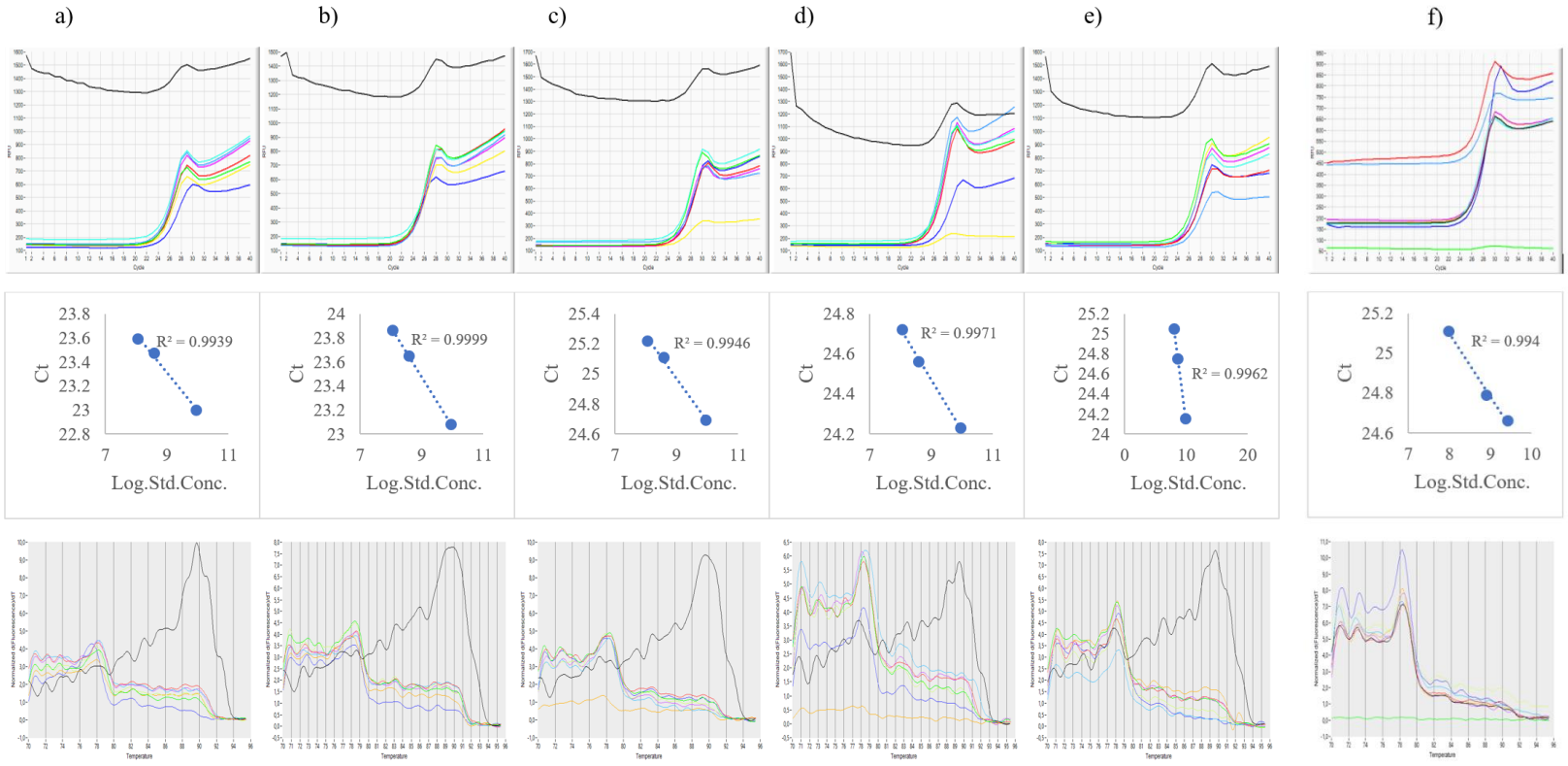

Figure 4.11. Amplification (top), standard (middle) and melting (bottom) curves of the qPCR analyses of *G. intestinalis* in winter effluents in CAS (a), BNR (b), SBR (c), CoFlUV (d), MBR (e) and CAS sludge (f). Ct, threshold cycle; RFU, reporter signal; Normalized d(Fluorescence)/dT, differential of fluorescence over temperature.

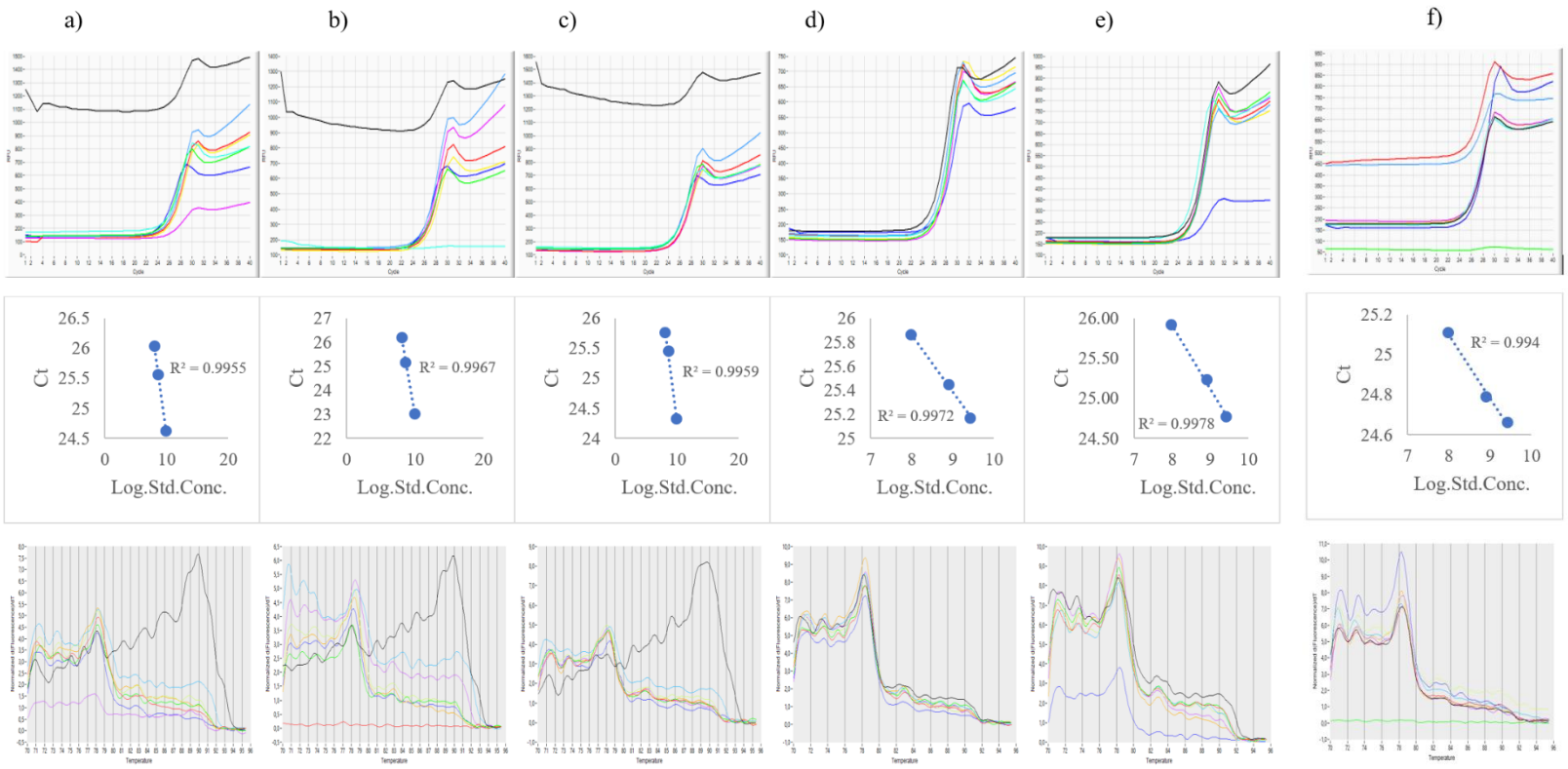

Figure 4.12. Amplification (top), standard (middle) and melting (bottom) curves of the qPCR analyses of *G. intestinalis* in spring effluents in CAS (a), BNR (b), SBR (c), CoFlUV (d), MBR (e) and CAS sludge (f). Ct, threshold cycle; RFU, reporter signal; Normalized d(Fluorescence)/dT, differential of fluorescence over temperature.

4.2.2 Quantitative analyses of *E. histolytica*

After the PCR optimization, standard curve was constructed by using Lambda DNA (Figure 4.13 to Figure 4.20). In all qPCR reactions R^2 values were higher than 0.99. The LOQ for *E. histolytica* was 11.30 log DNA copy number/L. The absolute abundances of *E. histolytica* were calculated by the normalization of DNA copy numbers to the sample volume used to generate the DNA copies per L

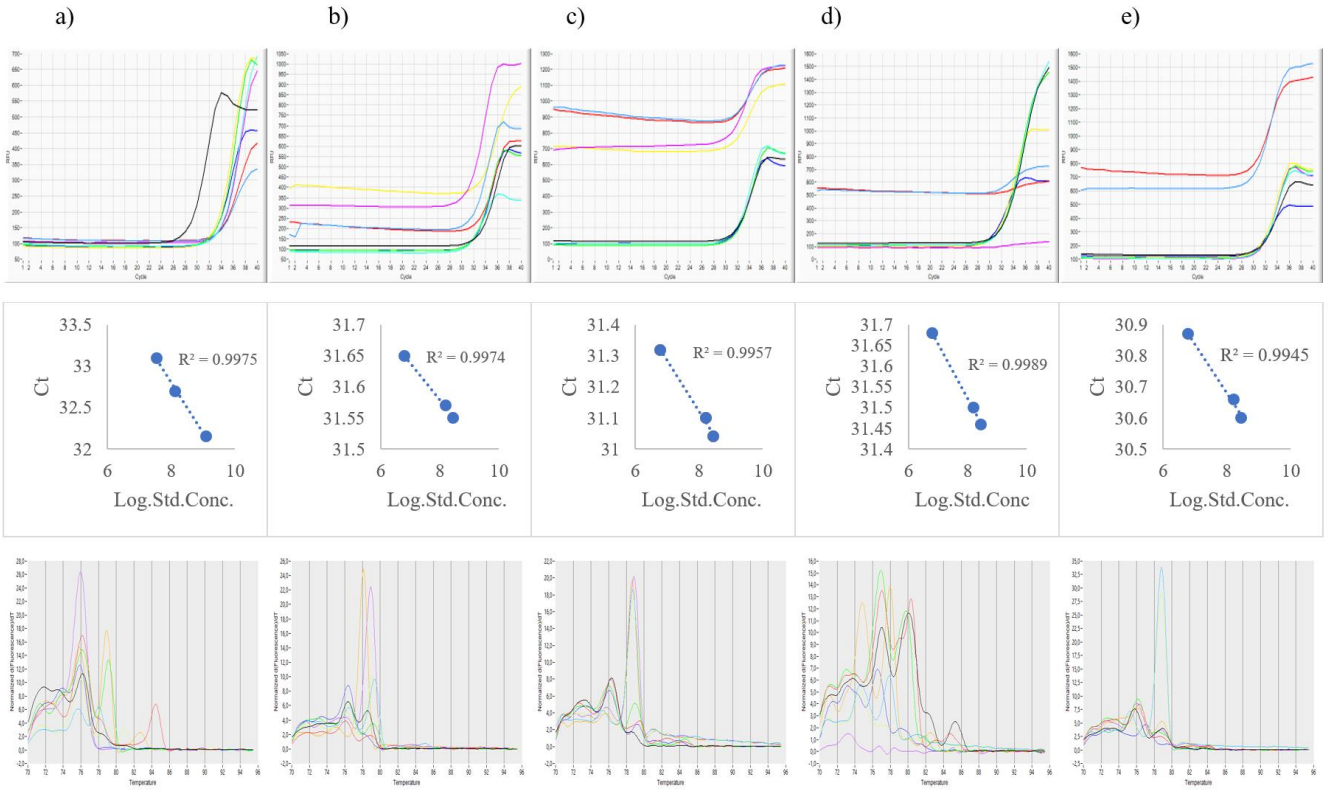

Figure 4.13. Amplification (top), standard (middle) and melting (bottom) curves of the qPCR analyses of *E. histolytica* in summer influents in CAS (a), BNR (b), SBR (c), CoFlUV (d) and MBR (e). Ct, threshold cycle; RFU, reporter signal; Normalized d(Fluorescence)/dT, differential of fluorescence over temperature.

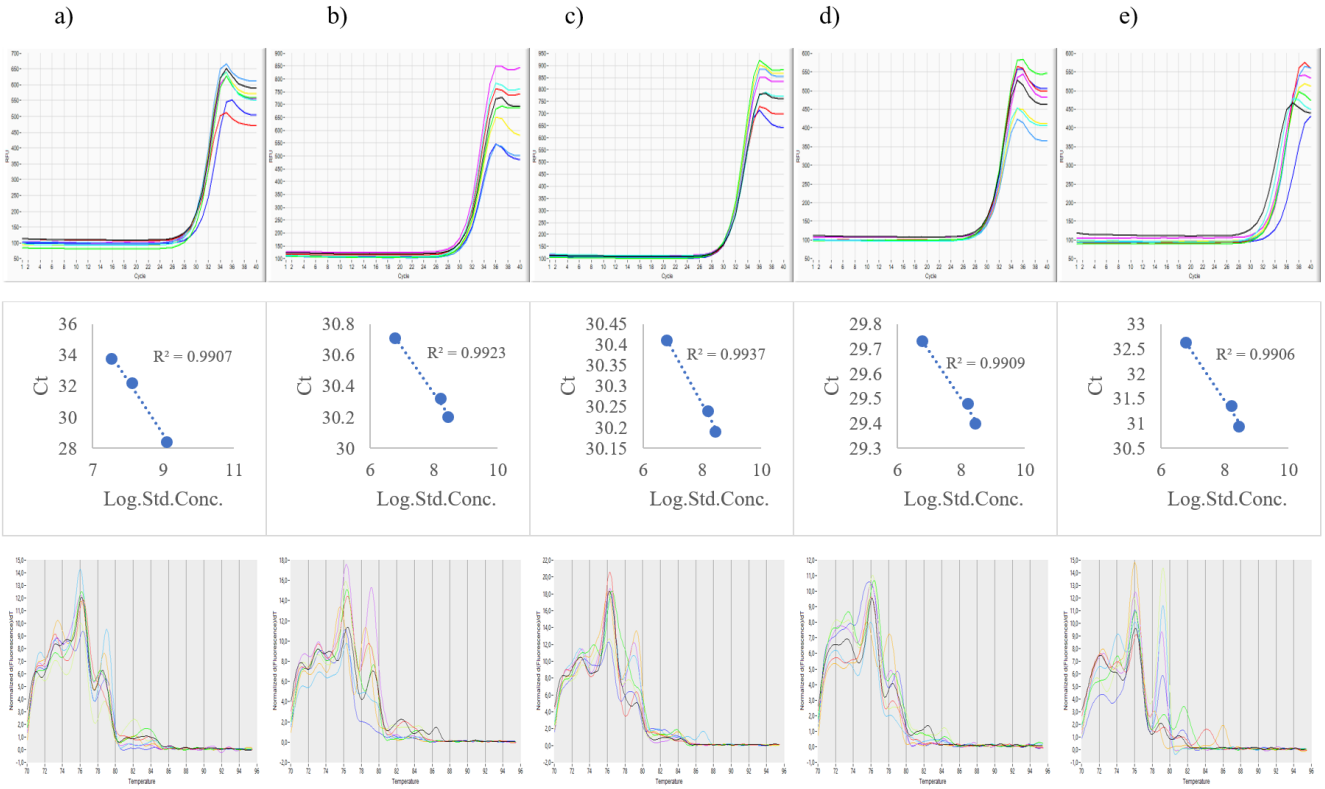

Figure 4.14. Amplification (top), standard (middle) and melting (bottom) curves of the qPCR analyses of *E. histolytica* in autumn influents in CAS (a), BNR (b), SBR (c), CoFlUV (d) and MBR (e). Ct, threshold cycle; RFU, reporter signal; Normalized d(Fluorescence)/dT, differential of fluorescence over temperature.

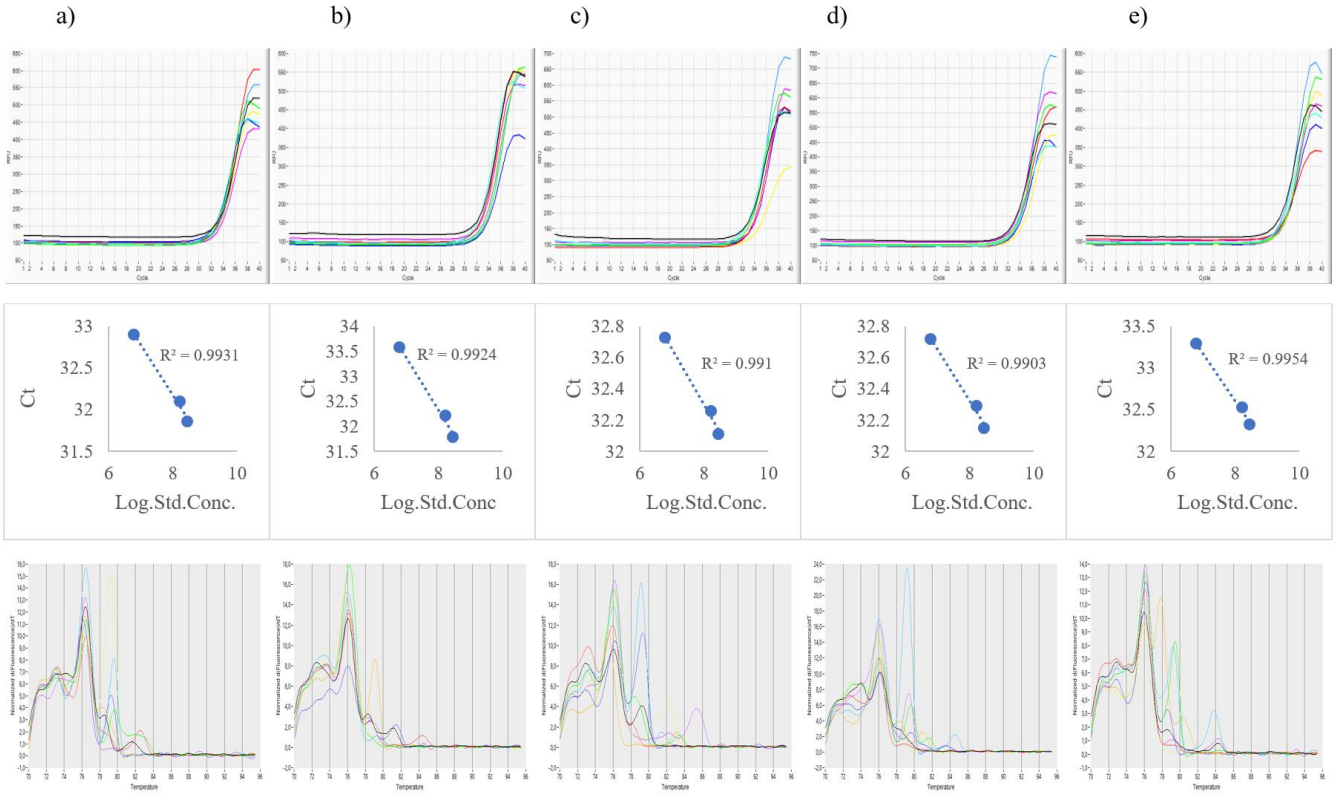

Figure 4.15. Amplification (top), standard (middle) and melting (bottom) curves of the qPCR analyses of *E. histolytica* in winter influents CAS (a), BNR (b), SBR (c), CoFlUV (d) and MBR (e). Ct, threshold cycle; RFU, reporter signal; Normalized d(Fluorescence)/dT, differential of fluorescence over temperature.

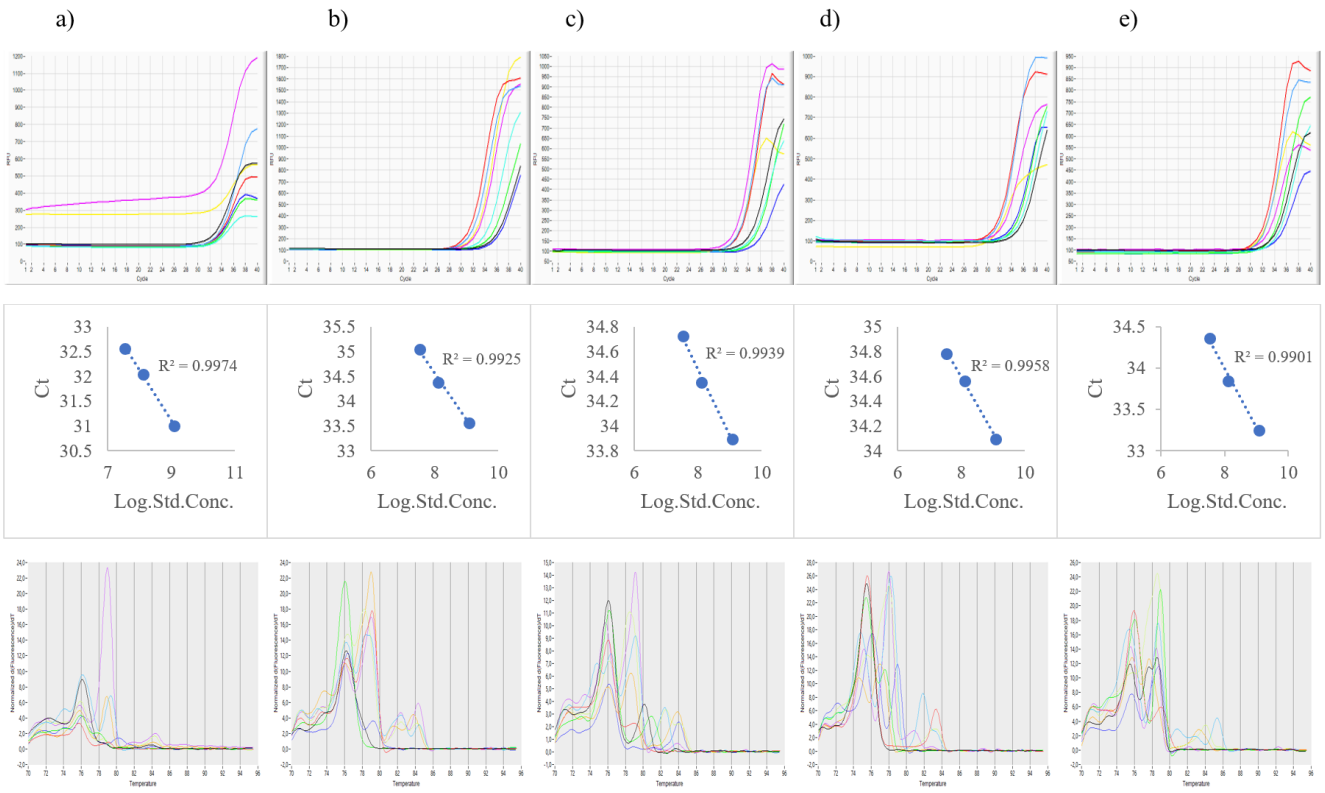

Figure 4.16. Amplification (top), standard (middle) and melting (bottom) curves of the qPCR analyses of *E. histolytica* in spring influents in CAS (a), BNR (b), SBR (c), CoFlUV (d) and MBR (e). Ct, threshold cycle; RFU, reporter signal; Normalized d(Fluorescence)/dT, differential of fluorescence over temperature.

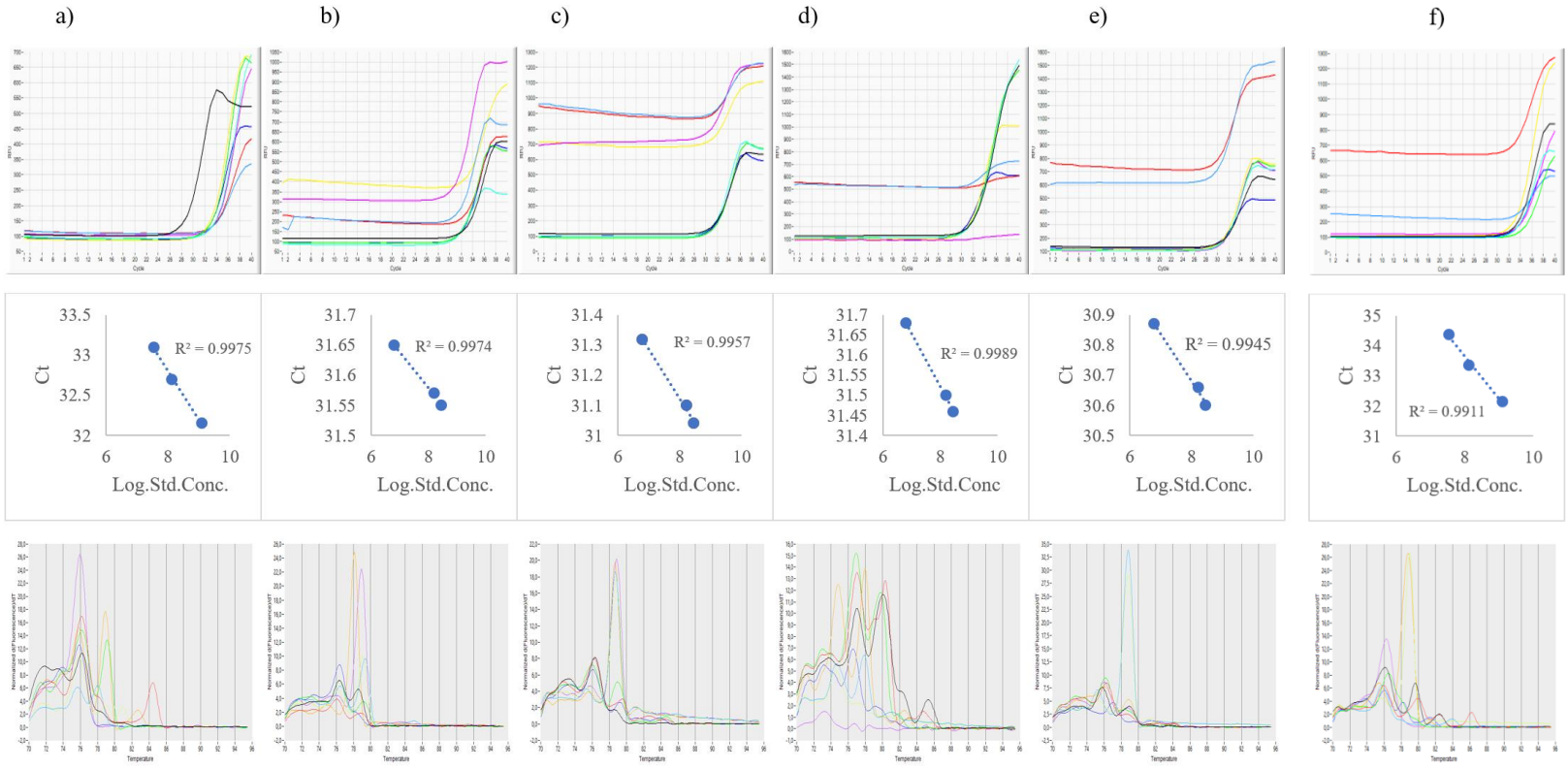

Figure 4.17. Amplification (top), standard (middle) and melting (bottom) curves of the qPCR analyses of *E. histolytica* in summer effluents in CAS (a), BNR (b), SBR (c), CoFlUV (d), MBR (e) and CAS sludge (f). Ct, threshold cycle; RFU, reporter signal; Normalized d(Fluorescence)/dT, differential of fluorescence over temperature.

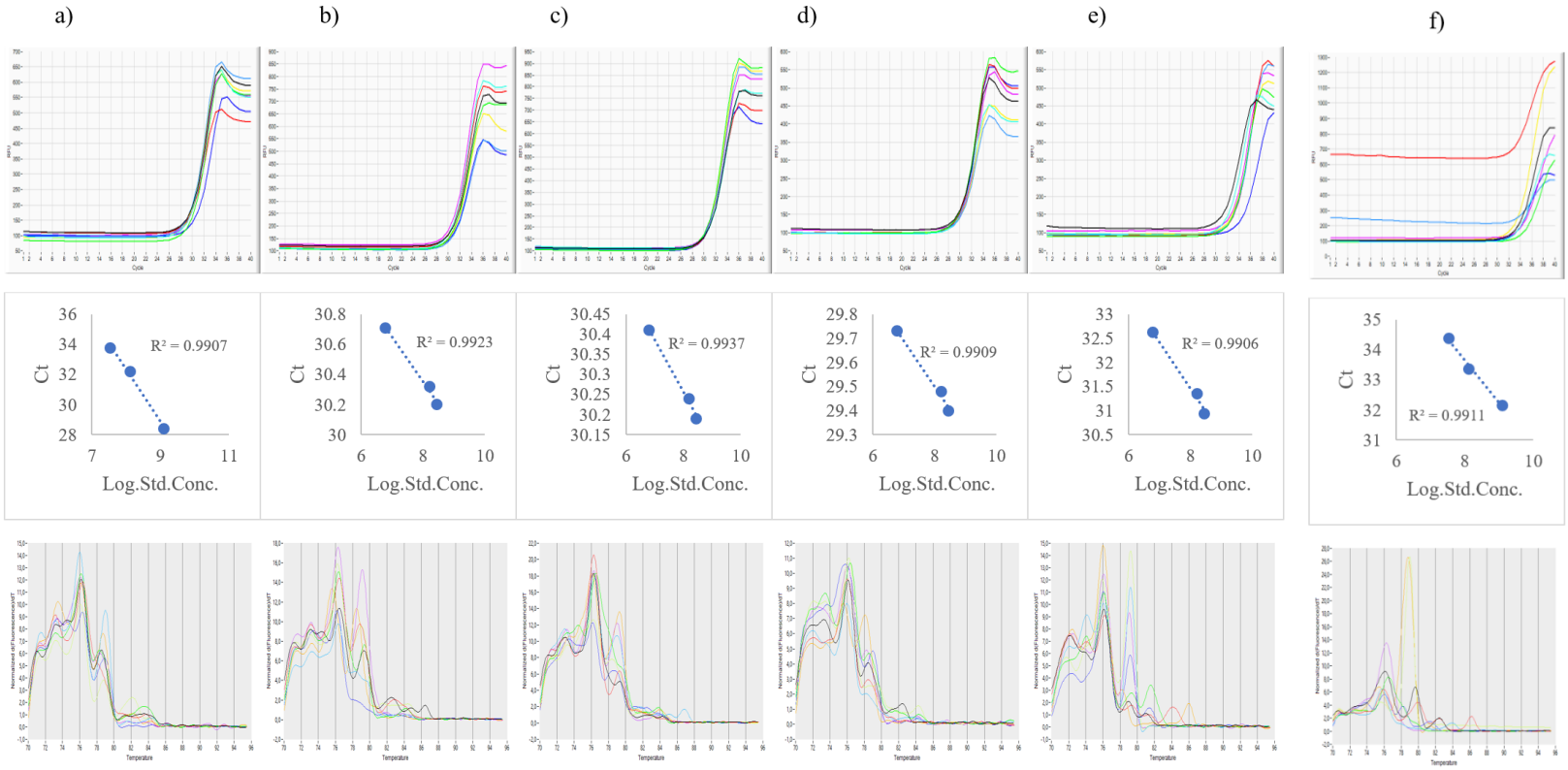

Figure 4.18. Amplification (top), standard (middle) and melting (bottom) curves of the qPCR analyses of *E. histolytica* in autumn effluents in CAS (a), BNR (b), SBR (c), CoFlUV (d), MBR (e) and CAS sludge (f). Ct, threshold cycle; RFU, reporter signal; Normalized d(Fluorescence)/dT, differential of fluorescence over temperature.

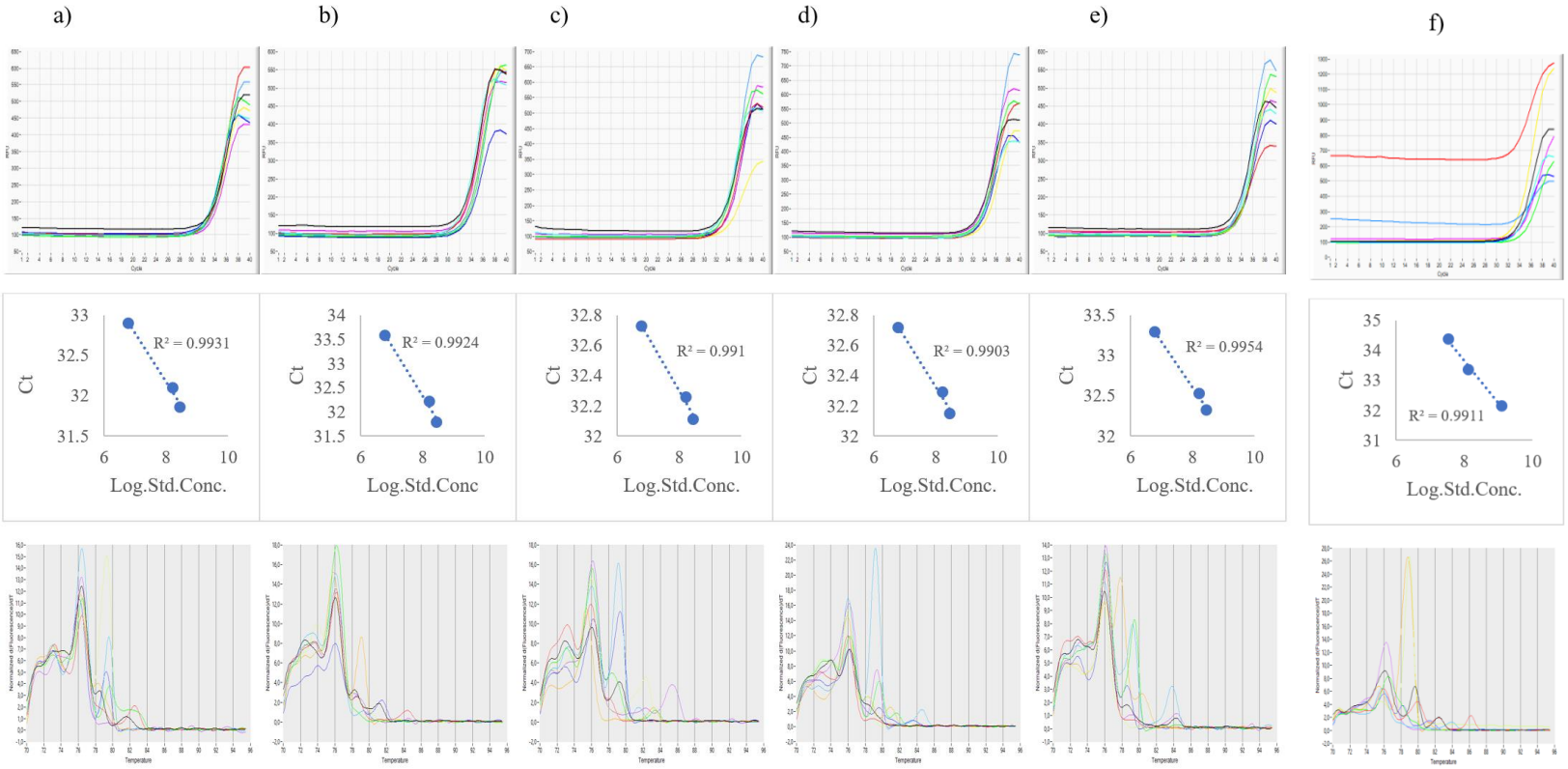

Figure 4.19. Amplification (top), standard (middle) and melting (bottom) curves of the qPCR analyses of *E. histolytica* in winter effluents in CAS (a), BNR (b), SBR (c), CoFlUV (d), MBR (e) and CAS sludge case (f). Ct, threshold cycle; RFU, reporter signal; Normalized d(Fluorescence)/dT, differential of fluorescence over temperature.

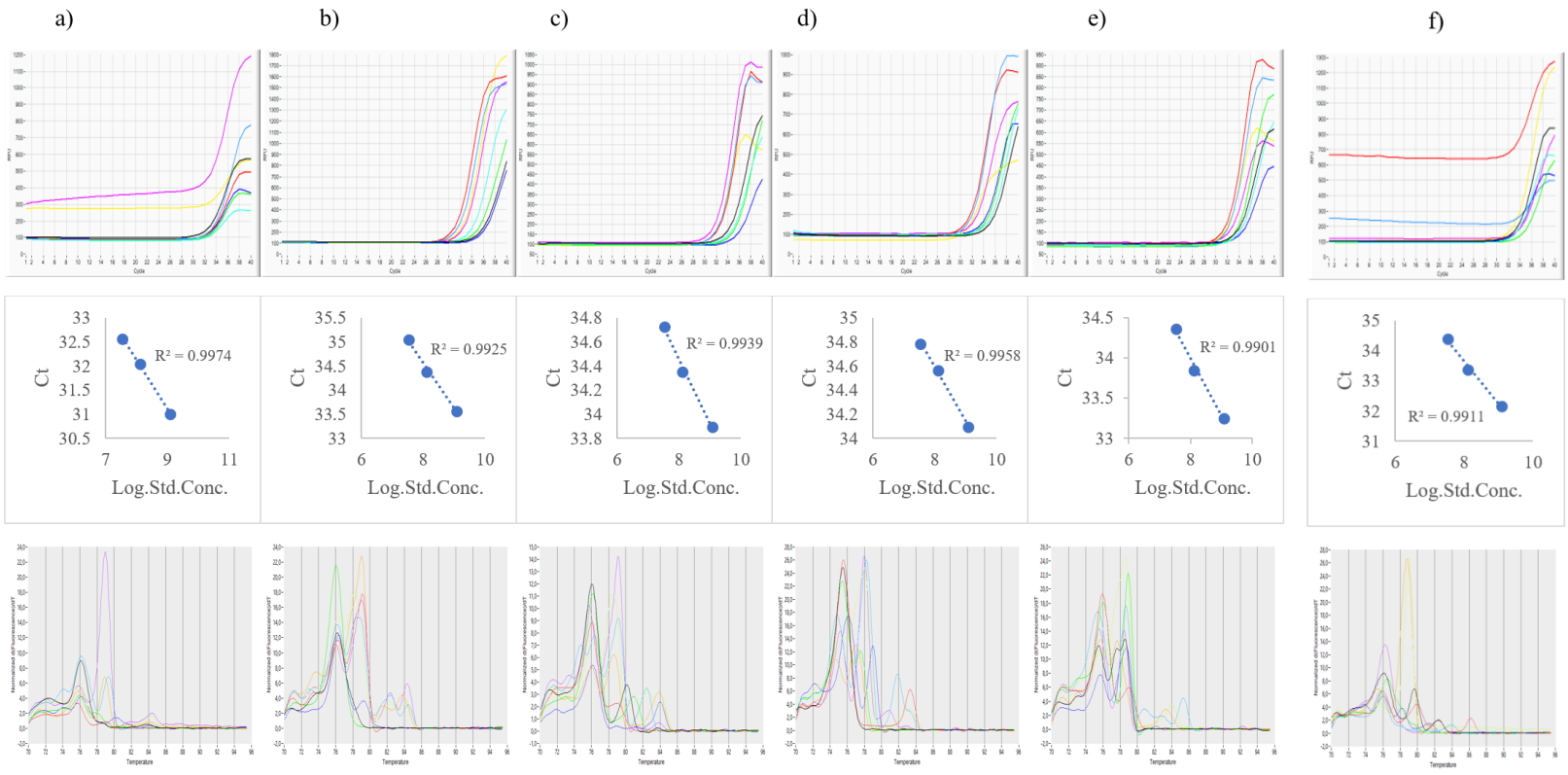

Figure 4.20. Amplification (top), standard (middle) and melting (bottom) curves of the qPCR analyses of *E. histolytica* in spring effluents in CAS (a), BNR (b), SBR (c), OSB (d), MBR (e) and CAS sludge (f). Ct, threshold cycle; RFU, reporter signal; Normalized d(Fluorescence)/dT, differential of fluorescence over temperature.

4.2.3 Quantitative analyses of *B. hominis*

After the PCR optimization, standard curve was constructed by using Lambda DNA (Figure 4.21 to Figure 4.28). In all qPCR reactions R^2 values were higher than 0.99. The LOQ for *B. hominis* was 10.94 log DNA copy number/L. The absolute abundances of *B. hominis* were calculated by the normalization of DNA copy numbers to the sample volume used to generate the DNA copies per L.

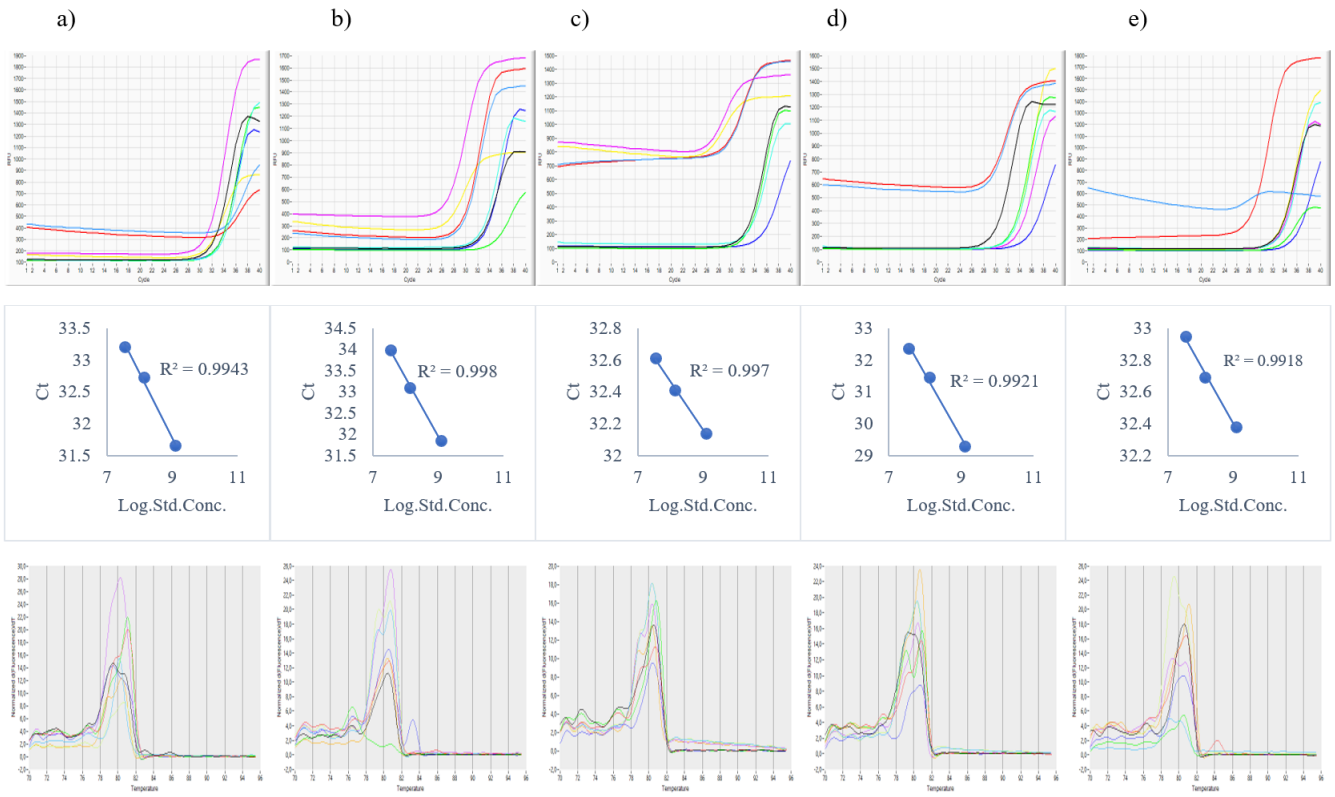

Figure 4.21. Amplification (top), standard (middle) and melting (bottom) curves of the qPCR analyses of *B. hominis* in summer influents in CAS (a), BNR (b), SBR (c), CoFlUV (d) and MBR (e). Ct, threshold cycle; RFU, reporter signal; Normalized d(Fluorescence)/dT, differential of fluorescence over temperature.

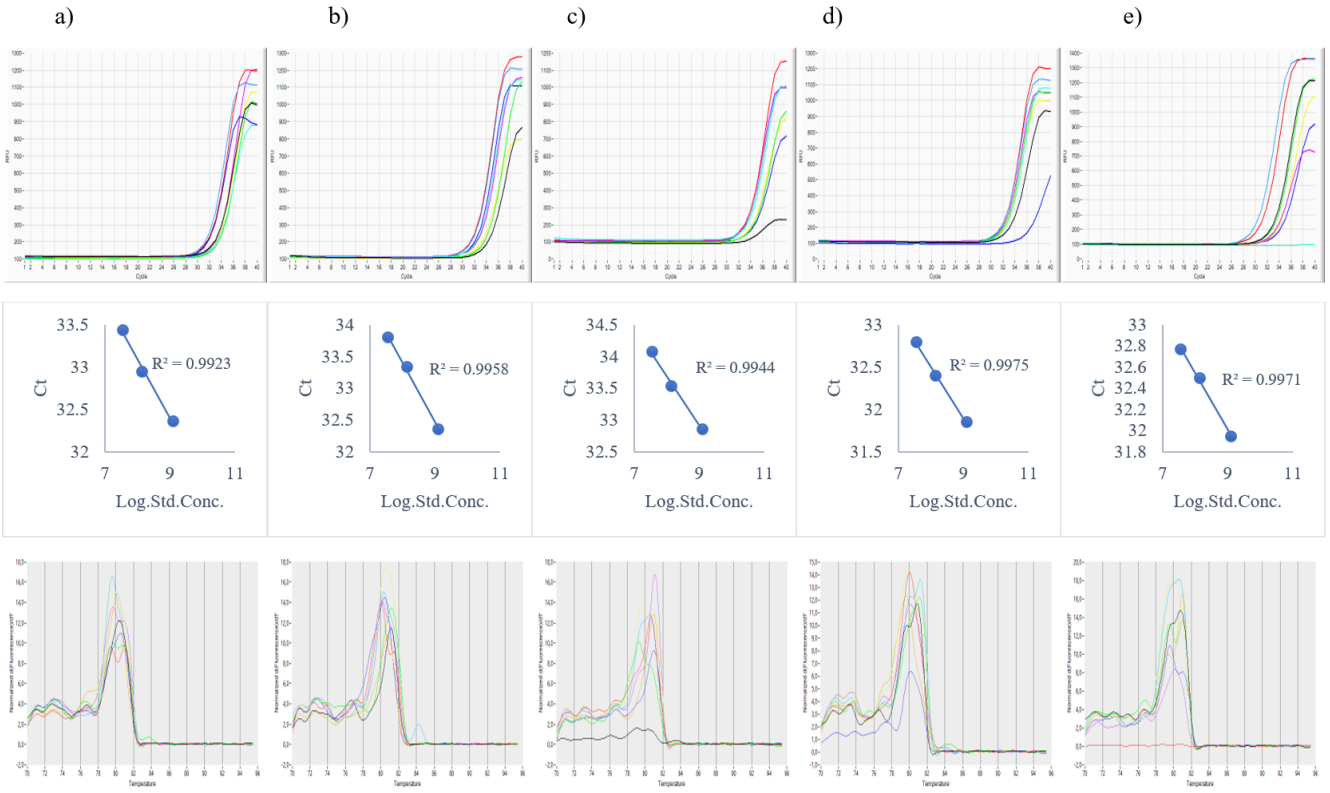

Figure 4.22. Amplification (top), standard (middle) and melting (bottom) curves of the qPCR analyses of *B. hominis* in autumn influents in CAS (a), BNR (b), SBR (c), CoFlUV (d) and MBR (e). Ct, threshold cycle; RFU, reporter signal; Normalized d(Fluorescence)/dT, differential of fluorescence over temperature.

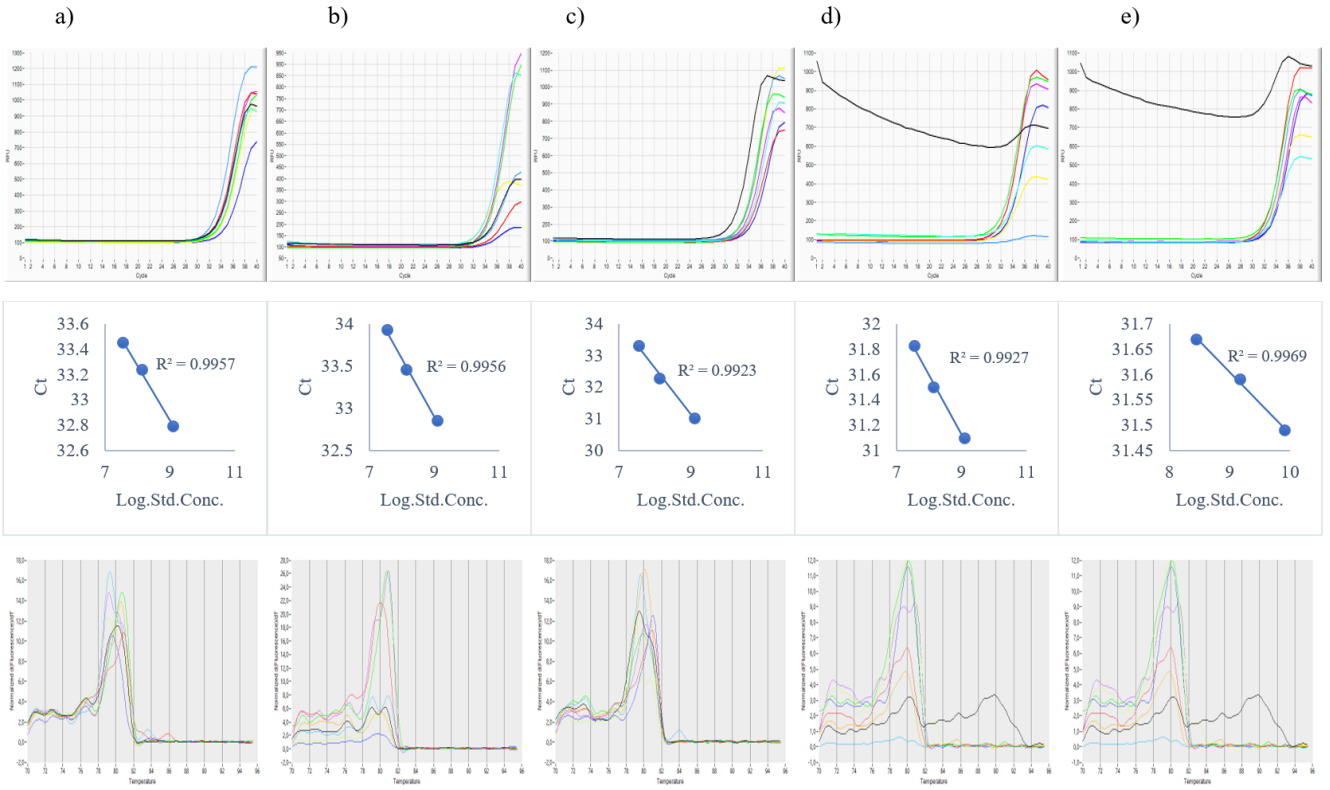

Figure 4.23. Amplification (top), standard (middle) and melting (bottom) curves of the qPCR analyses of *B. hominis* in winter influents in CAS (a), BNR (b), SBR (c), CoFlUV (d) and MBR (e). Ct, threshold cycle; RFU, reporter signal; Normalized d(Fluorescence)/dT, differential of fluorescence over temperature.

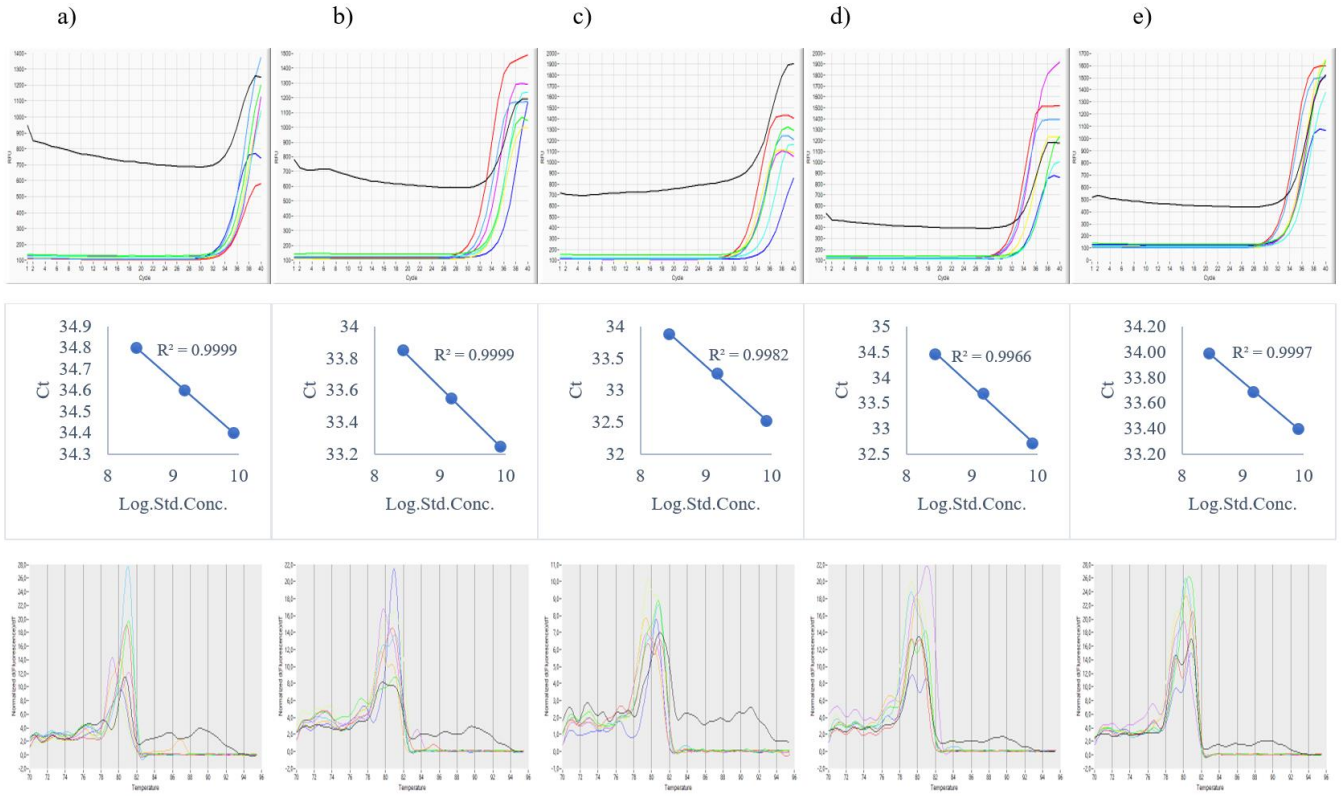

Figure 4.24. Amplification (top), standard (middle) and melting (bottom) curves of the qPCR analyses of *B. hominis* in spring influents in CAS (a), BNR (b), SBR (c), CoFlUV (d) and MBR (e). Ct, threshold cycle; RFU, reporter signal; Normalized d(Fluorescence)/dT, differential of fluorescence over temperature.

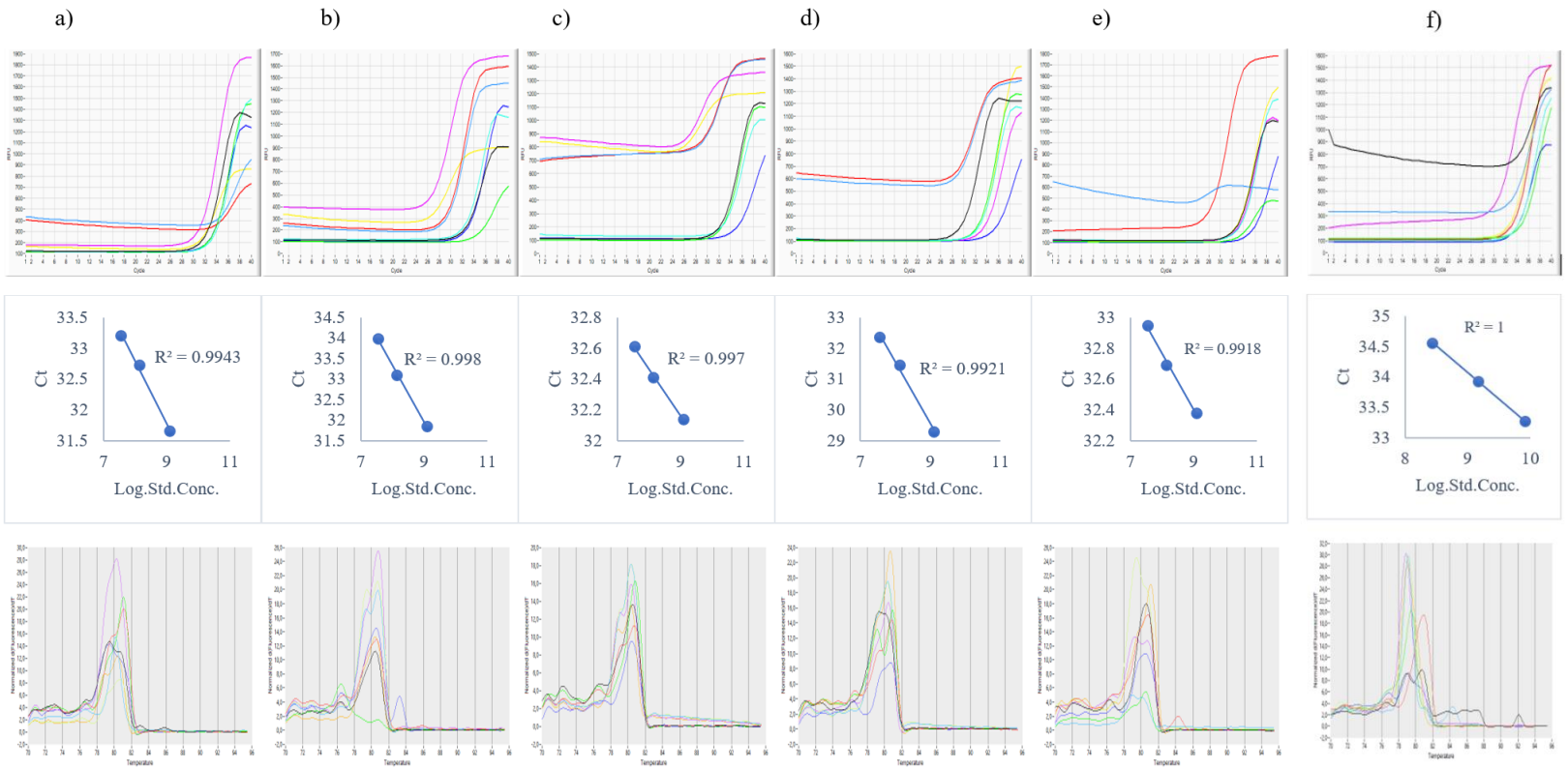

Figure 4.25. Amplification (top), standard (middle) and melting (bottom) curves of the qPCR analyses of *B. hominis* in summer effluents in CAS (a), BNR (b), SBR (c), CoFlUV (d), MBR (e) and CAS sludge (f). Ct, threshold cycle; RFU, reporter signal; Normalized d(Fluorescence)/dT, differential of fluorescence over temperature.

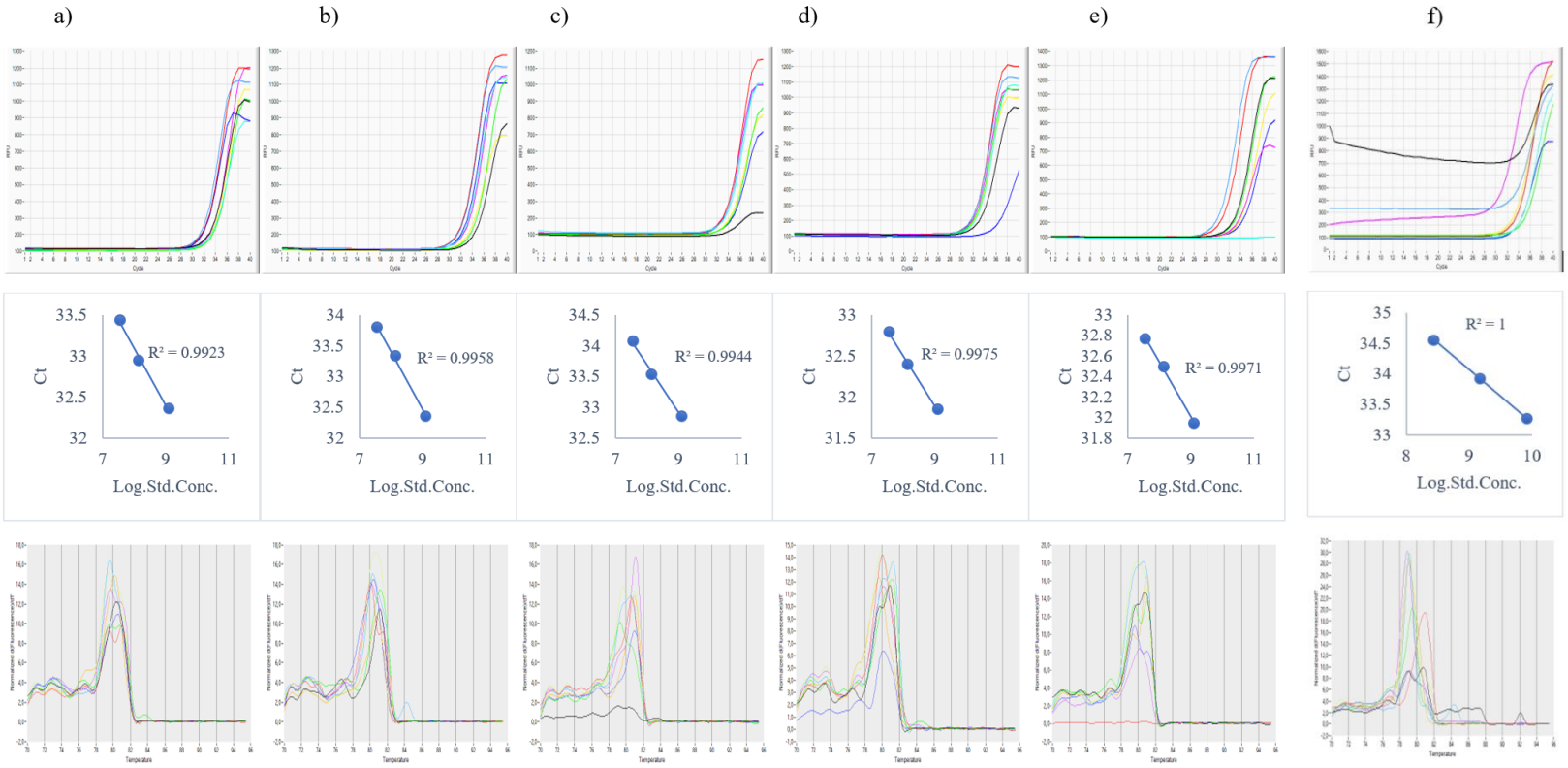

Figure 4.26. Amplification (top), standard (middle) and melting (bottom) curves of the qPCR analyses of *B. hominis* in autumn effluents in CAS (a), BNR (b), SBR (c), CoFlUV (d), MBR (e) and CAS sludge (f). Ct, threshold cycle; RFU, reporter signal; Normalized d(Fluorescence)/dT, differential of fluorescence over temperature.

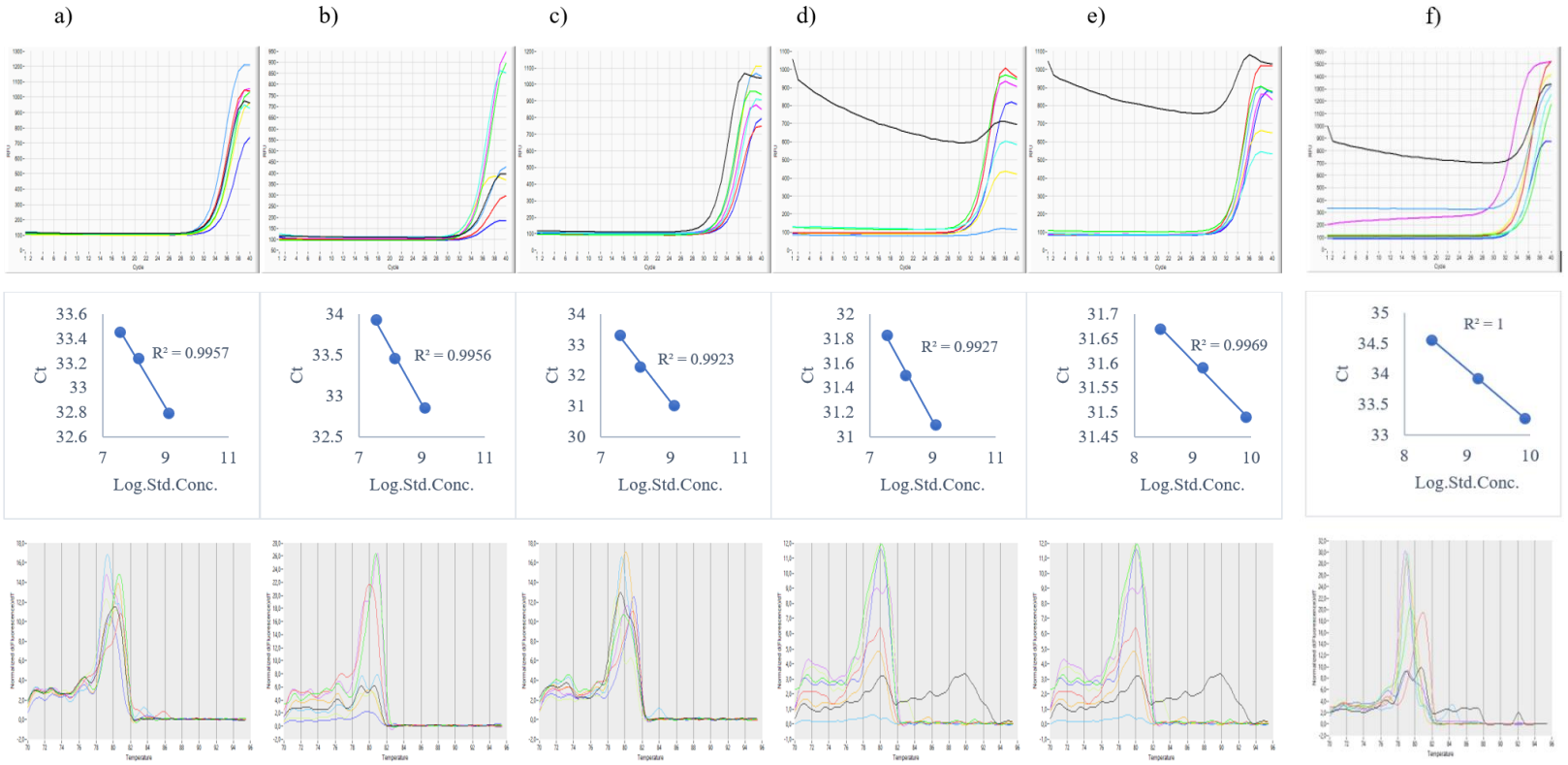

Figure 4.27. Amplification (top), standard (middle) and melting (bottom) curves of the qPCR analyses of *B. hominis* in winter effluents in CAS (a), BNR (b), SBR (c), CoFlUV (d), MBR (e) and CAS sludge (f). Ct, threshold cycle; RFU, reporter signal; Normalized d(Fluorescence)/dT, differential of fluorescence over temperature.

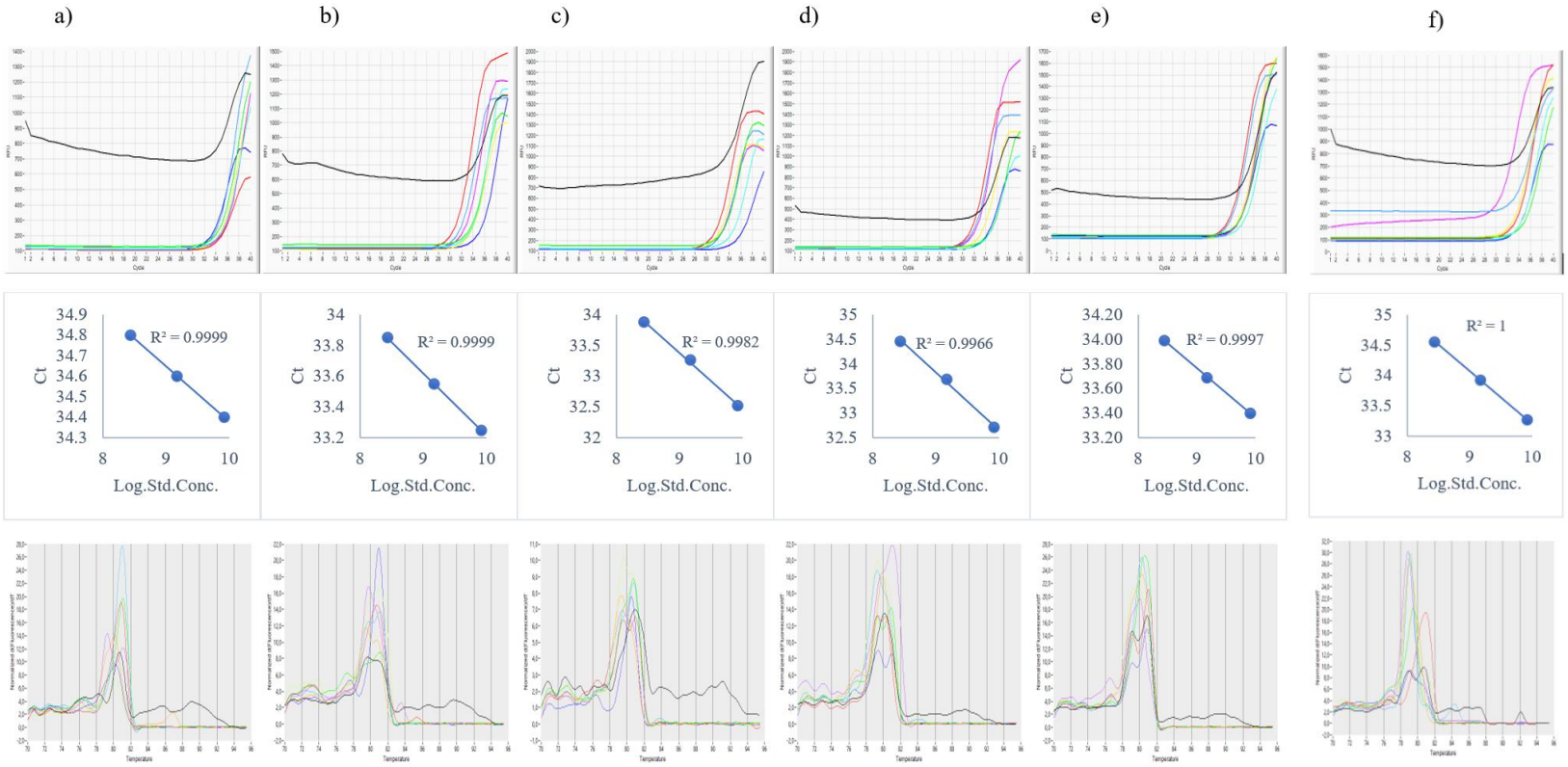

Figure 4.28. Amplification (top), standard (middle) and melting (bottom) curves of the qPCR analyses of *B. hominis* in spring effluents in CAS (a), BNR (b), SBR (c), CoFlUV (d), MBR (e) and CAS sludge (f). Ct, threshold cycle; RFU, reporter signal; Normalized d(Fluorescence)/dT, differential of fluorescence over temperature.

4.2.4 Quantitative analyses of *C. parvum*

After the PCR optimization, standard curve was constructed by using Lambda DNA (Figure 4.29 to Figure 4.36). In all qPCR reactions R^2 values were higher than 0.99. The LOQ for *C. parvum* was 10.91 log DNA copy number/L. The absolute abundances of *C. parvum* were calculated by the normalization of DNA copy numbers to the sample volume used to generate the DNA copies per L.

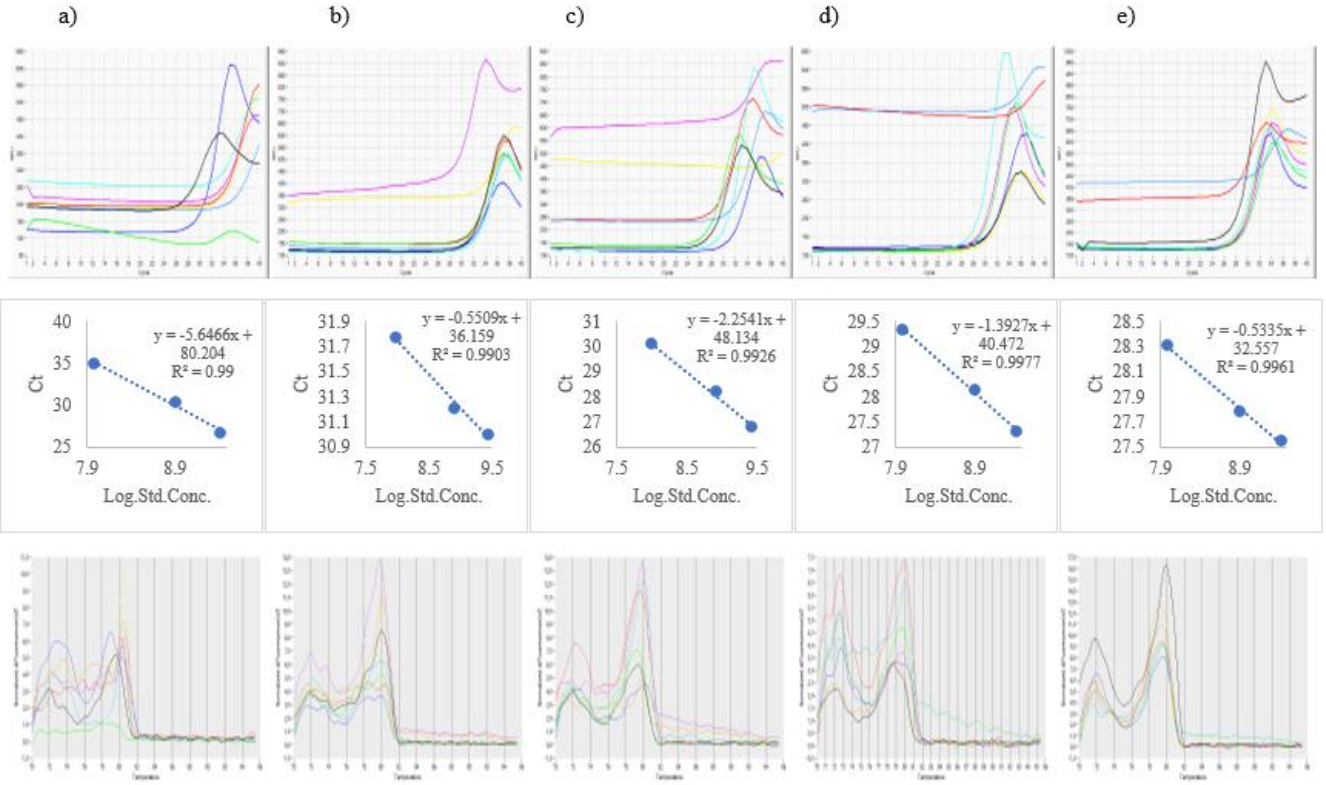

Figure 4.29. Amplification (top), standard (middle) and melting (bottom) curves of the qPCR analyses of C. parvum in summer influents in CAS (a), BNR (b), SBR (c), CoFlUV (d) and MBR (e). Ct, threshold cycle; RFU, reporter signal; Normalized d(Fluorescence)/dT, differential of fluorescence over temperature.

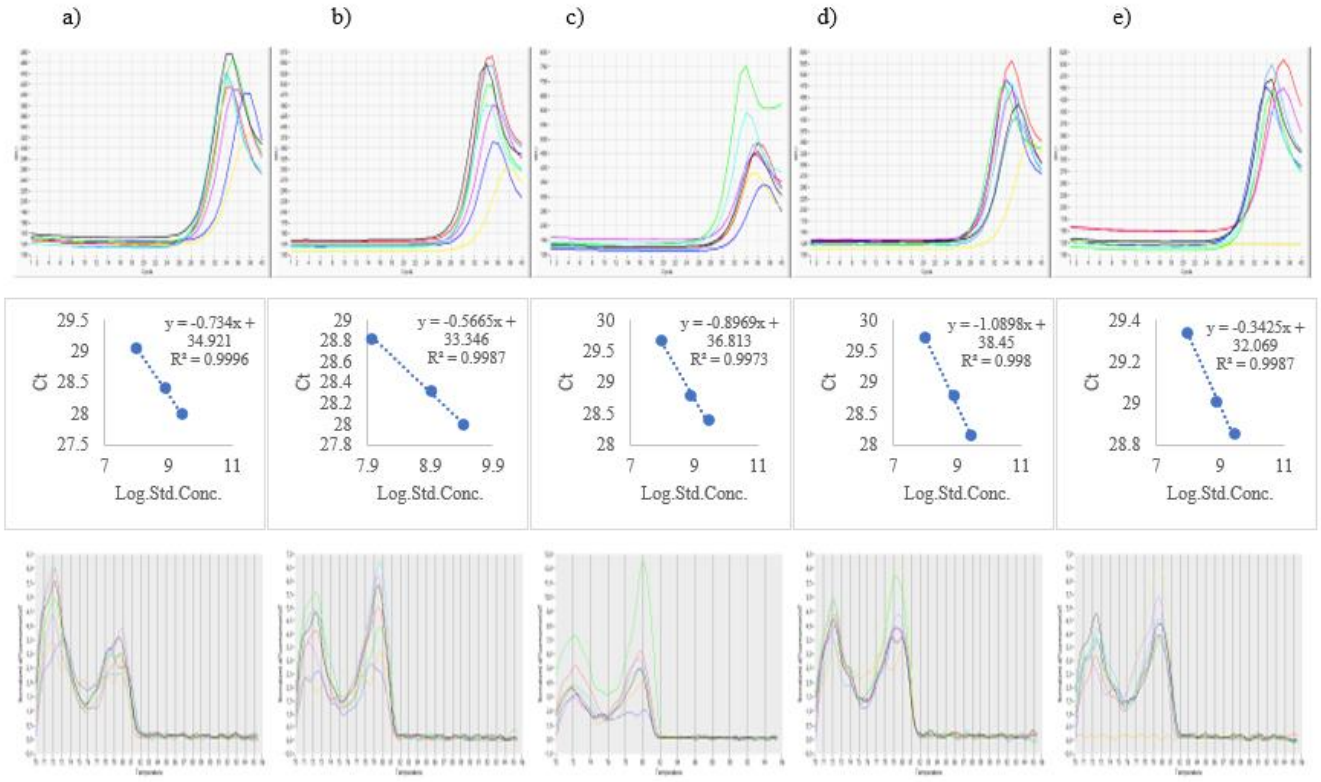

Figure 4.30. Amplification (top), standard (middle) and melting (bottom) curves of the qPCR analyses of *C. parvum* in autumn influents in CAS (a), BNR (b), SBR (c), CoFlUV (d) and MBR (e). Ct, threshold cycle; RFU, reporter signal; Normalized d(Fluorescence)/dT, differential of fluorescence over temperature.

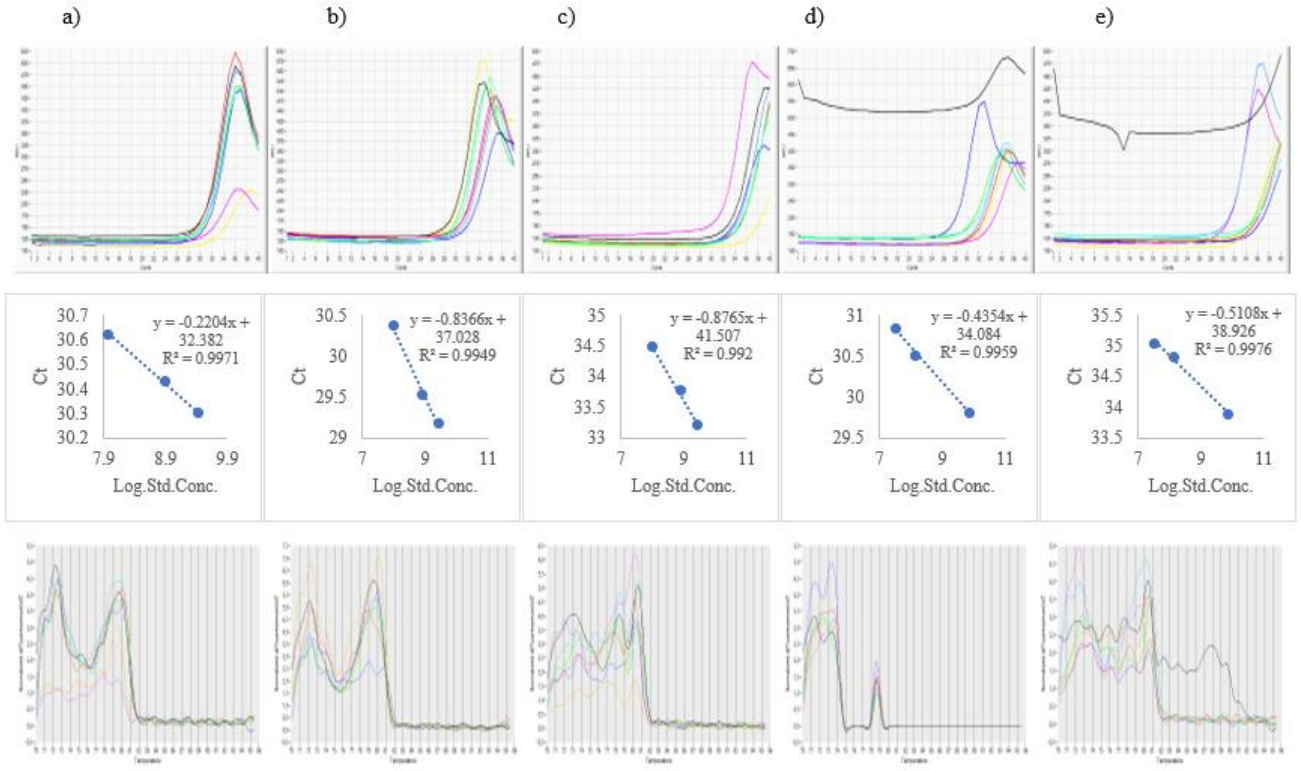

Figure 4.31. Amplification (top), standard (middle) and melting (bottom) curves of the qPCR analyses of *C. parvum* in winter influents in CAS (a), BNR (b), SBR (c), CoFlUV (d) and MBR (e). Ct, threshold cycle; RFU, reporter signal; Normalized d(Fluorescence)/dT, differential of fluorescence over temperature

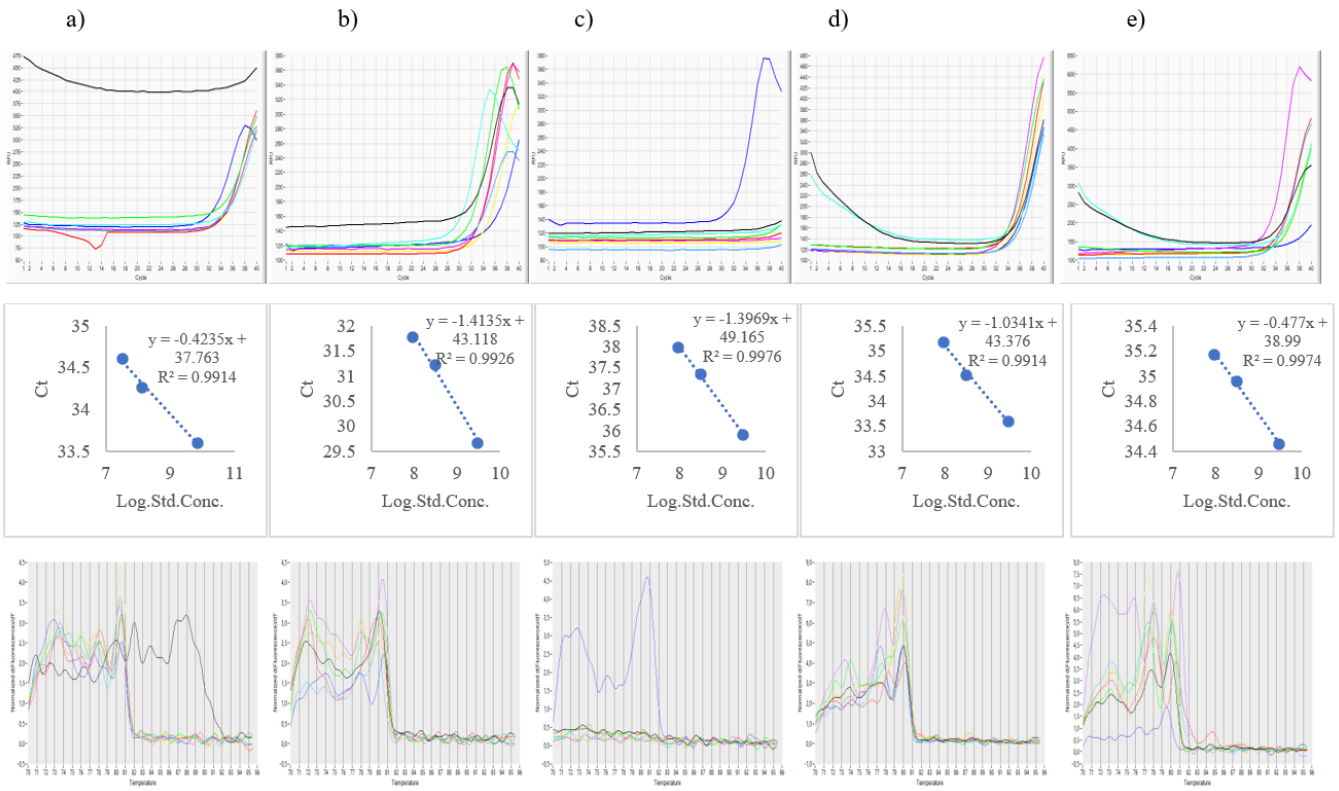

Figure 4.32. Amplification (top), standard (middle) and melting (bottom) curves of the qPCR analyses of *C. parvum* in spring influents in CAS (a), BNR (b), SBR (c), CoFlUV (d) and MBR (e). Ct, threshold cycle; RFU, reporter signal; Normalized d(Fluorescence)/dT, differential of fluorescence over temperature.

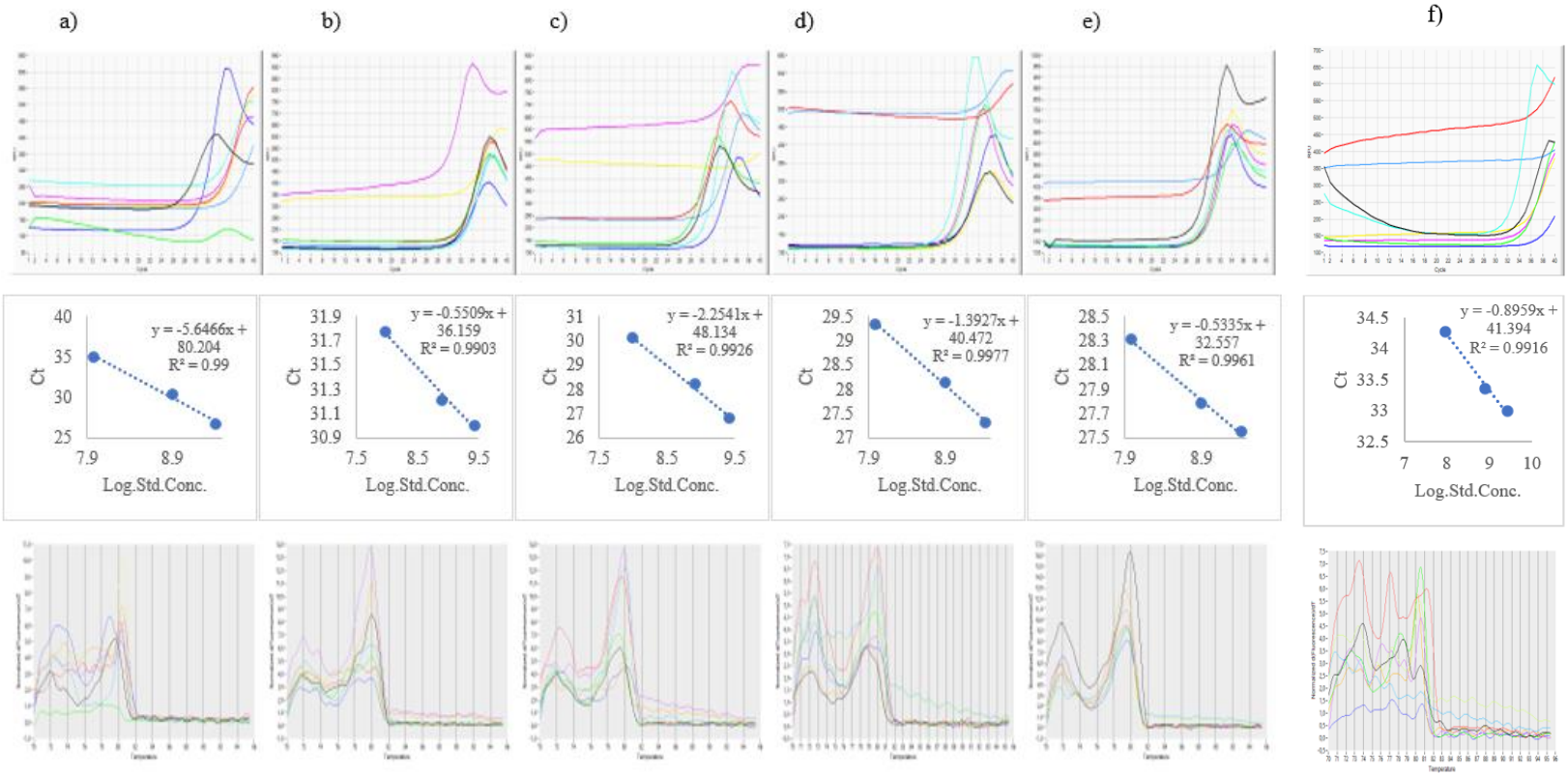

Figure 4.33. Amplification (top), standard (middle) and melting (bottom) curves of the qPCR analyses of *C. parvum* in summer effluents in CAS (a), BNR (b), SBR (c), CoFlUV (d) and MBR (e). Ct, threshold cycle; RFU, reporter signal; Normalized d(Fluorescence)/dT, differential of fluorescence over temperature.

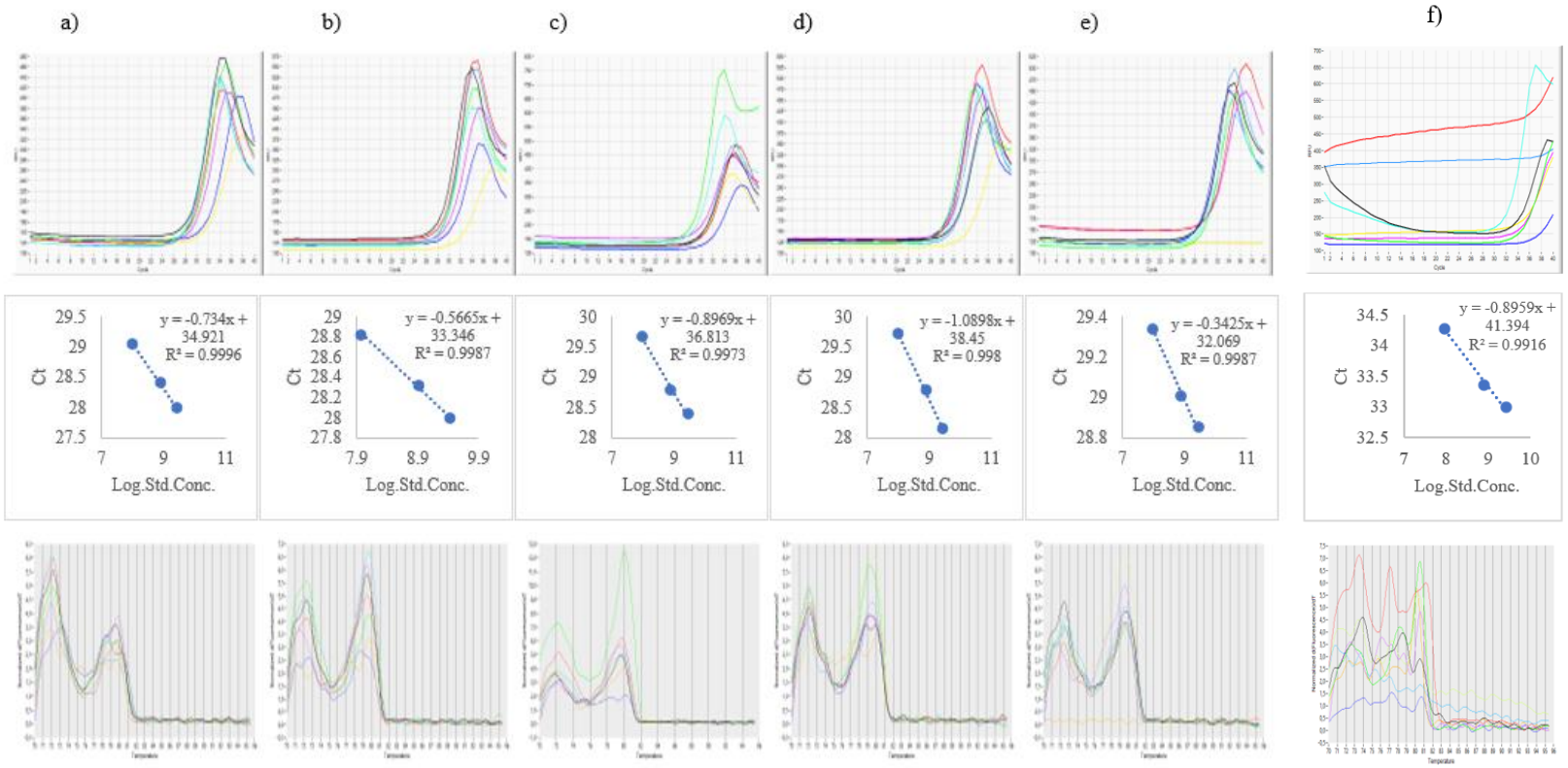

Figure 4.34. Amplification (top), standard (middle) and melting (bottom) curves of the qPCR analyses of *C. parvum* in autumn effluents in CAS (a), BNR (b), SBR (c), CoFlUV (d) and MBR (e). Ct, threshold cycle; RFU, reporter signal; Normalized d(Fluorescence)/dT, differential of fluorescence over temperature.

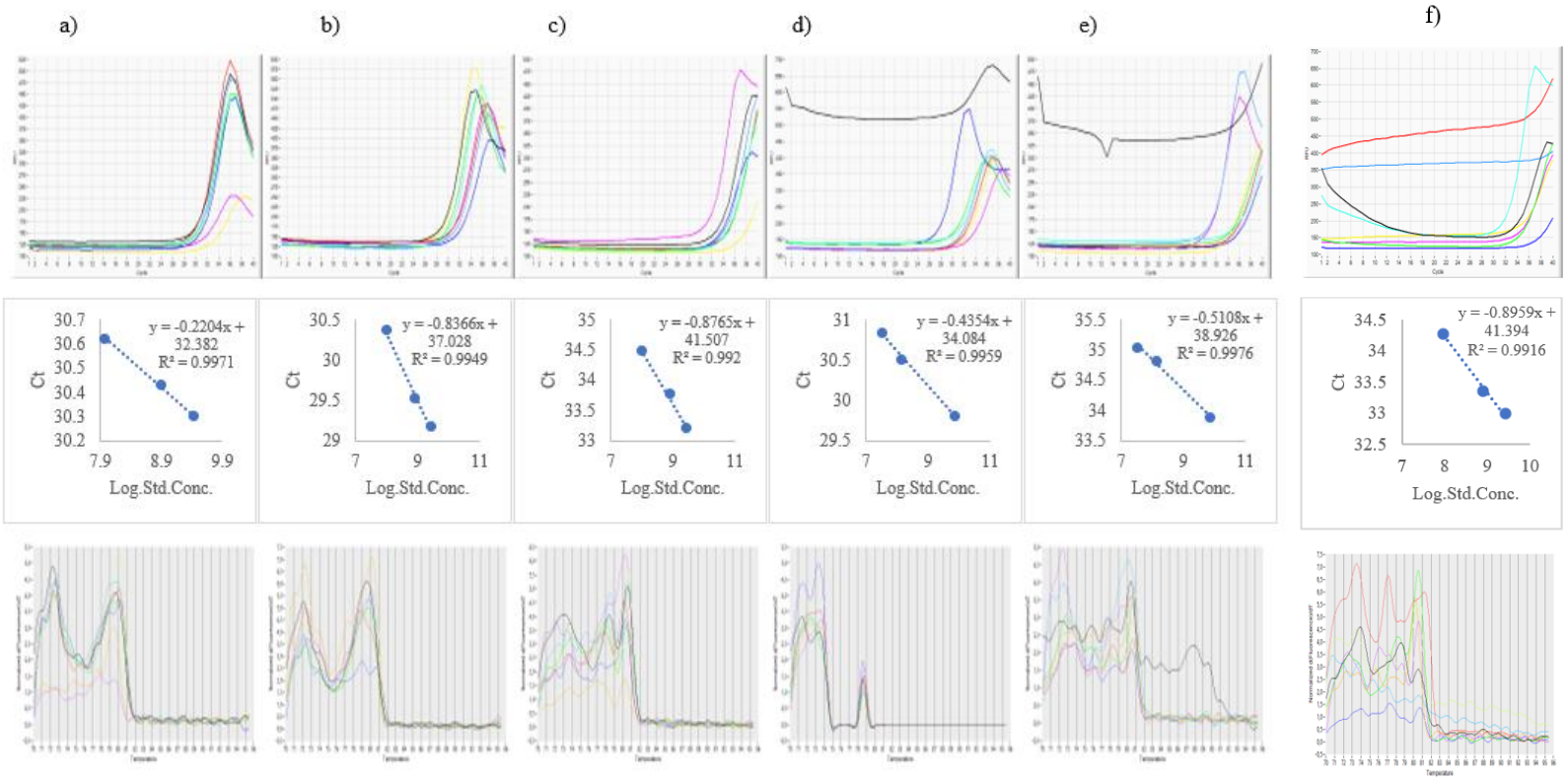

Figure 4.35. Amplification (top), standard (middle) and melting (bottom) curves of the qPCR analyses of *C. parvum* in winter effluents in CAS (a), BNR (b), SBR (c), CoFlUV (d) and MBR (e). Ct, threshold cycle; RFU, reporter signal; Normalized d(Fluorescence)/dT, differential of fluorescence over temperature

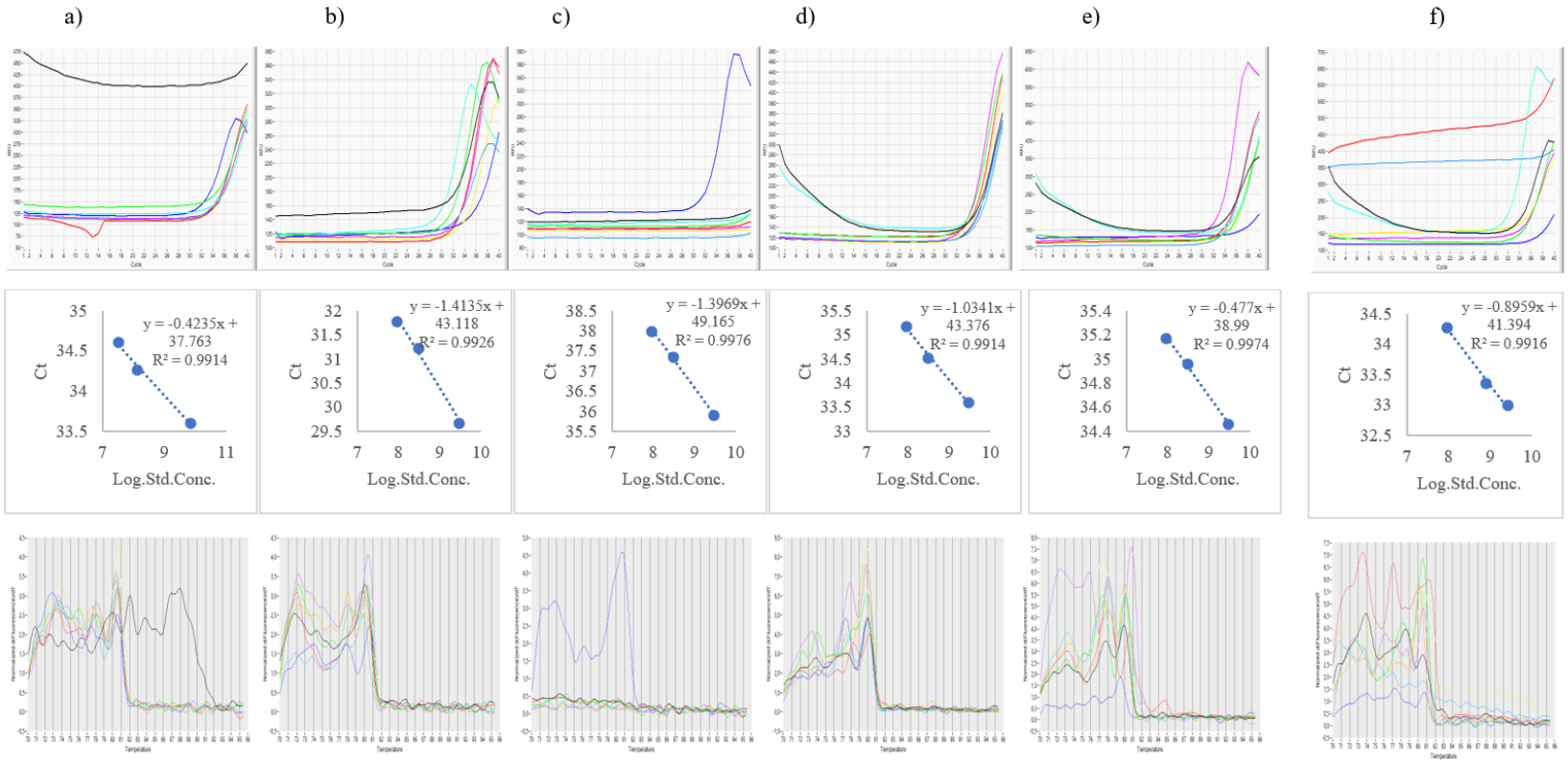

Figure 4.36. Amplification (top), standard (middle) and melting (bottom) curves of the qPCR analyses of C. parvum in winter effluents in CAS (a), BNR (b), SBR (c), CoFlUV (d) and MBR (e). Ct, threshold cycle; RFU, reporter signal; Normalized d(Fluorescence)/dT, differential of fluorescence over temperature

4.3 Parasitic protozoa removal capacities of WWTPs

WWTPs' removal capacities for four parasitic protozoa were determined by the qPCR analyses. Raw data obtained from the qPCR analyses are given in Appendix A. Statistical analyses for the seasonal variations in the removal capacities of WWTPs for four protozoan parasites are given in Appendix B.

4.3.1 in CAS

Figure 4.37 shows the schematic diagram of the CAS system sampled in the study. This system is made up of preliminary, primary, and secondary treatment stages. Preliminary treatment includes screening and an aerated grit chamber to remove the coarse solids and large particles. In the primary treatment stage, a primary sedimentation tank is used to remove the settleable organics and inorganics. Additionally, heavy metals and a fraction of the organic nitrogen and phosphorus may also be removed in primary treatment. Secondary treatment consists of aeration tanks and secondary sedimentation tanks. In this stage of the treatment process, aerobic microorganisms metabolize remaining organics and produce new cells as well as inorganic end-products. Then these microorganisms are separated from the wastewater via the secondary sedimentation tank. As a result of the secondary treatment stage, residual organics and suspended solids are removed from the wastewater. The settled biological (activated) sludge is then combined with the primary sludge to be sent to the sludge treatment where sludge is treated anaerobically (Metcalf & Eddy 2014). The CAS system sampled receives wastewater from Central Ankara and has a capacity of 765000 m^3/day. The biogas created because of the sludge treatment covers 80-85% of the energy needed by the plant. Average system operation parameters were 3 days SRT, 12 h HRT, and 60% RAS. Turkish Regulation on Water Pollution dictates that the effluent water discharge of a WWTP treating domestic wastewater and serving a population over 100000 should not have more than 35 mg/L BOD, 90 mg/L COD, 25 mg/L TSS, 10

mg/L N, 1 mg/L P and should have pH in the range of 6 and 9 (Republic of Turkey Environment and Urban Ministry 2004).The CAS system sampled was following the regulation during the sampling period except for the nitrogen and phosphorus values which were higher than the discharge standards (Table 3.1).

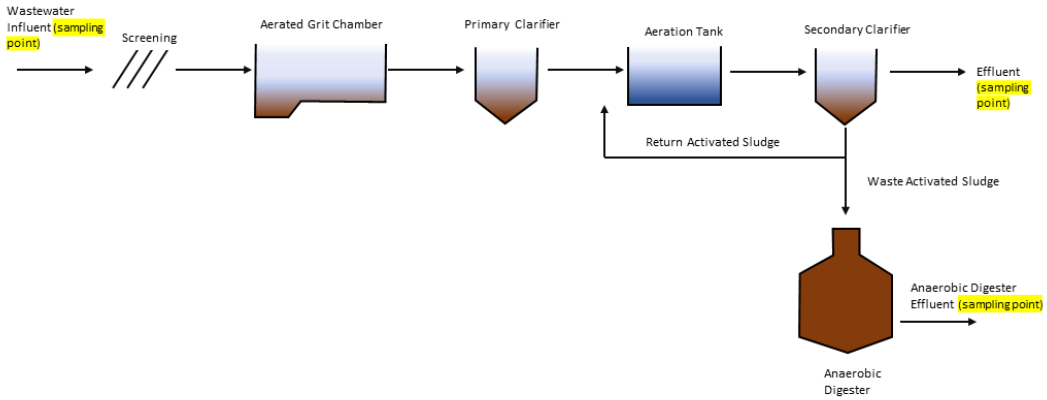

Figure 4.37. Schematic diagram of the CAS system tested in the study.

The CAS system sampled in this study removed protozoan parasites with LRV > 3 for *B. hominis* and *C. parvum* while the highest LRVs for *E. histolytica* and *G. intestinalis* were 2.93 and 1.44, respectively (Figure 4.38).

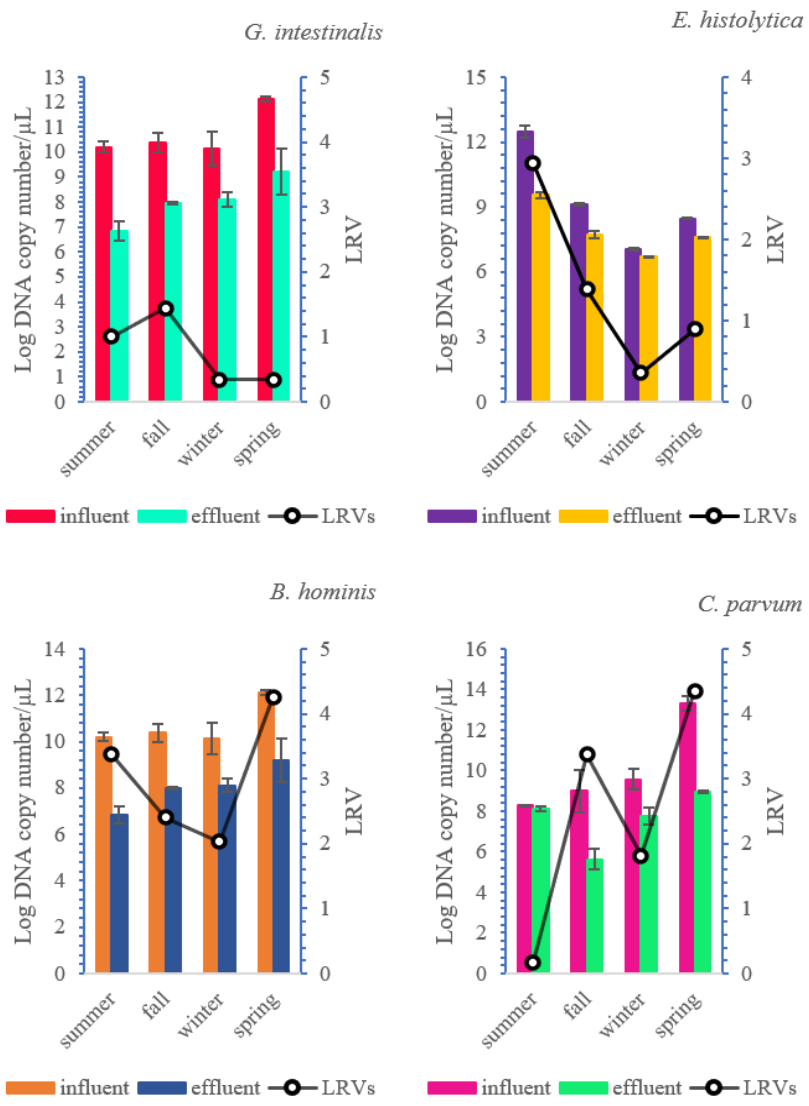

Figure 4.38. Seasonal LRVs for *G. intestinalis*, *E. histolytica*, *B. hominis* and *C. parvum* in CAS. Error bars correspond to the standard deviation of mean values of the three measurements for three replicates.

Significant seasonal variations were only observed for the removal efficiencies of *E. histolytica*, *B. hominis* and *C. parvum* ($p<0.05$) (Table 4.1).

Table 4.1. Seasonal LRVs in CAS

	LRV of CAS System			
	*B. hominis**	*E. histolytica**	*G. intestinalis*	*C. parvum**
Summer	3.368	2.934	1.004	0.177
Autumn	2.405	1.384	1.443	3.376
Winter	2.030	0.352	0.340	1.810
Spring	4.257	0.888	0.337	4.353

* seasonal significance ($p<0.05$)

The LRVs observed in the current study with the CAS process agreed with those observed in previous studies. Study conducted by Kistemann et.al. (2008) who reported LRVs > 2 for *G. intestinalis*. In another study conducted by Tonani et.al. (2011) CAS system shows LRVs lower than 2 for protozoan parasites. In their study, Ramo et.al. (2017) showed that activated sludge process shows removal only up to 2.34 LRVs for *Giardia* and 1.8 LRV for *Cryptosporidium*. Fu et.al. (2010) also showed 1.68 LRV for *Giardia* and 1.52 LRV for *Cryptosporidium* in CAS system. Berglund et.al. (2017) also reported that the CAS system removes protozoan parasites with LRVs ranging from 2 to 3, never reaching 3.

Sludge treatment, however, increased the copy numbers of *B. hominis* in winter, *E. histolytica* in winter and autumn, *G. intestinalis* in winter and autumn and *C. parvum* in winter (Figure 4.39). Significant seasonal variations were observed for the removal efficiencies of only *E. histolytica* ($p<0.05$) (Table 4.2).

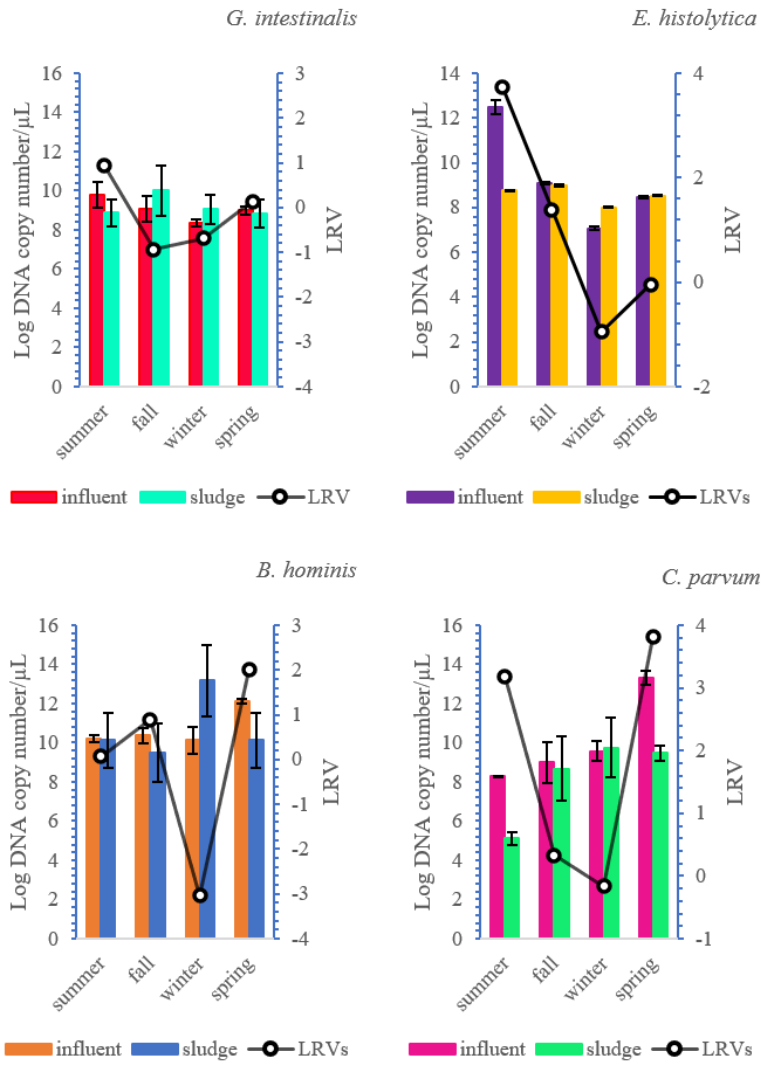

Figure 4.39. Seasonal LRVs for *G. intestinalis*, *E. histolytica*, *B. hominis* and *C. parvum* in CAS Sludge. Error bars correspond to the standard deviation of mean values of the three measurements for three replicates.

Table 4.2. Seasonal LRVs in CAS sludge

	LRV of CAS Sludge			
	B. hominis	*E. histolytica**	*G. intestinalis*	*C. parvum*
Summer	0.066	3.730	0.936	3.172
Autumn	0.885	1.384	-0.944	0.330
Winter	-3.035	-0.957	-0.683	-0.161
Spring	1.998	-0.050	0.137	3.811

* seasonal significance ($p<0.05$)

According to Naughton (2017), an average of 1.3 LRV of protozoan parasites can be expected from activated sludge systems. Naughton also argues that the main mechanism of pathogen removal in the activated sludge process is the adsorption of microorganisms onto sludge therefore the number of pathogens in sludge is enhanced (Naughton 2017). In addition, return activated sludge (RAS) that is collected from the bottom of the secondary sedimentation tank is introduced to the influent of the aeration tank. The cysts of the parasites can be retained in the RAS, then can be recycled into the aeration tank. With the cysts coming from the influent and the cysts that are recycled to the system parasitic protozoa cysts can be accumulated in the sludge (Naughton 2017). Certain types of protozoa such as ameba and metazoans that are predators of flocs and some ciliated protozoa that feed on free bacteria may also help to reduce bacteria living freely and that are in the floc form during activated sludge systems (Figure 4.40) (Naughton 2017).

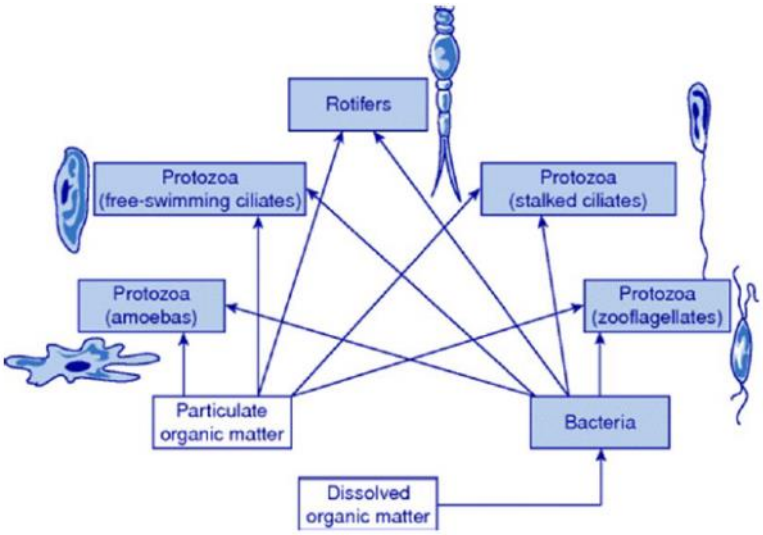

Figure 4.40. Food web of protozoa in CAS systems (Naughton 2017)

The highest removal rates were documented in summer and spring. Major pathogen removal and inactivation mechanisms in CAS were identified as; environmental factors, operational factors, microbiological factors, physico-chemical factors and adsorption onto sludge (Figure 4.41) (Naughton 2017).

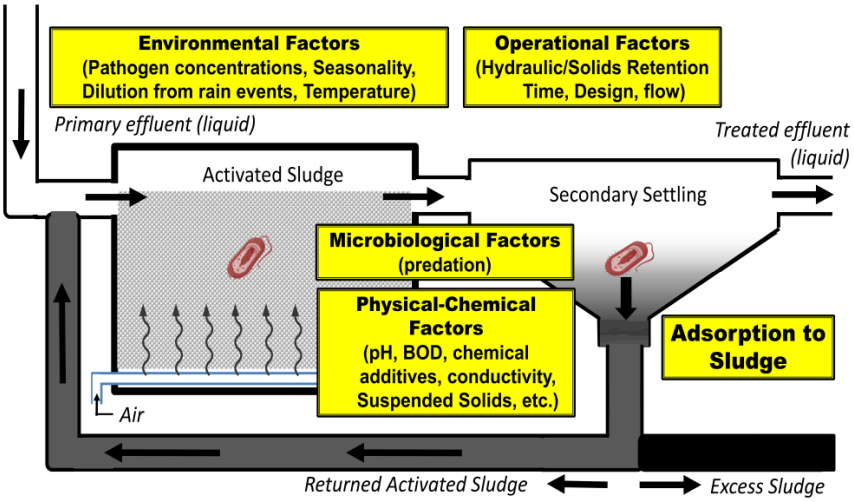

Figure 4.41. Major pathogen removal and inactivation mechanisms in CAS (Naughton 2017)

In one of the mechanisms, pathogens firstly adsorb onto the sludge in the aeration stage and then they are removed by sedimentation in the second stage of the activated sludge systems (Haramoto et al. 2007). Other parameters affecting pathogen removal in activated sludge systems are design and operational parameters such as hydraulic retention time (HRT), solids retention time (SRT), flow rate, and reactor configuration. In their paper, Fu et.al. (2010) suggest that a longer RT and higher sludge concentration increase the removal efficiency of WWTPs regarding pathogens (Fu et al. 2010). High RT is also suggested by Naughton et.al. (2017) as the main mechanism when removing protozoan cysts. Environmental factors such as ambient temperature and rainfall are also important factors effecting the pathogen removal in conventional activated sludge systems. King et.al. (2005) reported higher inactivation of cysts at greater temperatures when pathogens are exposed to higher UV radiation from sunlight. Rainy seasons and snowfall may dilute the wastewater and therefore pathogens in the wastewater, decreasing the removal efficiency of the WWTPs toward pathogens (Lucas et al. 2014). The study area receives rainfall throughout the year and snowfall in winters therefore this may be the reason the CAS system sampled in this study showed lower LRVs in autumn and winter seasons.

Dumontet et.al. (2001) reported no reduction of the protozoan cysts in sludge treatment. They also reported that cysts of these parasites can survive in sludge amended soil for at least 30 days. It has been shown that with thermophilic temperatures greater reduction of pathogens is reachable while with mesophilic temperatures it is less possible to achieve reduction (Protozoan Parasites in Sewage Sludge 2006). Lesser reduction in some seasons during sludge treatment might be caused by the mesophilic conditions that the anaerobic sludge treatment tank sampled in this study works under. Additionally, as adsorption to sludge is one of the main mechanisms for the removal of pathogens in activated sludge process, protozoan parasites were thought to be enriched due to adsorption as also indicated by Naughton et. al. (2017).

4.3.2 in BNR

A diagram of the BNR system having A^2O configuration sampled in this study is given in Figure 4.42. A^2O system includes three parts: nitrification, denitrification, and phosphorus removal happening in consecutive anaerobic, anoxic, and aerobic tanks. Nitrification consists of two stages, the first is the stage where *Nitrosomonas* oxidizes ammonium to nitrite and the second is where *Nitrobacter* oxidizes nitrite to nitrate (Tortora et al. 2016). The denitrification process on the other hand is the process in which nitrate ions are converted to nitrogen gas via denitrifying heterotrophic bacteria such as *Pseudomonas* (Tortora et al. 2016). The phosphorus removal in this process occurs in two stages. Firstly, under anaerobic conditions, Acinetobacter takes up organic matter and releases phosphorus and secondly, in the aerobic zone newly produced phosphorus accumulating organisms (PAOs) take up this previously released phosphorus. Phosphorus is accumulated in sludge and removed in the sedimentation stage with the sludge (Sathasivan n.d.). Throughout this study, the average system operation parameters of the BNR system sampled were 28 h HRT, 16-day SRT, and 85% RAS. The BNR system tested serves a village located in Ankara with a capacity of 41818 m^3/d. Turkish Regulation on Water

Pollution dictates that the effluent water discharge of a WWTP treating domestic wastewater and serving a population between 10000-100000 should not have more than 45 mg/L BOD, 100 mg/L COD, 30 mg/L TSS and should have pH in the range of 6 and 9 (Republic of Turkey Environment and Urban Ministry 2004). The BNR system tested in this study was following the regulation during the sampling period (Table 3.1).

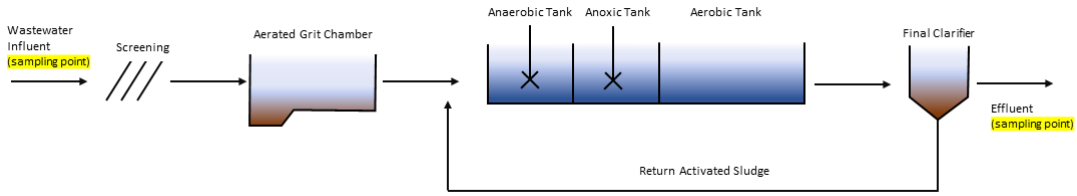

Figure 4.42. Schematic diagram of the BNR system tested in the study.

Wide-ranging LRVs up to 5 and 4 were observed for the removal of *C. parvum* and *B. hominis* in BNR process, respectively. The highest LRV 5 was recorded in summer for *C. parvum.* The seasonal change was only found to be significant for the removal efficiencies of *B. hominis* ($p<0.05$). BNR process displayed poor removal efficiency for *E. histolytica* and *G. intestinalis* (LRV often < 1) (Figure 4.43).

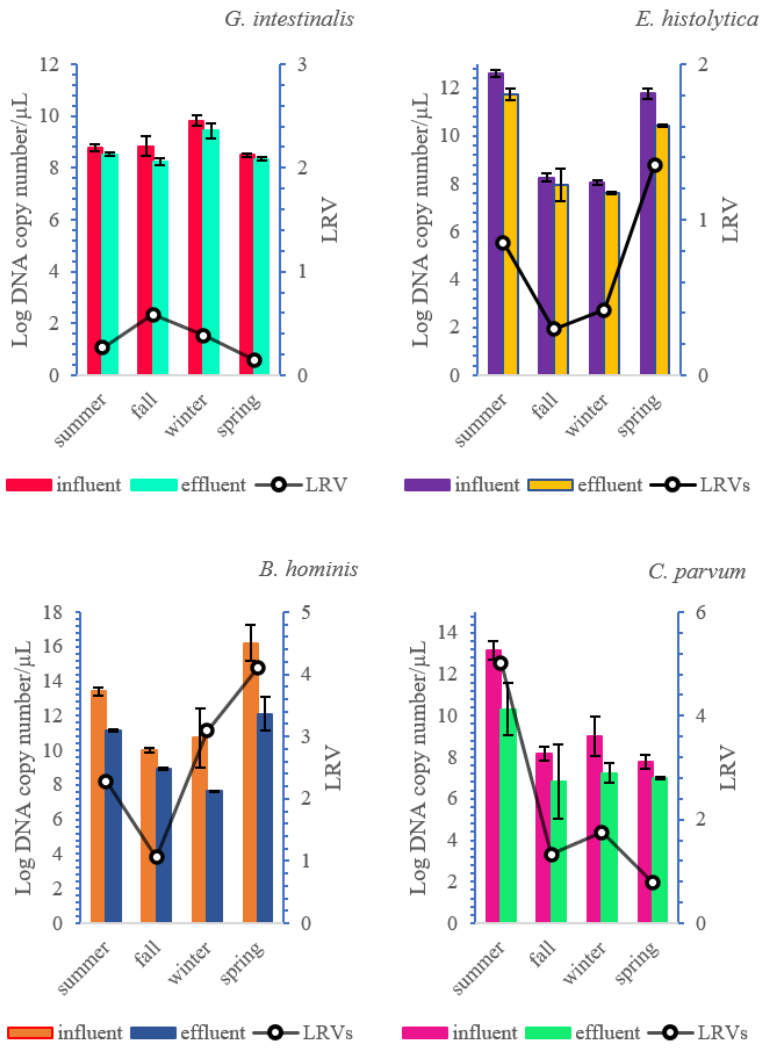

Figure 4.43.Seasonal LRVs for *G. intestinalis*, *E. histolytica*, *B. hominis* and *C. parvum* in BNR. Error bars correspond to the standard deviation of mean values of the three measurements for three replicates.

Table 4.3. Seasonal LRVs in BNR

LRV of BNR System				
	*B. hominis**	*E. histolytica*	*G. intestinalis*	*C. parvum*
Summer	2.283	0.851	0.246	5.025
Autumn	1.055	0.298	0.583	1.331
Winter	3.091	0.421	0.382	1.754
Spring	4.104	1.354	0.146	0.792

* seasonal significance ($p<0.05$)

Fu et.al. (2010) showed in their study that the BNR system removes *Giardia* with an LRV value of 2.04. In their study, Caccio et.al. (2003) reported that in these systems protozoan parasites are removed up to 1.23 LRV. A study conducted by Wang et.al. (2021) on the removal efficiencies of pathogens in different wastewater treatment systems. In this study, BNR (A^2O) system shows a range of LRVs from 1.3 to 1.7 for protozoan parasites (Wang et al. 2021). Another study was conducted by Wen et.al. (2009) on the fate of pathogens in activated sludge plants including BNR systems. BNR system removes an average of 2.41 LRV for *Cryptosporidium* and 2.49 LRV for *Giardia.*

In the current study, the BNR system showed LRVs < 2 for *E. histolytica* and *G. intestinalis* and the seasonal changes of LRVs were statistically significant for only *B. hominis* ($p < 0.05$) (Table 4.3). HRT, SRT, ambient temperature, and flow rate are some important parameters that can affect the removal rates of pathogens in biological nutrient removal systems (Naughton 2017). Longer HRT is recommended for pathogen predation, natural decay, and inactivation. In addition to that, longer SRT is also recommended for the pathogens to be able to adsorb onto the sludge (Naughton 2017). The sizes of protozoan parasites are in various ranges, so their tendency to attach to solid particles may differ affecting the removal rates in the BNR process (Wen et al. 2009). The size of *E. histolytica* cysts ranges from 12-15 µm, for *C. parvum* 4 to 5 µm and that of *G. intestinalis* ranges from 11 to 14 µm while for *B. hominis* this range is wider from 5 to 40 µm (CDC). Protozoa that have relatively smaller size and lower specific gravity of may lead to a lower settling velocity therefore a need for a higher retention time (Wen et al. 2009). This may be the reason the BNR system sampled in this study showed lower LRVs for some protozoa.

4.3.3 in SBR

The diagram of the SBR system sample in this study is given in Figure 4.44. This system consists of five different stages occurring in a single reactor which are fill,

react, settle, draw and idle. Treatment process starts with the fill phase when the reactor is filled with wastewater and then the reaction phase follows. In this phase both aeration and agitation are applied. Then comes the settle stage in which the agitation is stopped are sludge is left to settle. In the end, effluent is discharged to the receiving bodies in the draw phase. Once the draw phase is finished the reactor is filled again for another cycle. The idle stage is used only in a multi-task system (Metcalf & Eddy 2014). Even small changes in the concentrations or flow rate can affect the microbial growth and effluent quality of the SBR process (Yoo et al. 2004). The SBR sampled in this study was operated with 8 h HRT during this study. The SBR system treats wastewater coming from a village in Ankara with a capacity of 3000 m^3/d. Turkish Regulation on Water Pollution dictates that the effluent water discharge of a WWTP treating domestic wastewater and serving a population between 10000-100000 should not have more than 45 mg/L BOD, 100 mg/L COD, 30 mg/L TSS and should have pH in the range of 6 and 9 (Republic of Turkey Environment and Urban Ministry 2004). The SBR system tested in this study was following the regulation during the sampling period (Table 3.1)

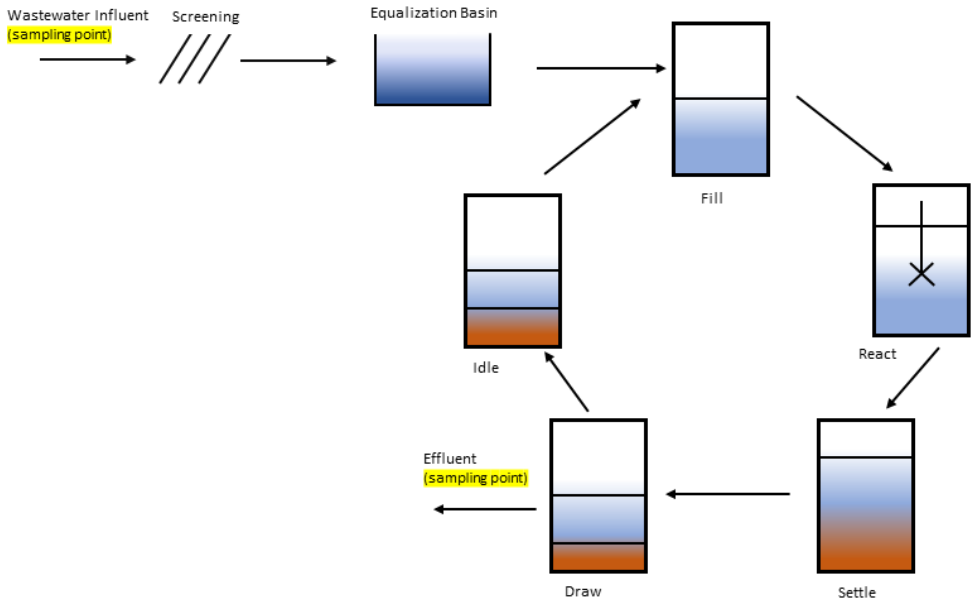

Figure 4.44 Schematic diagram of the SBR system tested in the study.

LRV > 3 was achievable for *B. hominis* in summer and *C. parvum* in spring in the SBR process. In the rest of the season for *B. hominis* along with in all seasons for *E. histolytica, C. parvum* and *G. intestinalis*, the SBR process displayed very poor removal efficiency with LRVs often < 1-2 (Figure 4.45). Seasonal variations were statistically significant for the removal of all the protozoan parasites except *C. parvum* ($p < 0.05$). A study was conducted by Supha et.al. (2015) on the long-term exposure of protozoan communities to TiO_2 in an SBR reactor. According to this research, the number of protozoan communities shows LRV 1 in the addition of TiO_2 to the SBR reactor.

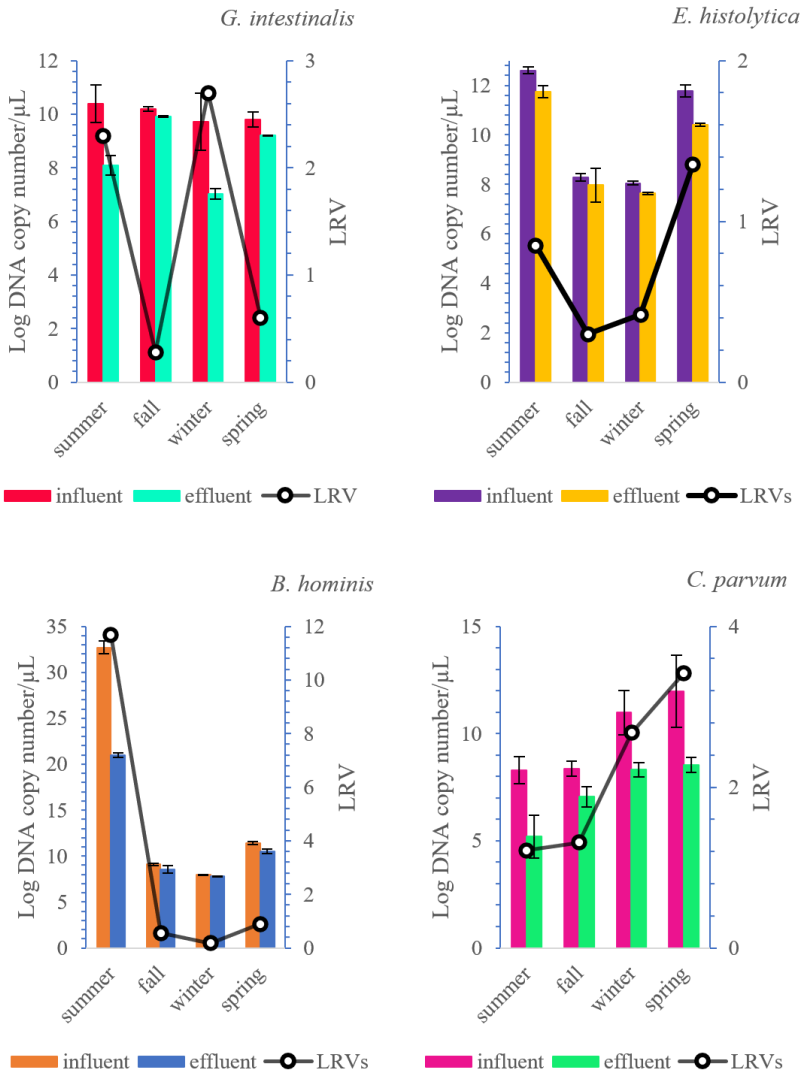

Figure 4.45. Seasonal LRVs for *G. intestinalis*, *E. histolytica*, *B. hominis* and *C. parvum* in SBR. Error bars correspond to the standard deviation of mean values of the three measurements for three replicates.

Table 4.4. Seasonal LRVs in SBR

	LRV of SBR System			
	*B. hominis**	*E. histolytica**	*G. intestinalis**	*C. parvum*
Summer	11.676	1.906	2.297	1.216
Autumn	0.555	0.650	0.280	1.311
Winter	0.179	0.546	2.698	2.675
Spring	0.887	1.551	0.603	3.421

* seasonal significance (p<0.05)

SBR performance depends on several parameters including characteristics of wastewater, cycle time, aeration rate, contact time, temperature, and SRT (Aziz et al. 2013), and the entire process uses a single basin instead of multiple basins due to lower total suspended solid values are obtained consistently the use of a separate clarifier is eliminated. This might explain the lower removal efficiencies of SBR for protozoan parasites.

4.3.4 in CoFlUV

The Figure 4.46 depicts the diagram of CoFlUV system sampled in this study. The coagulation flocculation unit aims to enhance the separation of particles that cannot be separated only by sedimentation and filtration. In this process, colloidal particles are brought together to form larger sized particles that can be more easily removed in the downstream processes (Shammas 2005). In this process, generally, a chemical coagulant is added to first destabilize these negatively charged colloids. Then a flocculant is added so that the larger flocs can be formed, and these smaller colloids can be removed from wastewater by sedimentation (Metcalf & Eddy 2014). UV disinfection, on the other hand, is used for the inactivation or destruction of microorganisms. Ultra-violet light when absorbed by the microorganisms can cause damage to the proteins or to the nucleic acids (thymine dimerization) (Linden and Murphy 2017). UV light is considered non-ionizing radiation as it has a longer wavelength and lower energy. When this radiation is absorbed by the DNA, adjacent thymine bases become cross-linked which forms a thymine dimer disrupting the normal base pairing of the DNA (Tortora et al. 2016). During this study the operational parameters of the CoFlUV system were 27 h HRT, 30day SRT, %100 RAS. The CoFlUV system tested in this study serves an Organized Industrial Zone located in Ankara. Turkish Regulation on Water Pollution dictates that the effluent water discharge of a WWTP treating industrial wastewater should not have more than 400 mg/L COD, 200 mg/L TSS and should have pH in the range of 6 and 9 (Republic of Turkey Environment and Urban Ministry 2004). The CoFlUV system

tested in this study was following the regulation during the sampling period (Table 3.1).

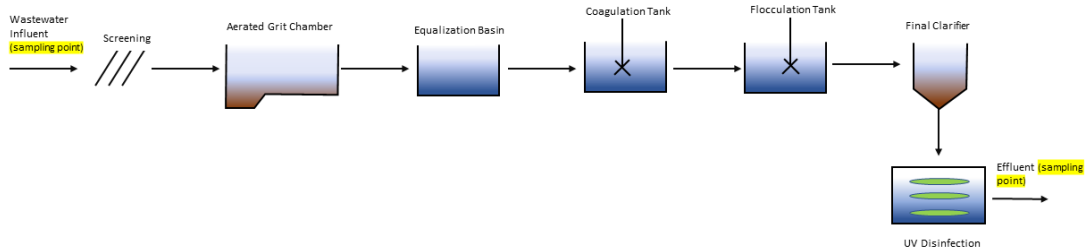

Figure 4.46. Schematic diagram of the CoFlUV system tested in the study.

The removal of *E. histolytica* with LRV > 3 was only obtained mainly in summertime in the CoFlUV process. Rest of the seasons for *E. histolytica* and in all seasons for *B. hominis, C. parvum* and *G. intestinalis*, the LRV was less than 3. Seasonal variations were significant for the removal efficiencies of *E. histolytica* and *B. hominis* (p<0.05) (Figure 4.47). In the coagulation stage since the protozoan cysts are naturally electronegative, precipitate enmeshment metal hydroxides may assure their reduction to more than LRV 2 (Bouzid et al. 2008). In their study, Fewtrell and Bartram (2001) reported that coagulation flocculation systems where ferric coagulants are used removes protozoan pathogen 1-2 LRVs. According to the study conducted by Chowdhury et al. (2022) coagulation-flocculation along with secondary sedimentation also leads LRVs 2-3 for *E. histolytica.* Hachich et.al. (2013) found that coagulation with ferric chloride removes *G. intestinalis* with 2.26 LRV. Betancourt et al. (2019) reported up to 3.41 LRV for *C. parvum.*

Previous study conducted by Neto et.al. (2006) showed that UV disinfection is only effective up to 1.96 LRV for *G. intestinalis* and 2.01 LRV for *C. parvum*. Linden et.al. (2017) however reported 2-4 LRVs for protozoan parasites in UV disinfection unit. A study was conducted by Rodriguez-Manzano et.al. (2012) on standard and new fecal indicators and pathogens in sewage treatment plants, microbiological parameters for improving the control of reclaimed water. According to this study, UV light shows 0.34 and 0.90 LRV for *Cryptosporidium* and *Giardia*, respectively. Although these removals are possible with UV light in the same study trophozoites

of these species are still found in the intestines of one Mouse providing evidence that the inactivation of cysts was not complete (Neto et al. 2006).

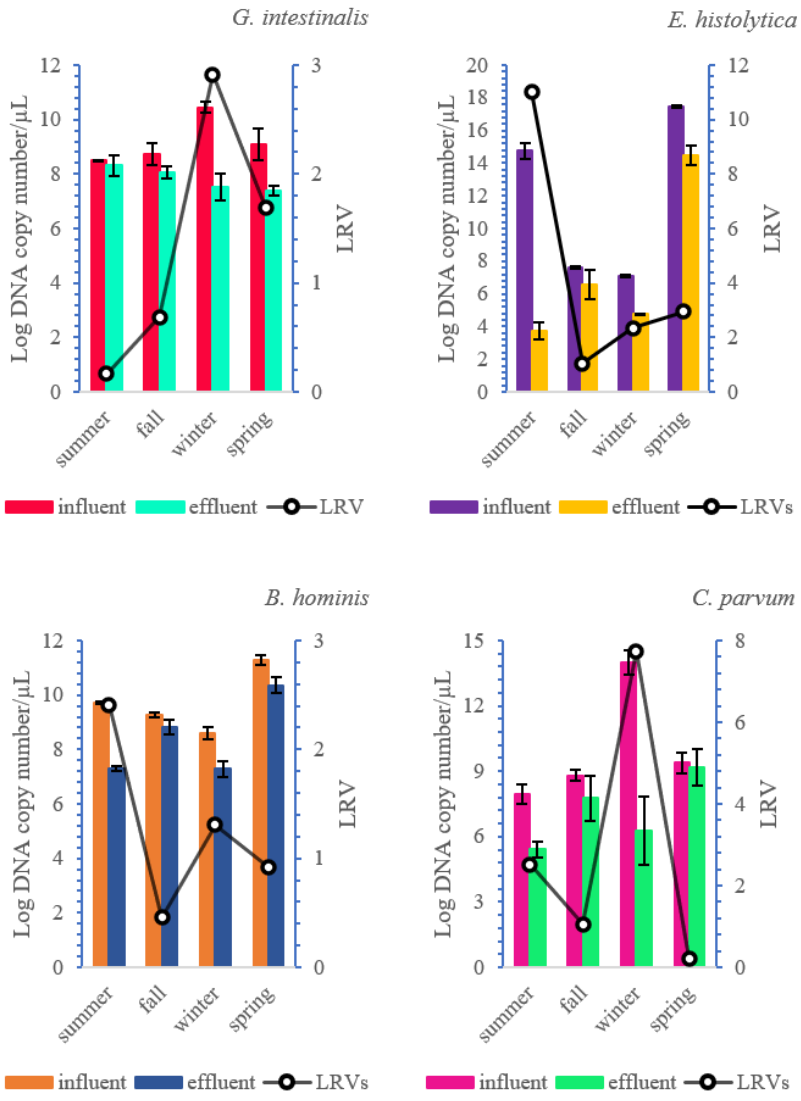

Figure 4.47. Seasonal LRVs for *G. intestinalis*, *E. histolytica*, *B. hominis* and *C. parvum* in CoFlUV. Error bars correspond to the standard deviation of mean values of the three measurements for three replicates.

Table 4.5. Seasonal LRVs in CoFlUV

	LRV of CoFlUV System			
	*B. hominis**	*E. histolytica**	*G. intestinalis*	*C. parvum*
Summer	2.410	11.035	0.166	2.508
Autumn	0.454	1.032	0.684	1.049
Winter	1.309	2.345	2.915	7.734
Spring	0.923	2.938	1.695	0.218

* seasonal significance (p<0.05)

Effective coagulation relies on accurate dosing and mixing of often highly variable influent loads and effective, well-controlled sludge removal. UV doses of 30 mJ/cm^2 is recorded as the best dose for pathogen inactivation. A lower dose of 15 mJ/cm^2 UV is applied in the current study might explain the lower LRVs for *B. hominis, C. parvum* and *G. intestinalis*. Considering the results of these previous studies, neither coagulation nor UV disinfection can remove ARGs as much as when they used in combination.

4.3.5 in MBR

The Figure 4.48 shows the schematic diagram of the MBR system sampled in this study. MBR systems are similar to activated sludge systems however they employ a micro- or ultra-filtration unit instead of secondary sedimentation tank for the removal of biomass. Some pathogen removal is achieved during the biological treatment however a much greater reduction is achieved during the filtration process (Verbyla and Rousselot 2018). Most MBR systems utilize microfiltration with 0.1 to 0.4 μm pore size or ultrafiltration with pore sizes ranging from 0.01 to 0.04 μm (Verbyla and Rousselot 2018). In MBR systems, continuous generation of new sludge and consumption of organic materials with decay in sludge mass occurs at the same time.

Therefore, a 44% reduction in sludge production is estimated in MBR systems comparing to CAS (Radjenovic et al. 2008). MBR system sampled was operated with 18 h HRT during this study. This system treats municipal wastewater collected from a university campus with daily capacity of 15000 m^3/d and has a total 540 m^2 membrane surface area and with membrane pore sizes of 0.038 µm. Turkish Regulation on Water Pollution dictates that the effluent water discharge of a WWTP treating domestic wastewater and serving to a population between 84-2000 should not have more than 45 mg/L BOD, 120 mg/L COD and should have pH in the range of 6 and 9 (Republic of Turkey Environment and Urban Ministry 2004). The MBR system tested in this study was following the regulation during the sampling period (Table 3.1).

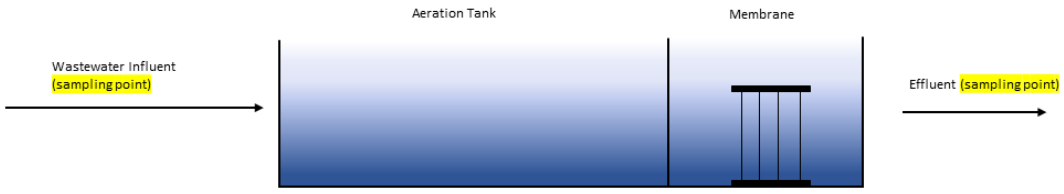

Figure 4.48. Schematic diagram of the MBR system tested in the study.

LRV > 3 was achievable for *B. hominis* for all seasons and for *C. parvum* in autumn and winter in the MBR process. This efficiency was only obtained in summertime for *E. histolytica* and the MBR system was showed LRV < 3 for *G. intestinalis* in all seasons. Seasonal changes were only significant for the removal efficiencies of *B. hominis* (p<0.05) (Figure 4.49).

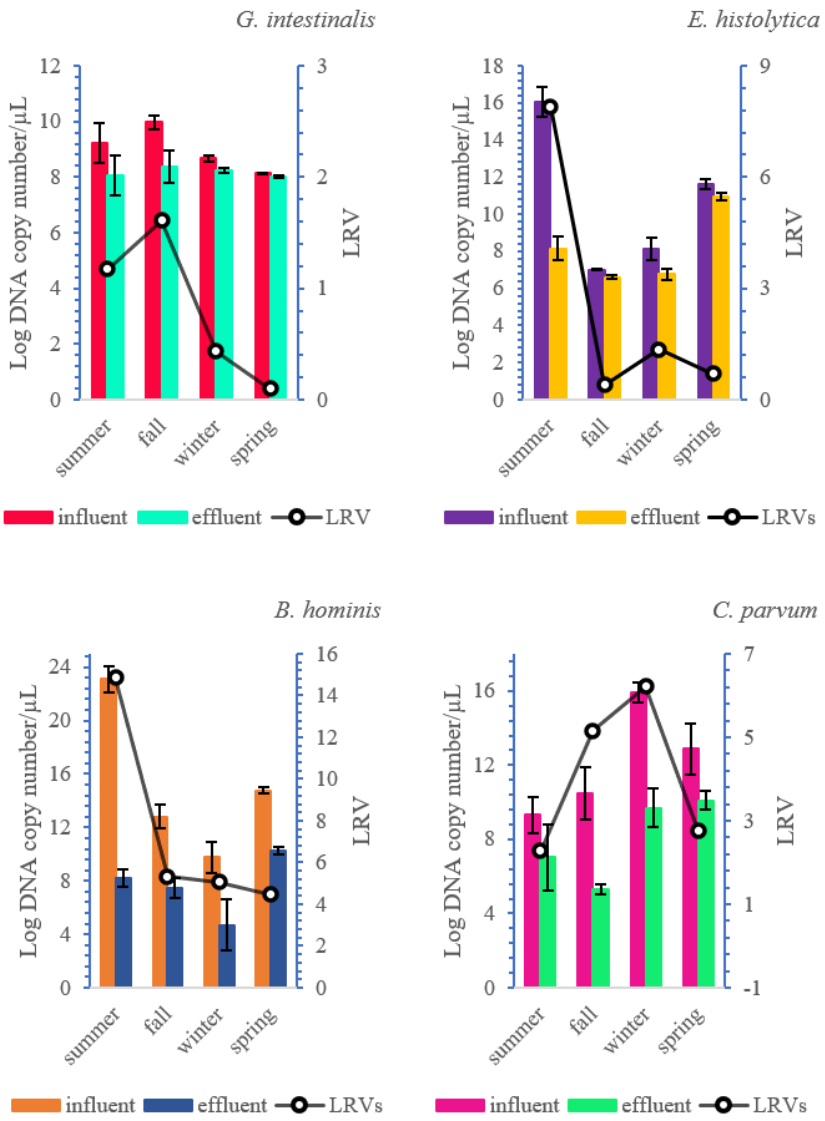

Figure 4.49. Seasonal LRVs for *B. hominis*, *E. histolytica*, and *G. intestinalis* in MBR. Error bars correspond to the standard deviation of mean values of the three measurements for three replicates.

Table 4.6. Seasonal LRVs in MBR

	LRV of MBR System			
	*B. hominis**	*E. histolytica*	*G. intestinalis*	*C. parvum*
Summer	14.852	7.900	1.174	2.275
Autumn	5.337	0.397	1.608	5.158
Winter	5.057	1.352	0.432	6.210
Spring	4.458	0.702	0.100	2.769

* seasonal significance (p<0.05)

A study was conducted by Fu et.al. (2010) on monitoring and evaluation of the removal of pathogens at municipal wastewater treatment plants. In this study, MBR shows LRVs higher than 1.84 for *Cryptosporidium* and higher than 2.40 for *Giardia* (Fu et al. 2010). With membrane technologies, Ben Ayed et al. (2017) report 3 to 4 LRVs for *Entamoeba* spp..

Protozoan cysts are significantly larger than the pores of the membrane filters, therefore efficient removal is expected according to Hai et.al. (2014). Even though the MBR system sampled in the current study showed high LRVs especially for *B. hominis*, the protozoan parasites were still detected up to 10^6 copy number/L in the effluent. Major pathogen removal mechanisms in MBR systems are size exclusion enhanced by the biological cake layer forming on the membrane (Verbyla and Rousselot 2018) (Figure 4.50).

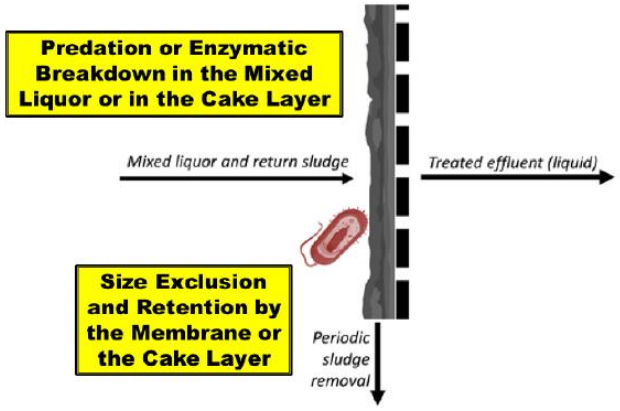

Figure 4.50. Major factors affecting pathogen removal in membrane bioreactors. (Verbyla and Rousselot 2018)

SRT, HRT, membrane integrity, variations in feed water and the extent of membrane fouling are also dome important factors affecting pathogen removal in MBR systems (Sidhu et al. 2015). MBR reactors maintain higher mixed liquor suspended solids (MLSS) compared to a CAS system therefore biomass properties and membrane fouling in an MBR system is highly affected by SRT. Since with longer SRTs higher biomass concentration in an MBR can be accomplished, longer SRT rises the treatment efficiency. Consequently, the change in the SRT may affect the removal rates of pathogens. However, high MLSS can accelerate the fouling of the membrane

by rapid deposition of sludge particles onto the membrane surface (Han et al. 2005). This might be the possible explanation of low LRVs obtained for *E. histolytica* and *G. intestinalis* in MBR systems in the current study.

4.4 Removal of protozoa in literature

A summary of selected parasitic protozoa LRVs in wastewater treatment plants observed in literature is given in Table 4.7.

Table 4.7. Removal of studied protozoa in literature

	LRVs recorded					
	CAS	BNR	SBR	CoFlUV	MBR	Reference
G. intestinalis	1.36					(Tonani et al., 2011)
	2.34					(Ramo et al., 2017)
	1.68	2.04			2.4	(Fu et al., 2010)
	0.62-2.5					(Berglund et al., 2017)
		1.23				(Cacciò et al., 2003)
		2.49				(Wen et al., 2009)
		1.3-1.7				(Wang et al., 2021)
			1.0			(Supha et al., 2015)
				1.0-2.0		(Fewtrell & Bartram, 2001)
				2.26		(Chowdhury et al., 2022)
				1.96		(Neto et al., 2006)
				2.0-4.0		(Linden & Murphy, 2017)
				0.90		(Rodriguez-Manzano et al., 2012)
E. histolytica	0.23-2.1					(Berglund et al., 2017)
		1.3-1.7				(Wang et al., 2021)
			1.0			(Supha et al., 2015)
				1.0-2.0		(Fewtrell & Bartram, 2001)
				2.0-3.0		(Chowdhury et al., 2022)
				2.0-4.0		(Linden & Murphy, 2017)
					3.0-4.0	(ben Ayed & Sabbahi, 2017)
B. hominis		1.3-1.7				(Wang et al., 2021)
			1.0			(Supha et al., 2015)
				1.0-2.0		(Fewtrell & Bartram, 2001)
				2.0-4.0		(Linden & Murphy, 2017)
C. parvum	1.8					(Ramo et al., 2017)
	1.52				1.84	(Fu et al., 2010)
		1.3-1.7				(Wang et al., 2021)
		2.41				(Wen et al., 2009)
			1.0			(Supha et al., 2015)
				1.0-2.0		(Fewtrell & Bartram, 2001)
				3.41		(Chowdhury et al., 2022)
				2.01		(Neto et al., 2006)
				2.0-4.0		(Linden & Murphy, 2017)
				0.34		(Rodriguez-Manzano et al., 2012)

CHAPTER 5

CONCLUSION AND RECOMMENDATIONS

5.1 Conclusion

In this study, common types of WWTPs namely, CAS, BNR, SBR, WWTP with coagulation-flocculation and UV disinfection units and MBR were investigated with respect to their seasonal removal capacities for 4 protozoan parasites including *G. intestinalis, E. histolytica*, *B. hominis* and *C. parvum* that are causative agents of commonly seen gastrointestinal diseases giardiasis, amebiasis, blastocytosis and cryptosporidiosis, respectively. Removal of parasitic protozoa in WWTPs was highly affected by the process and the season as summarized in the below given in Table 5.1.

Table 5.1. LRV for protozoan parasites

	LRV for *G. intestinalis*					
	CAS		BNR	SBR*	CoFlUV	MBR
	Sludge	Effluent				
Summer	0.94	1.00	0.25	2.30	0.17	1.17
Autumn	-0.94	1.44	0.58	0.28	0.68	1.61
Winter	-0.68	0.34	0.38	2.70	2.92	0.43
Spring	0.14	0.34	0.15	0.60	1.70	0.10

	LRV for *E. histolytica*					
	CAS*		BNR	SBR*	CoFlUV*	MBR
	Sludge	Effluent				
Summer	3.73	2.93	0.85	1.91	11.04	7.90
Autumn	1.38	1.38	0.30	0.65	1.03	0.40
Winter	-0.96	0.35	0.42	0.55	2.35	1.35
Spring	-0.05	0.89	1.35	1.55	2.94	0.70

Table 5.1. cont'd

	LRV for *B. hominis*					
	CAS*		BNR*	SBR*	CoFlUV*	MBR*
	Sludge	Effluent				
Summer	0.06	3.37	2.28	11.68	2.41	14.85
Autumn	0.89	2.41	1.06	0.56	0.45	5.34
Winter	-3.04	2.03	3.09	0.18	1.31	5.06
Spring	2.00	4.26	4.10	0.89	0.92	4.46

	LRV for *C. parvum*					
	CAS*		BNR	SBR	CoFlUV	MBR
	Sludge	Effluent				
Summer	3.17	0.18	5.03	1.22	2.51	2.28
Autumn	0.33	3.38	1.33	1.31	1.05	5.16
Winter	-0.16	1.81	1.75	2.68	7.73	6.21
Spring	3.81	4.35	0.79	3.42	0.22	2.77

*Seasonal significance ($p<0.05$)

This study pointed out that:

- In CAS, LRVs 1-2 were reachable for all protozoa. LRVs > 3 were reachable for *B. hominis* and *C. parvum*. Seasonal changes were significant for *E. histolytica, B. hominis* and *C. parvum* ($p<0.05$).
- In BNR, LRVs 1-2 were reachable for all protozoa except for *G. intestinalis.* LRVs > 3 were reachable for *B. hominis* and *C. parvum*. Seasonal changes were only significant for *B. hominis* ($p<0.05$).
- In SBR, LRVs 1-2 were reachable for all protozoa except for *B. hominis.* LRVs > 3 were reachable for *B. hominis* and *C. parvum*. Seasonal changes were significant for *G. intestinalis, E. histolytica,* and *B. hominis* ($p<0.05$).
- In CoFlUV, LRVs 1-2 were reachable for all protozoa. LRVs > 3 were reachable *E. histolytica* and *C. parvum*. Seasonal changes were significant for *E. histolytica* and *B. hominis* ($p<0.05$).
- In MBR, LRVs 1-2 were reachable for all protozoa. LRVs > 3 were reachable for all protozoa except for *G. intestinalis*. Seasonal changes were significant for only *B. hominis* ($p<0.05$).
- Sludge in the CAS increased the amount of *G. intestinalis* in autumn and winter, *E. histolytica* in winter and spring, *B. hominis* and *C. parvum* in

winter. Sludge treatment reached LRVs > 3 for only *E. histolytica* and *C. parvum* in summer for both and spring for only *C. parvum*.

Regardless of the process used in the treatment plants, it was observed that the removal efficiencies for *G. intestinalis* and *E. histolytica* were often lower than LRV 3. In most of the seasons removals efficiencies for these protozoa were observed to be around LRVs 1-2. Therefore, for especially *G. intestinalis* and *E. histolytica*, dissemination from the WWTPs can be considered as a significant threat to public health. Because of these results, discharge points of WWTPs should be monitored in terms of parasitic protozoa.

5.2 Future prospects and recommendations

1. Each unit process of WWTPs should be investigated in terms of their individual protozoa removal capacities.
2. Possible modifications on WWTP processes with the high protozoan parasite removal capacity should be investigated for the complete removal of parasites.
3. Installations of the high parasite removal capacity procedures into the other types of WWTPs should also be assessed.
4. Economic feasibility should be considered when proposing changes to the current WWTPs.
5. Regulation on protozoa discharge standard for each WWTP should be considered for public health.

Dissemination of protozoa, especially *G. intestinalis* and *E. histolytica*, from WWTPs raises a public health concern. The reuse of wastewater may be taken into consideration provided that an effluent irrigation scheme is built and managed. Irrigating crops, fruit, and vegetables, especially those intended for human consumption, using treated wastewater require special caution. Human exposure to biological pollution, including microorganisms like protozoa as well as the potential

for disease transmission are two main issues with the reuse. Since biological pollution is not typically eliminated by conventional secondary wastewater treatment, effluents of these WWTPs should be monitored and regulated.

REFERENCES

Aboelsoued, Dina et al. 2019. "Cellular Immune Response and Scanning Electron Microscopy in the Evaluation of Moringa Leaves Aqueous Extract Effect on *Cryptosporidium parvum* in Buffalo Intestinal Tissue Explants." *Journal of Parasitic Diseases* 43(3): 393–401.

Adam, Rodney D. 2001. "Biologia of *Giardia lamblia*." *Clinical Microbiology Reviews*: 447–75.

Adamska, M., M. Sawczuk, L. Kolodziejczyk, and B. Skotarczak. 2015. "Assessment of Molecular Methods as a Tool for Detecting Pathogenic Protozoa Isolated from Water Bodies." *Journal of Water and Health* 13(4): 953–59.

Aghalari, Zahra et al. 2020. "Effectiveness of Wastewater Treatment Systems in Removing Microbial Agents : A Systematic Review." : 1–11.

Akpolat, Nezahat, Fatih Çakır, Mutalip Çiçek, and Alican Bilden. 2022. "Retrospective Analysis of the Distribution of Intestinal Parasites in Patients Admitted to Dicle University Faculty of Medicine Between the Years 2011-2020." *Turkish Journal of Parasitology* 46(2): 119–23.

Al-Asheh, Sameer, Marzieh Bagheri, and Ahmed Aidan. 2021. "Membrane Bioreactor for Wastewater Treatment: A Review." *Case Studies in Chemical and Environmental Engineering* 4: 1-15

Alfredo Bonilla, J et al. 2015. "Quantification of Protozoa and Viruses from Small Water Volumes." *International Journal of Environmental Research and Public Health* 12(7): 7118–32.

Amini, Malihe, Habibollah Younesi, Ghasem Najafpour, and Ali Akbar Zinatizadeh. 2016. "Application of Response Surface Methodology for Simultaneous Carbon and Nitrogen (SND) Removal from Dairy Wastewater in Batch Systems." (December 2012).

Ben Ayed, Layla, and Sonia Sabbahi. 2017. "*Entamoeba histolytica*." *Global Water Pathogen Project* 151(17): 42.

Aziz, Shuokr Qarani et al. 2013. "Landfill Leachate Treatment Using Sequencing Batch Reactor (SBR) Process : Limitation of Operational Parameters and Performance Review Paper Landfill Leachate Treatment Using Sequencing Batch Reactor (SBR) Process : Limitation of Operational Parameter." (February).

Bartlett, John M S, and David Stirling. 1996. "YAC Protocols. Methods in Molecular Biology, Vol. 54." *FEBS Letters* 398(2–3): 338.

Benito, María et al. 2020. “Seeking the Reuse of Effluents and Sludge from Conventional Wastewater Treatment Plants: Analysis of the Presence of Intestinal Protozoa and Nematode Eggs.” *Journal of Environmental Management* 261(February).

Berglund, Björn et al. 2017. “Occurrence and Removal Efficiency of Parasitic Protozoa in Swedish Wastewater Treatment Plants.” *Science of the Total Environment* 598(November): 821–27. http://dx.doi.org/10.1016/j.scitotenv.2017.04.015.

Betancourt, Walter. 2019. “*Cryptosporidium* spp.*”* In *Water and Sanitation for the 21st Century: Health and Microbiological Aspects of Excreta and Wastewater Management (Global Water Pathogen Project)*, Michigan State University.

Bouzid, Maha, Dietmar Steverding, and Kevin M. Tyler. 2008. “Detection and Surveillance of Waterborne Protozoan Parasites.” *Current Opinion in Biotechnology* 19(3): 302–6.

Brittanica. 2021. “Polymerase Chain Reactions.” https://www.britannica.com/science/polymerase-chain-reaction (July 20, 2022).

Cacciò, Simone M, Marzia de Giacomo, Francesca A Aulicino, and Edoardo Pozio. 2003. “*Giardia* Cysts in Wastewater Treatment Plants in Italy.” *Applied and Environmental Microbiology* 69(6): 3393–98.

Carrero, Julio C, Magda Reyes-lópez, Jesús Serrano-luna, and Mineko Shibayama. 2020. “International Journal of Medical Microbiology Intestinal Amoebiasis : 160 Years of Its Fi Rst Detection and Still Remains as a Health Problem in Developing Countries.” *International Journal of Medical Microbiology* 310(1): 151358.

CDC. 2017. “Giardiasis.” https://www.cdc.gov/dpdx/giardiasis/index.html.

CDC. 2019. “Amebiasis.” https://www.cdc.gov/dpdx/amebiasis/index.html.

CDC. 2019. “*Blastocystis* Sp.” https://www.cdc.gov/dpdx/blastocystis/index.html.

CDC. 2019. “*Criptosporidium* Spp.”

CDC. 2019. “Cryptosporidiosis.” https://www.cdc.gov/dpdx/cryptosporidiosis/index.html.

CDC. 2021. “*Giardia*.” https://www.cdc.gov/parasites/giardia/pathogen.html.

CDC. 2022. “Transmission of Parasitic Diseases.” https://www.cdc.gov/parasites/transmission/index.html.

CDC. “*Entamoeba histolytica* and *Entamoeba dispar*.”

CDC. “Laboratory Diagnosis of Giardiasis.”

Chowdhury, Rakib Ahmed, Nwadiuto Esiobu, Daniel E Meeroff, and Fred Bloetscher. 2022. "Different Detection and Treatment Methods for *Entamoeba histolytica* and *Entamoeba dispar* in Water / Wastewater : A Review." (January).

Dadonaite, Bernedate, Hannah Ritchie, and Max Roser. 2019. "Diarrheal Diseases." https://ourworldindata.org/diarrheal-diseases#burden-of-diarrheal-diseases.

Domenech, Eva, Inmaculada Amorós, Yolanda Moreno, and José L. Alonso. 2018. "*Cryptosporidium* and *Giardia* Safety Margin Increase in Leafy Green Vegetables Irrigated with Treated Wastewater." *International Journal of Hygiene and Environmental Health* 221(1): 112–19.

Dumontet, Stefano et al. 2001. "Sewage Sludge paper The Importance of Pathogenic Organisms in Sewage and Sewage Sludge."

Dungeni, M, and M N B Momba. 2010. "The abundance of *Cryptosporidium* and *Giardia* spp. in treated effluents produced by four wastewater treatment plantts in the Gauteng Province of South Africa ." 36(4): 425–32.

EPA. 1999. "Wastewater Technology Fact Sheet Sequencing Batch Reactors."

EPA. 2007. Biological Nutrient Removal Processes and Costs.

Fewtrell, Lorna, and Jamie Bartram. 2001. "Water Treatment and Pathogen Control World Health Organization Titles with IWA Publishing."

Fontaine, Melanie, and Emmanuelle Guillot. 2002. "Development of a TaqMan Quantitative PCR Assay Specific for Cryptosporidium Parvum ." *FEMS Microbiology Letters* 214(1): 13–17.

Fu, C Y et al. 2010. "Monitoring and Evaluation of Removal of Pathogens at Municipal Wastewater Treatment Plants."

Gallas-Lindemann, Carmen et al. 2016. "*Giardia* and *Cryptosporidium* Spp. Dissemination during Wastewater Treatment and Comparative Detection via Immunofluorescence Assay (IFA), Nested Polymerase Chain Reaction (Nested PCR) and Loop Mediated Isothermal Amplification (LAMP)." *Acta Tropica* 158: 43–51.

Garibyan, Lilit, and Nidhi Avashia. 2013. "Polymerase Chain Reaction." *Journal of Investigative Dermatology* 133(3): 1–4.

Ghangrekar, M M, and West Bengal. 2014. 3 Comprehensive Water Quality and Purification *3 . 5 Suspended Growth Treatment Processes*. Elsevier Ltd.

Gilbride, K. A., D. Y. Lee, and L. A. Beaudette. 2006. "Molecular Techniques in Wastewater: Understanding Microbial Communities, Detecting Pathogens, and Real-Time Process Control." *Journal of Microbiological Methods* 66(1): 1–20.

Gross, Andrej et al. 2015. "Improved Drinking Water Disinfection with UVC-LEDs for *Escherichia coli* and *Bacillus subtilis* Utilizing Quartz Tubes as Light Guide." *Water (Switzerland)* 7(9): 4605–21.

Guidelines for Canadian Drinking Water Quality Guideline Technical Document Enteric Protozoa*: Giardia* and *Cryptosporidium*. 2019.

Gülmez, Dolunay, Zeynep Saribaş, Yakut Akyön, and Sibel Ergüven. 2013. "[The Results of Hacettepe University Faculty of Medicine Parasitology Laboratory in 2003-2012: Evaluation of 10 Years]." *Türkiye parazitoloji dergisi / Türkiye Parazitoloji Derneği = Acta parasitologica Turcica / Turkish Society for Parasitology* 37(2): 97–101.

Gutiérrez, Antonio Marty Quispe. 2017. "Giardiasis Epidemiology." In *Current Topics in Giardiasis*, InTech.

Guy, Rebecca A, Pierre Payment, Ulrich J Krull, and Paul A Horgen. 2003. "Real-Time PCR for Quantification of *Giardia* and *Cryptosporidium* in Environmental Water Samples and Sewage." 69(9): 5178–85.

Hachich, Elayse M et al. 2013. "Pathogenic Parasites and Enteroviruses in Wastewater : Support for a Reguiation on Water Reuse." (December 2009): 1512–19.

Hai, Faisal I. et al. 2014. "Removal of Pathogens by Membrane Bioreactors: A Review of the Mechanisms, Influencing Factors and Reduction in Chemical Disinfectant Dosing." *Water (Switzerland)* 6(12): 3603–30.

Han, Sung-soo, Tae-hyun Bae, Gyung-gug Jang, and Tae-moon Tak. 2005. "Influence of Sludge Retention Time on Membrane Fouling and Bioactivities in Membrane Bioreactor System." 40: 2393–2400.

Haramoto, E, H Katayama, K Oguma, and S Ohgaki. 2007. "Quantitative Analysis of Human Enteric Adenoviruses in Aquatic Environments." 103: 2153–59.

Hemmati, Arash, Elham Hooshmand, and Mohammad Javad Hosseini. 2015. "Identification of *Entamoeba histolytica* by Molecular Method in Surface Water of Rasht City , Iran." 44(2): 238–43.

Hooshyar, Hossein, Parvin Rostamkhani, Mohsen Arbabi, and Mahdi Delavari. 2019. "*Giardia lamblia* Infection: Review of Current Diagnostic Strategies." *Gastroenterology and Hepatology from Bed to Bench* 12(1): 3–12.

Ibrahim, Suha, Wafaa Choumane, and Amal Dayoub. 2020. "Occurrence and Seasonal Variations of Giardia in Wastewater and River Water from Al-Jinderiyah Region in Latakia, Syria." *International Journal of Environmental Studies* 77(3): 370–81.

Karim, M.A., and James L. Mark. 2017. "A Preliminary Comparative Analysis of MBR and CAS Wastewater Treatment Systems." *International Journal of Water and Wastewater Treatment* 3(2): 1-6

King, Brendon J, Alexandra R Keegan, Paul T Monis, and Christopher P Saint. 2005. "Environmental Temperature Controls *Cryptosporidium* Oocyst Metabolic Rate and Associated Retention of Infectivity." 71(7): 3848–57.

Kistemann, Thomas et al. 2008. "A Comparison of Efficiencies of Microbiological Pollution Removal in six Sewage Treatment Plants with Different Treatment Systems." *International Journal of Hygine and Environmental Health*.154: 341-358

Kitajima, Masaaki, Eiji Haramoto, Brandon C Iker, and Charles P Gerba. 2014. "Science of the Total Environment Occurrence of *Cryptosporidium* , *Giardia* , and *Cyclospora* in influent and effluent Water at Wastewater Treatment Plants in Arizona." *Science of the Total Environment, The* 484: 129–36.

Koloren, Zeynep, Berivan Basak, and Panagiotis Karanis. 2018. "Acta Tropica Molecular Identi Fi Cation of *Blastocystis* Sp . Subtypes in Water Samples Collected from Black Sea , Turkey." *Acta Tropica* 180(October 2017): 58–68.

Kralik, Petr, and Matteo Ricchi. 2017. "A Basic Guide to Real Time PCR in Microbial Diagnostics: Definitions, Parameters, and Everything." *Frontiers in Microbiology* 8(FEB): 1-9

de la Cruz, Christian, and Rune Stensvol. 2017. "Part Three . Specıfic Excreted Pathogens : Envıronmental And Epıdemıology Aspects Copyright :" *Global Water Pathogen Project*.

Lee, Pei Yun, John Costumbrado, Chih Yuan Hsu, and Yong Hoon Kim. 2012. "Agarose Gel Electrophoresis for the Separation of DNA Fragments." *Journal of Visualized Experiments* (62): 1–5.

Leitch, Gordon J., and Qing He. 2011. "Cryptosporidiosis-an Overview." *Journal of Biomedical Research* 25(1): 1–16.

Lemarchand, K et al. 2005. "Optimization of Microbial DNA Extraction and Purification from Raw Wastewater Samples for Downstream Pathogen Detection by Microarrays." *Journal of Microbiological Methods* 63(2): 115–26.

van Lieshout, L., and M. Roestenberg. 2015. “Clinical Consequences of New Diagnostic Tools for Intestinal Parasites.” *Clinical Microbiology and Infection* 21(6): 520–28.

Linden, Karl, and Joanna R. Murphy. 2017. “Physical Agents.” *Global Water Pathogen Project* (September): 1–20.

Lucas, Françoise S et al. 2014. “Variation of Raw Wastewater Microbiological Quality in Dry and Wet Weather Conditions.” : 5318–28.

Madigan, Michael T., and John M. Martinko. 2006. *Brock Biology of Microorganisms*. 11th ed. ed. Gary Carlson. Pearson.

Metcalf & Eddy. 2014. *Wastewater Engineering*. 5th ed. McGraw - Hill.

Minarovi, Jana, Č O V Á Eva, Kaclíková Klára, and Krascsenicsová Peter. 2007. “Detection of Cryptosporidium Parvum by Polymerase Chain Reaction.” 46(2): 58–62.

Moreno, Y. et al. 2018. “Multiple Identification of Most Important Waterborne Protozoa in Surface Water Used for Irrigation Purposes by 18S RRNA Amplicon-Based Metagenomics.” *International Journal of Hygiene and Environmental Health* 221(1): 102–11.

Nathanson,J.A. 2022. “Wastewater Treatment.” https://www.britannica.com/technology/wastewater-treatment (July 13, 2022).

Naughton, Colleen. 2017. “Part Four . Management Of Risk From Excreta And Wastewater Activated Sludge Copyright : *Global Water Pathogen Project*.

Neto, R. Cantusio, J. U. Santos, and R. M.B. Franco. 2006. “Evaluation of Activated Sludge Treatment and the Efficiency of the Disinfection of *Giardia* Species Cysts and *Cryptosporidium* Oocysts by UV at a Sludge Treatment Plant in Campinas, South-East Brazil.” *Water Science and Technology* 54(3): 89–94.

Nikaeen, M et al. 2003. “Sensitive Detection of *Giardia* Cysts by Polymerase Chain Reaction (PCR).” 32(1): 15–18.

Nosala, Christopher, and Scott C. Dawson. 2015. “The Critical Role of the Cytoskeleton in the Pathogenesis of *Giardia*.” *Current Clinical Microbiology Reports* 2(4): 155–62.

Oakley, Stewart. 2019. “Pathogen Reduction and Survival in Complete Treatment Works.” *Global Water Pthogen Project*.

Pelczar, Michael J. 2020. “Microbiology.” *Encyclopedia Brittanica*. https://www.britannica.com/science/microbiology (July 13, 2022).

Peterson, Kristine M, Upinder Singh, and William A Petri. 2011. 25 Tropical Infectious Diseases: Principles, Pathogens and Practice *PART H : Protozoan Infections CHAPTER 92*. Thrid Edit. Elsevier Inc. http://dx.doi.org/10.1016/B978-0-7020-3935-5.00092-6.

Plutzer, Judit, and Panagiotis Karanis. 2016. "Neglected Waterborne Parasitic Protozoa and Their Detection in Water." *Water Research* 101: 318–32.

Protozoan Parasites in Sewage Sludge. 2006. Copenhagen.

Radjenovic, Jelena et al. 2008. "Membrane Bioreactor (MBR) as an Advanced Wastewater Treatment Technology." *Hdb Env Chem* 5(November 2007): 401–34.

Ramo, Ana, Emilio del Cacho, Caridad Sánchez-Acedo, and Joaquín Quílez. 2017. "Occurrence and Genetic Diversity of *Cryptosporidium* and *Giardia* in Urban Wastewater Treatment Plants in North-Eastern Spain." *Science of the Total Environment* 598: 628–38.

Republic of Turkey Environment and Urban Ministry. 2004. "Turkish Regulation on Water Pollution Control." (d).

Rodriguez-Manzano, J. et al. 2012. "Standard and New Faecal Indicators and Pathogens in Sewage Treatment Plants, Microbiological Parameters for Improving the Control of Reclaimed Water." *Water Science and Technology* 66(12): 2517–23.

Saleh, Tawfik Abdo, and Vinod Kumar Gupta. 2016. "An Overview of Membrane Science and Technology." *Nanomaterial and Polymer Membranes*.

Sánchez, Claudia et al. 2018. "Molecular Detection and Genotyping of Pathogenic Protozoan Parasites in Raw and Treated Water Samples from Southwest Colombia." *Parasites and Vectors* 11(1).

Sathasivan, A. "Biological Phosphorus Removal Processes For Wastewater Treatment." *Water And Wastewater Treatment Technologies*.

Shammas, Nazih K. 2005. "Coagulation and Flocculation." 3.

Shiek, Abdul Gaffar et al. 2021. "Design of Control Strategies for Nutrient Removal in a Biological Wastewater Treatment Process." : 12092–106.

Sidhu, J P S et al. 2015. *Development of Validation Protocol for Activated Sludge Process in Water Recycling Project Leader Partners About the Australian Water Recycling Centre of Excellence*. www.australianwaterrecycling.com.au.

Skotarczak, B. 2009. "Methods for Parasitic Protozoans Detection in the Environmental Samples." *Parasite* 16(3): 183–90.

Smith, Cindy J., and A. Mark Osborn. 2009. “Advantages and Limitations of Quantitative PCR (Q-PCR)-Based Approaches in Microbial Ecology.” *FEMS Microbiology Ecology* 67(1): 6–20.

Sow, Samba O et al. 2016. “The Burden of *Cryptosporidium* Diarrheal Disease among Children < 24 Months of Age in Moderate / High Mortality Regions of Sub- Saharan Africa and South Asia , Utilizing Data from the Global Enteric Multicenter Study (GEMS).” : 1–20.

Sroka, Jacek et al. 2013. “Occurrence of *Cryptosporidium* Oocysts and *Giardia* Cysts in Effluent from Sewage Treatment Plant from Eastern Poland.” *Annals of agricultural and environmental medicine : AAEM* . 1(1): 57–62.

Stalder, Thibault et al. 2012. “Integron Involvement in Environmental Spread of Antibiotic Resistance.” *Frontiers in Microbiology* 3(APR).

Stenzel, D J, and P F L Boreham. 1996. “*Blastocystis hominis* Revisited.” 9(4): 563–84.

Sukprasert, S. et al. 2008. “PCR Detection of *Entamoeba* Spp from Surface and Waste Water Samples Using Genus-Specific Primers.” *the Southeast Asian Journal of Tropical Medicine and Public Health* · 39(January): 39 Suppl1(1):6-9.

Supha, Chitpisud, Yuphada Boonto, and Manee Jindakaraked. 2015. “Long-Term Exposure of Bacterial and Protozoan Communities to TiO 2 Nanoparticles in an Aerobic-Sequencing Batch Reactor.” *Science and Technology of Advanced Materials* 16(3): 34609.

Suresh, K, H V Smith, and T C Tan. 2005. “Viable *Blastocystis* Cysts in Scottish and Malaysian Sewage Samples.” 71(9): 5619–20.

Tan, Kevin S W. 2008. “New Insights on Classification , Identification , and Clinical Relevance of *Blastocystis* Spp .” 21(4): 639–65.

Tanrıverdi Çaycı, Yeliz, Kübra Hacıeminoğlu, and Asuman Birinci. 2017. “Ondokuz Mayıs Üniversitesi Hastanesi Tıbbi Parazitoloji Laboratuvarında 2014-2016 Yılları Arasında Saptanan Bağırsak Parazitlerinin Dağılımı.” *Kocaeli Üniversitesi Sağlık Bilimleri Dergisi* 3(3): 6–8.

Teel, Lydia et al. 2022. “Science of the Total Environment Protozoa Reduction through Secondary Wastewater Treatment in Two Water Reclamation Facilities.” 807.

Tonani, K. A.A. et al. 2011. “Behavior of Metals, Pathogen Parasites, and Indicator Bacteria in Sewage Effluents during Biological Treatment by Activated Sludge.” *Biological Trace Element Research* 143(2): 1193–1201.

Tortora, Gerard J, Berdell R Funke, and Christine L Case. 2016. *Microbiology, An Introduction*. 12th ed. Harlow: Pearson Education Limited.

van der Velden, Vhj et al. 2003. “REVIEW Detection of Minimal Residual Disease in Hematologic Malignancies by Real-Time Quantitative PCR: Principles, Approaches, and Laboratory Aspects.” www.nature.com/leu.

Verbyla, Matthew, and Olivier Rousselot. 2018. “Membrane Bioreactors.”

Verweij, Jaco J., Roy A. Blangé, et al. 2004. “Simultaneous Detection of Entamoeba Histolytica, Giardia Lamblia, and Cryptosporidium Parvum in Fecal Samples by Using Multiplex Real-Time PCR.” *Journal of Clinical Microbiology* 42(3): 1220–23.

Verweij, Jaco J., and Lisette van Lieshout. 2011. “Intestinal Parasitic Infections in an Industrialized Country; A New Focus on Children with Better DNA-Based Diagnostics.” *Parasitology* 138(12): 1492–98.

Wang, Mian, Julia Zhu, and Xinwei Mao. 2021. “Removal of Pathogens in Onsite Wastewater Treatment Systems: A Review of Design Considerations and Influencing Factors.” *Water (Switzerland)* 13(9).

Water Environment Federation. 2007. “Biological Nutrient Removal Processes.” *Operation of Municipal Wastewater Treatment Plants*: 22-1-22–65.

Water, Global, and Pathogen Project. “Part One . The Health Hazards Of Excreta : Theory And Control Envıronmental Aspects And Features Of Crıtıcal Copyright :*Global Waer Pathogen Project*

Wawrzyniak, Ivan et al. 2013. “*Blastocystis,* an Unrecognized Parasite: An Overview of Pathogenesis and Diagnosis.” *Therapeutic Advances in Infectious Disease* 1(5): 167–78.

Wen, Qinxue, Candani Tutuka, Alexandra Keegan, and Bo Jin. 2009. “Fate of Pathogenic Microorganisms and Indicators in Secondary Activated Sludge Wastewater Treatment Plants.” *Journal of Environmental Management* 90(3): 1442–47.

Whelan, Joseph A, Nick B Russell, and Michael A Whelan. 2003. “A Method for the Absolute Quantification of cDNA Using Real-Time PCR.” *Journal of Immunological Methods* 278(1–2): 261–69.

WHO. 2022. “Diarrhoeal Disease.” https://www.who.int/news-room/fact-sheets/detail/diarrhoeal-disease.

Wiser, Mark F. 2021. “Nutrition and Protozoan Pathogens of Humans: A Primer.” *Nutrition and Infectious Diseases* (February): 165–87.

Yoo, Chang Kyoo, Dae Sung Lee, and Peter A. Vanrolleghem. 2004. “Application of Multiway ICA for On-Line Process Monitoring of a Sequencing Batch Reactor.” *Water Research* 38(7): 1715–32.

Zacharia, Abdallah, Anne H Outwater, Billy Ngasala, and Rob van Deun. 2018. “Pathogenic Parasites in Raw and Treated Wastewater in Africa : A Review.” *Resources and Environment* 8(5): 232–40.

APPENDICES

A. Raw data obtained from the qPCR analyses of protozoan parasites

Table A.1. qPCR analyses of protozoan parasites of CAS

	CAS											
	Summer			Autumn			Winter			Spring		
	Influent ($\times 10^4$)	Effluent ($\times 10^4$)	LRV	Influent ($\times 10^4$)	Effluent ($\times 10^4$)	LRV	Influent ($\times 10^4$)	Effluent ($\times 10^4$)	LRV	Influent ($\times 10^4$)	Effluent ($\times 10^4$)	LRV
G. intestinalis	8.36 ± 0.19	0.82 ± 0.38	1.004	1.54 ± 0.40	0.06 ± 0.05	1.443	0.31 ± 0.67	0.14 ± 0.29	0.340	1.27 ± 0.09	0.58 ± 0.94	0.337
	Influent ($\times 10^7$)	Effluent ($\times 10^5$)	LRV	Influent ($\times 10^4$)	Effluent ($\times 10^3$)	LRV	Influent ($\times 10^3$)	Effluent ($\times 10^3$)	LRV	Influent ($\times 10^4$)	Effluent ($\times 10^4$)	LRV
E. histolytica	5.70 ± 0.29	0.67 ± 0.12	2.934	2.40 ± 0.05	0.99 ± 0.15	1.384	0.21 ± 0.07	0.09 ± 0.01	0.325	0.56 ± 0.05	0.07 ± 0.04	0.888
	Influent ($\times 10^5$)	Effluent ($\times 10^3$)	LRV	Influent ($\times 10^5$)	Effluent ($\times 10^3$)	LRV	Influent ($\times 10^5$)	Effluent ($\times 10^3$)	LRV	Influent ($\times 10^7$)	Effluent ($\times 10^3$)	LRV
B. hominis	2.07 ± 0.19	0.08 ± 0.338	3.368	3.04 ± 0.40	1.19 ± 0.05	2.405	1.78 ± 0.67	1.66 ± 0.29	2.030	1.70 ± 0.09	0.96 ± 0.94	4.257
	Influent ($\times 10^3$)	Effluent ($\times 10^3$)	LRV	Influent ($\times 10^4$)	Effluent ($\times 10^0$)	LRV	Influent ($\times 10^4$)	Effluent ($\times 10^3$)	LRV	Influent ($\times 10^8$)	Effluent ($\times 10^4$)	LRV
C. parvum	2.50 ± 0.02	1.68 ± 0.10	0.177	1.33 ± 1.004	5.60 ± 0.53	3.376	4.86 ± 0.52	0.75 ± 0.44	1.810	2.60 ± 0.35	1.14 ± 0.05	4.353

CAS, conventional activated sludge; LRV, logarithmic removal value; ±, standard deviation

Table A.2. qPCR analyses of protozoan parasites of CAS Sludge

	CAS Sludge											
	Summer			Autumn			Winter			Spring		
	Influent ($x 10^4$)	Effluent ($x 10^3$)	LRV	Influent ($x 10^4$)	Effluent ($x 10^4$)	LRV	Influent ($x 10^4$)	Effluent ($x 10^4$)	LRV	Influent ($x 10^4$)	Effluent ($x 10^4$)	LRV
G. intestinalis	8.36 ± 0.19	9.68 ± 0.67	0.936	1.54 ± 0.40	1.35 ± 1.27	-0.94	0.31 ± 0.67	1.48 ± 0.74	-0.68	1.27 ± 0.09	9.32 ± 0.71	0.137
	Influent ($x 10^7$)	Effluent ($x 10^4$)	LRV	Influent ($x 10^4$)	Effluent ($x 10^3$)	LRV	Influent ($x 10^3$)	Effluent ($x 10^3$)	LRV	Influent ($x 10^4$)	Effluent ($x 10^3$)	LRV
E. histolytica	5.70 ± 0.29	1.07 ± 0.03	3.73	2.40 ± 0.05	0.99 ± 0.04	1.384	0.21 ± 0.07	1.94 ± 0.02	-0.96	0.56 ± 0.05	6.35 ± 0.02	-0.05
	Influent ($x 10^5$)	Effluent ($x 10^5$)	LRV	Influent ($x 10^5$)	Effluent ($x 10^4$)	LRV	Influent ($x 10^5$)	Effluent ($x 10^8$)	LRV	Influent ($x 10^7$)	Effluent ($x 10^5$)	LRV
B. hominis	2.07 ± 0.19	1.78 ± 1.41	0.066	3.04 ± 0.40	3.96 ± 1.47	0.885	1.78 ± 0.67	1.90 ± 1.83	-3.04	1.70 ± 0.09	1.73 ± 1.38	1.998
	Influent ($x 10^3$)	Effluent ($x 10^0$)	LRV	Influent ($x 10^4$)	Effluent ($x 10^3$)	LRV	Influent ($x 10^4$)	Effluent ($x 10^4$)	LRV	Influent ($x 10^8$)	Effluent ($x 10^4$)	LRV
C. parvum	2.50 ± 0.02	1.7 ± 0.31	3.172	1.33 ±1.004	6.25 ± 1.62	0.330	4.86 ± 0.52	7.04 ± 1.52	-0.16	2.60 ± 0.35	3.99 ± 0.38	3.811

CAS, conventional activated sludge; LRV, logarithmic removal value; ±, standard deviation

Table A.3. qPCR analyses of protozoan parasites of BNR

	BNR											
	Summer			Autumn			Winter			Spring		
	Influent ($\times 10^3$)	Effluent ($\times 10^3$)	LRV	Influent ($\times 10^3$)	Effluent ($\times 10^3$)	LRV	Influent ($\times 10^4$)	Effluent ($\times 10^4$)	LRV	Influent ($\times 10^3$)	Effluent ($\times 10^3$)	LRV
G. intestinalis	7.80 ± 0.13	4.28 ± 0.06	0.264	8.98 ± 0.38	2.34 ± 0.13	0.583	8.75 ± 0.21	3.62 ± 0.29	0.382	4.01 ± 0.05	2.86 ± 0.08	0.146
	Influent ($\times 10^7$)	Effluent ($\times 10^6$)	LRV	Influent ($\times 10^3$)	Effluent ($\times 10^3$)	LRV	Influent ($\times 10^3$)	Effluent ($\times 10^3$)	LRV	Influent ($\times 10^7$)	Effluent ($\times 10^5$)	LRV
E. histolytica	8.20 ± 0.14	3.46 ± 0.25	1.375	3.48 ± 0.15	1.75 ± 0.68	0.298	2.09 ± 0.08	0.08 ± 0.06	0.421	1.00 ± 0.23	4.91 ± 0.06	1.354
	Influent ($\times 10^8$)	Effluent ($\times 10^6$)	LRV	Influent ($\times 10^5$)	Effluent ($\times 10^4$)	LRV	Influent ($\times 10^5$)	Effluent ($\times 10^3$)	LRV	Influent ($\times 10^{11}$)	Effluent ($\times 10^7$)	LRV
B. hominis	3.00 ± 0.22	2.00 ± 0.04	2.283	1.29 ± 0.12	1.14 ± 0.05	1.055	6.92 ± 1.72	0.56 ± 0.03	3.091	2.00 ± 1.04	2.00 ± 0.96	4.104
	Influent ($\times 10^8$)	Effluent ($\times 10^3$)	LRV	Influent ($\times 10^3$)	Effluent ($\times 10^2$)	LRV	Influent ($\times 10^4$)	Effluent ($\times 10^3$)	LRV	Influent ($\times 10^3$)	Effluent ($\times 10^3$)	LRV
C. parvum	1.78 ± 0.44	1.68 ± 1.24	5.025	1.91 ± 0.32	0.89 ± 1.79	1.331	1.28 ± 0.95	0.23 ± 0.46	1.754	0.78 ± 0.35	0.13 ± 0.06	0.792

BNR, biological nutrient removal; LRV, logarithmic removal value; ±, standard deviation

Table A.4. qPCR analyses of protozoan parasites of SBR

	SBR											
	Summer			Autumn			Winter			Spring		
	Influent (x 10^5)	Effluent (x 10^3)	LRV	Influent (x 10^5)	Effluent (x 10^5)	LRV	Influent (x 10^4)	Effluent (x 10^3)	LRV	Influent (x 10^5)	Effluent (x 10^5)	LRV
G. intestinalis	3.21 ± 0.69	1.62 ± 0.36	2.297	2.03 ± 0.07	1.06 ± 0.03	0.280	6.86 ± 1.07	0.14 ± 0.19	2.698	0.84 ± 0.27	0.21 ± 0.02	0.603
	Influent (x 10^8)	Effluent (x 10^6)	LRV	Influent (x 10^3)	Effluent (x 10^2)	LRV	Influent (x 10^2)	Effluent (x 10^2)	LRV	Influent (x 10^8)	Effluent (x 10^7)	LRV
E. histolytica	1.50 ± 0.47	1.90 ± 0.18	1.906	2.59 ± 0.08	5.81 ± 0.09	0.650	0.20 ± 0.11	0.06 ± 0.80	0.546	7.00 ± 0.23	2.00 ± 0.05	1.551
	Influent (x 10^{27})	Effluent (x 10^{16})	LRV	Influent (x 10^4)	Effluent (x 10^3)	LRV	Influent (x 10^3)	Effluent (x 10^3)	LRV	Influent (x 10^6)	Effluent (x 10^5)	LRV
B. hominis	6.00 ± 0.69	1.00 ± 0.25	11.68	1.73 ± 0.11	4.81 ± 0.38	0.555	1.21 ± 0.02	0.81 ± 0.05	0.179	3.00 ± 0.18	4.27 ± 0.25	0.887
	Influent (x 10^3)	Effluent (x 10^3)	LRV	Influent (x 10^3)	Effluent (x 10^3)	LRV	Influent (x 10^6)	Effluent (x 10^3)	LRV	Influent (x 10^7)	Effluent (x 10^3)	LRV
C. parvum	2.57 ± 0.62	0.16 ± 0.98	1.216	3.03 ± 0.33	0.15 ± 0.47	1.311	1.26 ± 1.02	2.67 ± 0.34	2.675	1.20 ± 1.68	4.53 ± 0.35	3.421

SBR, sequencing batch reactor; LRV, logarithmic removal value; ±, standard deviation

Table A.5. qPCR analyses of protozoan parasites of CoFlUV

	CoFlUV											
	Summer			Autumn			Winter			Spring		
	Influent ($\times 10^3$)	Effluent ($\times 10^3$)	LRV	Influent ($\times 10^3$)	Effluent ($\times 10^3$)	LRV	Influent ($\times 10^5$)	Effluent ($\times 10^3$)	LRV	Influent ($\times 10^4$)	Effluent ($\times 10^3$)	LRV
G. intestinalis	4.02 ± 0.02	2.74 ± 0.38	0.166	7.21 ± 0.41	1.49 ± 0.23	0.684	3.63 ± 0.19	0.44 ± 0.48	2.915	1.62 ± 0.59	0.33 ± 0.17	1.695
	Influent ($\times 10^{10}$)	Effluent ($\times 10^0$)	LRV	Influent ($\times 10^3$)	Effluent ($\times 10^2$)	LRV	Influent ($\times 10^3$)	Effluent ($\times 10^0$)	LRV	Influent ($\times 10^{12}$)	Effluent ($\times 10^9$)	LRV
E. histolytica	1.00 ± 0.51	0.09 ± 0.52	11.04	0.74 ± 0.05	0.69 ± 0.93	1.032	0.24 ± 0.06	1.10 ± 0.04	2.345	5.20 ± 0.07	5.90 ± 0.59	2.938
	Influent ($\times 10^4$)	Effluent ($\times 10^3$)	LRV	Influent ($\times 10^4$)	Effluent ($\times 10^3$)	LRV	Influent ($\times 10^3$)	Effluent ($\times 10^3$)	LRV	Influent ($\times 10^6$)	Effluent ($\times 10^6$)	LRV
B. hominis	6.78 ± 0.03	0.26 ± 0.09	2.41	2.46 ± 0.08	8.67 ± 0.27	0.454	5.09 ± 0.21	0.25 ± 0.29	1.309	2.00 ± 0.19	2.95 ± 0.28	0.923
	Influent ($\times 10^3$)	Effluent ($\times 10^0$)	LRV	Influent ($\times 10^3$)	Effluent ($\times 10^3$)	LRV	Influent ($\times 10^9$)	Effluent ($\times 10^2$)	LRV	Influent ($\times 10^4$)	Effluent ($\times 10^4$)	LRV
C. parvum	1.09 ± 0.44	3.40 ± 0.37	2.508	8.41 ± 0.26	0.75 ± 1.02	1.049	1.31 ± 0.54	0.24 ± 1.57	7.734	3.15 ± 0.47	1.91 ± 0.82	0.218

CoFlUV, WWTP with coagulation-flocculation units and UV disinfection; LRV, logarithmic removal value; ±, standard deviation

Table A.6. qPCR analyses of protozoan parasites of MBR

	MBR											
	Summer			Autumn			Winter			Spring		
	Influent (x 10^5)	Effluent (x 10^3)	LRV	Influent (x 10^5)	Effluent (x 10^3)	LRV	Influent (x 10^3)	Effluent (x 10^3)	LRV	Influent (x 10^3)	Effluent (x 10^3)	LRV
G. intestinalis	2.15 ± 0.72	1.44 ± 0.72	1.174	1.22 ± 0.26	3.00 ± 0.57	1.608	6.02 ± 0.11	2.22 ± 0.08	0.432	1.74 ± 0.01	1.38 ± 0.04	0.100
	Influent (x 10^{11})	Effluent (x 10^3)	LRV	Influent (x 10^3)	Effluent (x 10^2)	LRV	Influent (x 10^3)	Effluent (x 10^2)	LRV	Influent (x 10^6)	Effluent (x 10^6)	LRV
E. histolytica	2.10 ± 0.80	2.65 ± 0.65	7.900	0.18 ± 0.03	0.74 ± 0.08	0.397	2.52 ± 0.61	1.12 ± 0.29	1.352	7.85 ± 0.25	1.56 ± 0.19	0.702
	Influent (x 10^{18})	Effluent (x 10^3)	LRV	Influent (x 10^7)	Effluent (x 10^3)	LRV	Influent (x 10^4)	Effluent (x 10^0)	LRV	Influent (x 10^9)	Effluent (x 105)	LRV
B. hominis	1.60 ± 0.93	2.26 ± 0.66	14.85	8.00 ± 0.88	0.38 ± 0.73	5.337	7.61 ± 1.16	0.66 ± 1.94	5.057	7.00 ± 0.22	2.57 ± 0.28	4.458
	Influent (x 10^4)	Effluent (x 10^3)	LRV	Influent (x 10^5)	Effluent (x 10^0)	LRV	Influent (x 10^{11})	Effluent (x 10^4)	LRV	Influent (x 10^7)	Effluent (x 10^5)	LRV
C. parvum	2.67 ± 0.96	0.14 ± 1.76	2.275	3.81 ± 1.41	2.64 ± 0.25	5.158	1.01 ± 0.53	6.24 ± 1.04	6.210	9.80 ± 1.36	1.66 ± 0.53	2.769

MBR, membrane bioreactor; LRV, logarithmic removal value; ±, standard deviation

B. Statistical analyses of the qPCR results

Table B.1. Seasonal variations for the removal of *G. intestinalis* in CAS

(I) seasons		Mean Difference (I-J)	Std. Error	Sig.	95% Confidence Interval Lower Bound	95% Confidence Interval Upper Bound
Autumn	Spring	39.0973	26.73886	0.500	-46.5299	124.7246
	Summer	19.5437	26.73886	0.882	-66.0836	105.1709
	Winter	32.5420	26.73886	0.634	-53.0853	118.1693
Spring	Autumn	-39.0973	26.73886	0.500	-124.7246	46.5299
	Summer	-19.5537	26.73886	0.882	-105.1809	66.0736
	Winter	-6.5553	26.73886	0.994	-92.1826	79.0719
Summer	Autumn	-19.5437	26.73886	0.882	-105.1709	66.0836
	Spring	19.5537	26.73886	0.882	-66.0736	105.1809
	Winter	12.9983	26.73886	0.960	-72.6289	98.6256
Winter	Autumn	-32.5420	26.73886	0.634	-118.1693	53.0853
	Spring	6.5553	26.73886	0.994	-79.0719	92.1826
	Summer	-12.9983	26.73886	0.960	-98.6256	72.6289

Multiple comparisons, dependent variable: removal rate, Tukey honest significant difference.
Based on observed means. The error term is Mean Square (Error) = 1072.450. Highlights show significant difference at the 0.05 level. std, standard; sig, significance.

Table B.2. Seasonal variations for the removal of *G. intestinalis* in CAS Sludge

(I) seasons		Mean Difference (I-J)	Std. Error	Sig.	95% Confidence Interval	
					Lower Bound	Upper Bound
Autumn	Spring	-7508.2930	5312.79345	0.526	-24521.7278	9505.1418
	Summer	-7504.1590	5312.79345	0.526	-24517.5938	9509.2758
	Winter	-7181.9267	5312.79345	0.559	-24195.3614	9831.5081
Spring	Autumn	7508.2930	5312.79345	0.526	-9505.1418	24521.7278
	Summer	4.1340	5312.79345	1.000	-17009.3008	17017.5688
	Winter	326.3663	5312.79345	1.000	-16687.0684	17339.8011
Summer	Autumn	7504.1590	5312.79345	0.526	-9509.2758	24517.5938
	Spring	-4.1340	5312.79345	1.000	-17017.5688	17009.3008
	Winter	322.2323	5312.79345	1.000	-16691.2024	17335.6671
Winter	Autumn	7181.9267	5312.79345	0.559	-9831.5081	24195.3614
	Spring	-326.3663	5312.79345	1.000	-17339.8011	16687.0684
	Summer	-322.2323	5312.79345	1.000	-17335.6671	16691.2024

Multiple comparisons, dependent variable: removal rate, Tukey honest significant difference.
Based on observed means. The error term is Mean Square (Error) = 42228661.398. Highlights show significant difference at the 0.05 level. std, standard; sig, significance.

Table B.3. Seasonal variations for the removal of *G. intestinalis* in BNR

(I) seasons		Mean Difference (I-J)	Std. Error	Sig.	95% Confidence Interval Lower Bound	95% Confidence Interval Upper Bound
Autumn	Spring	35.7460	21.12142	0.386	-31.8922	103.3842
	Summer	22.0920	21.12142	0.729	-45.5462	89.7302
	Winter	9.8710	21.12142	0.964	-57.7672	77.5092
Spring	Autumn	-35.7460	21.12142	0.386	-103.3842	31.8922
	Summer	-13.6540	21.12142	0.914	-81.2922	53.9842
	Winter	-25.8750	21.12142	0.630	-93.5132	41.7632
Summer	Autumn	-22.0920	21.12142	0.729	-89.7302	45.5462
	Spring	13.6540	21.12142	0.914	-53.9842	81.2922
	Winter	-12.2210	21.12142	0.936	-79.8592	55.4172
Winter	Autumn	-9.8710	21.12142	0.964	-77.5092	57.7672
	Spring	25.8750	21.12142	0.630	-41.7632	93.5132
	Summer	12.2210	21.12142	0.936	-55.4172	79.8592

Multiple comparisons, dependent variable: removal rate, Tukey honest significant difference.
Based on observed means. The error term is Mean Square (Error) = 669.171. Highlights show significant difference at the 0.05 level. std, standard; sig, significance.

Table B.4. Seasonal variations for the removal of *G. intestinalis* in SBR

(I) seasons		Mean Difference (I-J)	Std. Error	Sig.	95% Confidence Interval	
					Lower Bound	Upper Bound
Autumn	Spring	-21.5360	9.69448	0.197	-52.5811	9.5091
	Summer	-50.6673*	9.69448	0.004	-81.7125	-19.6222
	Winter	-50.5117*	9.69448	0.004	-81.5568	-19.4665
Spring	Autumn	21.5360	9.69448	0.197	-9.5091	52.5811
	Summer	-29.1313	9.69448	0.066	-60.1765	1.9138
	Winter	-28.9757	9.69448	0.068	-60.0208	2.0695
Summer	Autumn	50.6673*	9.69448	0.004	19.6222	81.7125
	Spring	29.1313	9.69448	0.066	-1.9138	60.1765
	Winter	0.1557	9.69448	1.000	-30.8895	31.2008
Winter	Autumn	50.5117*	9.69448	0.004	19.4665	81.5568
	Spring	28.9757	9.69448	0.068	-2.0695	60.0208
	Summer	-0.1557	9.69448	1.000	-31.2008	30.8895

Multiple comparisons, dependent variable: removal rate, Tukey honest significant difference.
Based on observed means. The error term is Mean Square (Error) = 140.974. Highlights show significant difference at the 0.05 level. std, standard; sig, significance.

Table B.5. Seasonal variations for the removal of *G. intestinalis* in CoFlUV

(I) seasons		Mean Difference (I-J)	Std. Error	Sig.	95% Confidence Interval Lower Bound	95% Confidence Interval Upper Bound
Autumn	Spring	-26.4047	23.45655	0.685	-101.5208	48.7115
	Summer	34.0523	23.45655	0.505	-41.0638	109.1685
	Winter	-12.1873	23.45655	0.952	-87.3035	62.9288
Spring	Autumn	26.4047	23.45655	0.685	-48.7115	101.5208
	Summer	60.4570	23.45655	0.121	-14.6591	135.5731
	Winter	14.2173	23.45655	0.927	-60.8988	89.3335
Summer	Autumn	-34.0523	23.45655	0.505	-109.1685	41.0638
	Spring	-60.4570	23.45655	0.121	-135.5731	14.6591
	Winter	-46.2397	23.45655	0.274	-121.3558	28.8765
Winter	Autumn	12.1873	23.45655	0.952	-62.9288	87.3035
	Spring	-14.2173	23.45655	0.927	-89.3335	60.8988
	Summer	46.2397	23.45655	0.274	-28.8765	121.3558

Multiple comparisons, dependent variable: removal rate, Tukey honest significant difference.
Based on observed means. The error term is Mean Square (Error) = 825.314. Highlights show significant difference at the 0.05 level. std, standard; sig, significance.

Table B.6. Seasonal variations for the removal of *G. intestinalis* in MBR

(I) seasons		Mean Difference (I-J)	Std. Error	Sig.	95% Confidence Interval Lower Bound	95% Confidence Interval Upper Bound
Autumn	Spring	74.8013*	8.68271	0.000	46.9963	102.6064
	Summer	10.7970	8.68271	0.619	-17.0081	38.6021
	Winter	34.8277*	8.68271	0.016	7.0226	62.6327
Spring	Autumn	-74.8013*	8.68271	0.000	-102.6064	-46.9963
	Summer	-64.0043*	8.68271	0.000	-91.8094	-36.1993
	Winter	-39.9737*	8.68271	0.008	-67.7787	-12.1686
Summer	Autumn	-10.7970	8.68271	0.619	-38.6021	17.0081
	Spring	64.0043*	8.68271	0.000	36.1993	91.8094
	Winter	24.0307	8.68271	0.092	-3.7744	51.8357
Winter	Autumn	-34.8277*	8.68271	0.016	-62.6327	-7.0226
	Spring	39.9737*	8.68271	0.008	12.1686	67.7787
	Summer	-24.0307	8.68271	0.092	-51.8357	3.7744

Multiple comparisons, dependent variable: removal rate, Tukey honest significant difference.
Based on observed means. The error term is Mean Square (Error) = 113.084. Highlights show significant difference at the 0.05 level. std, standard; sig, significance.

Table B.7. Seasonal variations for the removal of *E. histolytica* in CAS

(I) seasons		Mean Difference (I-J)	Std. Error	Sig.	95% Confidence Interval Lower Bound	95% Confidence Interval Upper Bound
Autumn	Spring	8.7017	69.17482	0.999	-212.8204	230.2238
	Summer	97.8300	69.17482	0.525	-123.6921	319.3521
	Winter	41.0163	69.17482	0.931	-180.5058	262.5384
Spring	Autumn	-8.7017	69.17482	0.999	-230.2238	212.8204
	Summer	89.1283	69.17482	0.594	-132.3938	310.6504
	Winter	32.3147	69.17482	0.964	-189.2074	253.8368
Summer	Autumn	-97.8300	69.17482	0.525	-319.3521	123.6921
	Spring	-89.1283	69.17482	0.594	-310.6504	132.3938
	Winter	-56.8137	69.17482	0.843	-278.3358	164.7084
Winter	Autumn	-41.0163	69.17482	0.931	-262.5384	180.5058
	Spring	-32.3147	69.17482	0.964	-253.8368	189.2074
	Summer	56.8137	69.17482	0.843	-164.7084	278.3358

Multiple comparisons, dependent variable: removal rate, Tukey honest significant difference.
Based on observed means. The error term is Mean Square (Error) = 7177.733. Highlights show significant difference at the 0.05 level. std, standard; sig, significance.

Table B.8. Seasonal variations for the removal of *E. histolytica* in CAS Sludge

(I) seasons		Mean Difference (I-J)	Std. Error	Sig.	95% Confidence Interval	
					Lower Bound	Upper Bound
Autumn	Spring	109.8303	90.99868	0.640	-181.5795	401.2401
	Summer	13.3150	90.99868	0.999	-278.0948	304.7248
	Winter	926.5410*	90.99868	0.000	635.1312	1217.9508
Spring	Autumn	-109.8303	90.99868	0.640	-401.2401	181.5795
	Summer	-96.5153	90.99868	0.721	-387.9251	194.8945
	Winter	816.7107*	90.99868	0.000	525.3009	1108.1205
Summer	Autumn	-13.3150	90.99868	0.999	-304.7248	278.0948
	Spring	96.5153	90.99868	0.721	-194.8945	387.9251
	Winter	913.2260*	90.99868	0.000	621.8162	1204.6358
Winter	Autumn	-926.5410*	90.99868	0.000	-1217.9508	-635.1312
	Spring	-816.7107*	90.99868	0.000	-1108.1205	-525.3009
	Summer	-913.2260*	90.99868	0.000	-1204.6358	-621.8162

Multiple comparisons, dependent variable: removal rate, Tukey honest significant difference.
Based on observed means. The error term is Mean Square (Error) = 12421.139. Highlights show significant difference at the 0.05 level. std, standard; sig, significance.

Table B.9. Seasonal variations for the removal of *E. histolytica* in BNR

(I) seasons		Mean Difference (I-J)	Std. Error	Sig.	95% Confidence Interval	
					Lower Bound	Upper Bound
Autumn	Spring	-47.6777*	8.14016	0.002	-73.7453	-21.6100
	Summer	-47.8613*	8.14016	0.002	-73.9290	-21.7937
	Winter	-13.7033	8.14016	0.391	-39.7710	12.3643
Spring	Autumn	47.6777*	8.14016	0.002	21.6100	73.7453
	Summer	-0.1837	8.14016	1.000	-26.2513	25.8840
	Winter	33.9743*	8.14016	0.013	7.9067	60.0420
Summer	Autumn	47.8613*	8.14016	0.002	21.7937	73.9290
	Spring	0.1837	8.14016	1.000	-25.8840	26.2513
	Winter	34.1580*	8.14016	0.013	8.0903	60.2257
Winter	Autumn	13.7033	8.14016	0.391	-12.3643	39.7710
	Spring	-33.9743*	8.14016	0.013	-60.0420	-7.9067
	Summer	-34.1580*	8.14016	0.013	-60.2257	-8.0903

Multiple comparisons, dependent variable: removal rate, Tukey honest significant difference.
Based on observed means. The error term is Mean Square (Error) = 99.393. Highlights show significant difference at the 0.05 level. std, standard; sig, significance.

Table B.10. Seasonal variations for the removal of *E. histolytica* in SBR

(I) seasons		Mean Difference (I-J)	Std. Error	Sig.	95% Confidence Interval Lower Bound	95% Confidence Interval Upper Bound
Autumn	Spring	-19.7513	14.76630	0.567	-67.0382	27.5356
	Summer	-19.1510	14.76630	0.589	-66.4379	28.1359
	Winter	12.0820	14.76630	0.844	-35.2049	59.3689
Spring	Autumn	19.7513	14.76630	0.567	-27.5356	67.0382
	Summer	0.6003	14.76630	1.000	-46.6866	47.8872
	Winter	31.8333	14.76630	0.215	-15.4536	79.1202
Summer	Autumn	19.1510	14.76630	0.589	-28.1359	66.4379
	Spring	-0.6003	14.76630	1.000	-47.8872	46.6866
	Winter	31.2330	14.76630	0.227	-16.0539	78.5199
Winter	Autumn	-12.0820	14.76630	0.844	-59.3689	35.2049
	Spring	-31.8333	14.76630	0.215	-79.1202	15.4536
	Summer	-31.2330	14.76630	0.227	-78.5199	16.0539

Multiple comparisons, dependent variable: removal rate, Tukey honest significant difference.
Based on observed means. The error term is Mean Square (Error) = 327.065. Highlights show significant difference at the 0.05 level. std, standard; sig, significance.

Table B.11. Seasonal variations for the removal of *E. histolytica* in CoFlUV

(I) seasons		Mean Difference (I-J)	Std. Error	Sig.	95% Confidence Interval Lower Bound	95% Confidence Interval Upper Bound
Autumn	Spring	-8.2963	3.29681	0.131	-18.8539	2.2612
	Summer	-8.9203	3.29681	0.101	-19.4779	1.6372
	Winter	-8.4653	3.29681	0.122	-19.0229	2.0922
Spring	Autumn	8.2963	3.29681	0.131	-2.2612	18.8539
	Summer	-0.6240	3.29681	0.997	-11.1815	9.9335
	Winter	-0.1690	3.29681	1.000	-10.7265	10.3885
Summer	Autumn	8.9203	3.29681	0.101	-1.6372	19.4779
	Spring	0.6240	3.29681	0.997	-9.9335	11.1815
	Winter	0.4550	3.29681	0.999	-10.1025	11.0125
Winter	Autumn	8.4653	3.29681	0.122	-2.0922	19.0229
	Spring	0.1690	3.29681	1.000	-10.3885	10.7265
	Summer	-0.4550	3.29681	0.999	-11.0125	10.1025

Multiple comparisons, dependent variable: removal rate, Tukey honest significant difference.
Based on observed means. The error term is Mean Square (Error) = 16.303. Highlights show significant difference at the 0.05 level. std, standard; sig, significance.

Table B.12. Seasonal variations for the removal of *E. histolytica* in MBR

(I) seasons		Mean Difference (I-J)	Std. Error	Sig.	95% Confidence Interval Lower Bound	95% Confidence Interval Upper Bound
Autumn	Spring	-19.1397*	4.04661	0.006	-32.0983	-6.1810
	Summer	-39.7857*	4.04661	0.000	-52.7443	-26.8270
	Winter	-30.0193*	4.04661	0.000	-42.9780	-17.0607
Spring	Autumn	19.1397*	4.04661	0.006	6.1810	32.0983
	Summer	-20.6460*	4.04661	0.004	-33.6047	-7.6873
	Winter	-10.8797	4.04661	0.103	-23.8383	2.0790
Summer	Autumn	39.7857*	4.04661	0.000	26.8270	52.7443
	Spring	20.6460*	4.04661	0.004	7.6873	33.6047
	Winter	9.7663	4.04661	0.152	-3.1923	22.7250
Winter	Autumn	30.0193*	4.04661	0.000	17.0607	42.9780
	Spring	10.8797	4.04661	0.103	-2.0790	23.8383
	Summer	-9.7663	4.04661	0.152	-22.7250	3.1923

Multiple comparisons, dependent variable: removal rate, Tukey honest significant difference.
Based on observed means. The error term is Mean Square (Error) = 24.563. Highlights show significant difference at the 0.05 level. std, standard; sig, significance.

Table B.13. Seasonal variations for the removal of *B. hominis* in CAS

(I) seasons		Mean Difference (I-J)	Std. Error	Sig.	95% Confidence Interval Lower Bound	95% Confidence Interval Upper Bound
Autumn	Spring	-0.7060	0.71069	0.757	-2.9819	1.5699
	Summer	-0.6530	0.71069	0.796	-2.9289	1.6229
	Winter	1.4043	0.71069	0.272	-0.8715	3.6802
Spring	Autumn	0.7060	0.71069	0.757	-1.5699	2.9819
	Summer	0.0530	0.71069	1.000	-2.2229	2.3289
	Winter	2.1103	0.71069	0.069	-0.1655	4.3862
Summer	Autumn	0.6530	0.71069	0.796	-1.6229	2.9289
	Spring	-0.0530	0.71069	1.000	-2.3289	2.2229
	Winter	2.0573	0.71069	0.077	-0.2185	4.3332
Winter	Autumn	-1.4043	0.71069	0.272	-3.6802	0.8715
	Spring	-2.1103	0.71069	0.069	-4.3862	0.1655
	Summer	-2.0573	0.71069	0.077	-4.3332	0.2185

Multiple comparisons, dependent variable: removal rate, Tukey honest significant difference.
Based on observed means. The error term is Mean Square (Error) = 0.758. Highlights show significant difference at the 0.05 level. std, standard; sig, significance.

Table B.14. Seasonal variations for the removal of *B. hominis* in CAS Sludge

(I) seasons		Mean Difference (I-J)	Std. Error	Sig.	95% Confidence Interval	
					Lower Bound	Upper Bound
Autumn	Spring	-5.9510	30536.02582	1.000	-97793.0545	97781.1525
	Summer	146.5477	30536.02582	1.000	-97640.5558	97933.6512
	Winter	44396.8013	30536.02582	0.504	-53390.3022	142183.9048
Spring	Autumn	5.9510	30536.02582	1.000	-97781.1525	97793.0545
	Summer	152.4987	30536.02582	1.000	-97634.6048	97939.6022
	Winter	44402.7523	30536.02582	0.504	-53384.3512	142189.8558
Summer	Autumn	-146.5477	30536.02582	1.000	-97933.6512	97640.5558
	Spring	-152.4987	30536.02582	1.000	-97939.6022	97634.6048
	Winter	44250.2537	30536.02582	0.507	-53536.8498	142037.3572
Winter	Autumn	-44396.8013	30536.02582	0.504	-142183.9048	53390.3022
	Spring	-44402.7523	30536.02582	0.504	-142189.8558	53384.3512
	Summer	-44250.2537	30536.02582	0.507	-142037.3572	53536.8498

Multiple comparisons, dependent variable: removal rate, Tukey honest significant difference.
Based on observed means. The error term is Mean Square (Error) = 1398693309.011. Highlights show significant difference at the 0.05 level. std, standard; sig, significance.

Table B.15. Seasonal variations for the removal of *B. hominis* in BNR

(I) seasons		Mean Difference (I-J)	Std. Error	Sig.	95% Confidence Interval Lower Bound	95% Confidence Interval Upper Bound
Autumn	Spring	-9.1747	15.97728	0.937	-60.3395	41.9902
	Summer	-8.7197	15.97728	0.945	-59.8845	42.4452
	Winter	14.9397	15.97728	0.788	-36.2252	66.1045
Spring	Autumn	9.1747	15.97728	0.937	-41.9902	60.3395
	Summer	0.4550	15.97728	1.000	-50.7099	51.6199
	Winter	24.1143	15.97728	0.475	-27.0505	75.2792
Summer	Autumn	8.7197	15.97728	0.945	-42.4452	59.8845
	Spring	-0.4550	15.97728	1.000	-51.6199	50.7099
	Winter	23.6593	15.97728	0.490	-27.5055	74.8242
Winter	Autumn	-14.9397	15.97728	0.788	-66.1045	36.2252
	Spring	-24.1143	15.97728	0.475	-75.2792	27.0505
	Summer	-23.6593	15.97728	0.490	-74.8242	27.5055

Multiple comparisons, dependent variable: removal rate, Tukey honest significant difference.
Based on observed means. The error term is Mean Square (Error) = 382.910. Highlights show significant difference at the 0.05 level. std, standard; sig, significance.

Table B.16. Seasonal variations for the removal of *B. hominis* in SBR

(I) seasons		Mean Difference (I-J)	Std. Error	Sig.	95% Confidence Interval Lower Bound	95% Confidence Interval Upper Bound
Autumn	Spring	-17.9417	16.89631	0.720	-72.0496	36.1663
	Summer	-33.8893	16.89631	0.262	-87.9973	20.2186
	Winter	32.7580	16.89631	0.286	-21.3499	86.8659
Spring	Autumn	17.9417	16.89631	0.720	-36.1663	72.0496
	Summer	-15.9477	16.89631	0.783	-70.0556	38.1603
	Winter	50.6997	16.89631	0.066	-3.4083	104.8076
Summer	Autumn	33.8893	16.89631	0.262	-20.2186	87.9973
	Spring	15.9477	16.89631	0.783	-38.1603	70.0556
	Winter	66.6473*	16.89631	0.018	12.5394	120.7553
Winter	Autumn	-32.7580	16.89631	0.286	-86.8659	21.3499
	Spring	-50.6997	16.89631	0.066	-104.8076	3.4083
	Summer	-66.6473*	16.89631	0.018	-120.7553	-12.5394

Multiple comparisons, dependent variable: removal rate, Tukey honest significant difference.
Based on observed means. The error term is Mean Square (Error) = 428.228. Highlights show significant difference at the 0.05 level. std, standard; sig, significance.

Table B.17. Seasonal variations for the removal of *B. hominis* in CoFlUV

(I) seasons		Mean Difference (I-J)	Std. Error	Sig.	95% Confidence Interval Lower Bound	95% Confidence Interval Upper Bound
Autumn	Spring	-23.5377	15.75109	0.483	-73.9782	26.9029
	Summer	-39.0200	15.75109	0.139	-89.4605	11.4205
	Winter	-32.6367	15.75109	0.240	-83.0772	17.8039
Spring	Autumn	23.5377	15.75109	0.483	-26.9029	73.9782
	Summer	-15.4823	15.75109	0.763	-65.9229	34.9582
	Winter	-9.0990	15.75109	0.936	-59.5395	41.3415
Summer	Autumn	39.0200	15.75109	0.139	-11.4205	89.4605
	Spring	15.4823	15.75109	0.763	-34.9582	65.9229
	Winter	6.3833	15.75109	0.976	-44.0572	56.8239
Winter	Autumn	32.6367	15.75109	0.240	-17.8039	83.0772
	Spring	9.0990	15.75109	0.936	-41.3415	59.5395
	Summer	-6.3833	15.75109	0.976	-56.8239	44.0572

Multiple comparisons, dependent variable: removal rate, Tukey honest significant difference.
Based on observed means. The error term is Mean Square (Error) = 372.145. Highlights show significant difference at the 0.05 level. std, standard; sig, significance.

Table B.18. Seasonal variations for the removal of *B. hominis* in MBR

(I) seasons		Mean Difference (I-J)	Std. Error	Sig.	95% Confidence Interval Lower Bound	95% Confidence Interval Upper Bound
Autumn	Spring	.0027*	0.00041	0.001	0.0014	0.0040
	Summer	-0.0007	0.00041	0.414	-0.0020	0.0006
	Winter	-0.0003	0.00041	0.845	-0.0016	0.0010
Spring	Autumn	-.0027*	0.00041	0.001	-0.0040	-0.0014
	Summer	-.0033*	0.00041	0.000	-0.0046	-0.0020
	Winter	-.0030*	0.00041	0.000	-0.0043	-0.0017
Summer	Autumn	0.0007	0.00041	0.414	-0.0006	0.0020
	Spring	.0033*	0.00041	0.000	0.0020	0.0046
	Winter	0.0003	0.00041	0.845	-0.0010	0.0016
Winter	Autumn	0.0003	0.00041	0.845	-0.0010	0.0016
	Spring	.0030*	0.00041	0.000	0.0017	0.0043
	Summer	-0.0003	0.00041	0.845	-0.0016	0.0010

Multiple comparisons, dependent variable: removal rate, Tukey honest significant difference.
Based on observed means. The error term is Mean Square (Error) = 2.5×10^{-7}. Highlights show significant difference at the 0.05 level. std, standard; sig, significance.

Table B.19. Seasonal variations for the removal of *C. parvum* in CAS

(I) seasons		Mean Difference (I-J)	Std. Error	Sig.	95% Confidence Interval Lower Bound	95% Confidence Interval Upper Bound
Autumn	Spring	6.9033	8.86125	0.862	-21.4735	35.2802
	Summer	65.1383*	8.86125	0.000	36.7615	93.5152
	Winter	6.4623	8.86125	0.883	-21.9145	34.8392
Spring	Autumn	-6.9033	8.86125	0.862	-35.2802	21.4735
	Summer	58.2350*	8.86125	0.001	29.8582	86.6118
	Winter	-0.4410	8.86125	1.000	-28.8178	27.9358
Summer	Autumn	-65.1383*	8.86125	0.000	-93.5152	-36.7615
	Spring	-58.2350*	8.86125	0.001	-86.6118	-29.8582
	Winter	-58.6760*	8.86125	0.001	-87.0528	-30.2992
Winter	Autumn	-6.4623	8.86125	0.883	-34.8392	21.9145
	Spring	0.4410	8.86125	1.000	-27.9358	28.8178
	Summer	58.6760*	8.86125	0.001	30.2992	87.0528

Multiple comparisons, dependent variable: removal rate, Tukey honest significant difference.
Based on observed means. The error term is Mean Square (Error) = 117.783. Highlights show significant difference at the 0.05 level. std, standard; sig, significance.

Table B.20. Seasonal variations for the removal of *C. parvum* in CAS Sludge

(I) seasons		Mean Difference (I-J)	Std. Error	Sig.	95% Confidence Interval	
					Lower Bound	Upper Bound
Autumn	Spring	-1009.0660	723.46588	0.536	-3325.8584	1307.7264
	Summer	-1068.2930	723.46588	0.492	-3385.0854	1248.4994
	Winter	-854.0987	723.46588	0.655	-3170.8911	1462.6938
Spring	Autumn	1009.0660	723.46588	0.536	-1307.7264	3325.8584
	Summer	-59.2270	723.46588	1.000	-2376.0194	2257.5654
	Winter	154.9673	723.46588	0.996	-2161.8251	2471.7598
Summer	Autumn	1068.2930	723.46588	0.492	-1248.4994	3385.0854
	Spring	59.2270	723.46588	1.000	-2257.5654	2376.0194
	Winter	214.1943	723.46588	0.990	-2102.5981	2530.9868
Winter	Autumn	854.0987	723.46588	0.655	-1462.6938	3170.8911
	Spring	-154.9673	723.46588	0.996	-2471.7598	2161.8251
	Summer	-214.1943	723.46588	0.990	-2530.9868	2102.5981

Multiple comparisons, dependent variable: removal rate, Tukey honest significant difference.
Based on observed means. The error term is Mean Square (Error) = 785104.328. Highlights show significant difference at the 0.05 level. std, standard; sig, significance.

Table B.21. Seasonal variations for the removal of *C. parvum* in BNR

(I) seasons		Mean Difference (I-J)	Std. Error	Sig.	95% Confidence Interval Lower Bound	95% Confidence Interval Upper Bound
Autumn	Spring	5.2037	15.05640	0.985	-43.0122	53.4196
	Summer	-4.2593	15.05640	0.991	-52.4752	43.9566
	Winter	13.0643	15.05640	0.821	-35.1516	61.2802
Spring	Autumn	-5.2037	15.05640	0.985	-53.4196	43.0122
	Summer	-9.4630	15.05640	0.920	-57.6789	38.7529
	Winter	7.8607	15.05640	0.951	-40.3552	56.0766
Summer	Autumn	4.2593	15.05640	0.991	-43.9566	52.4752
	Spring	9.4630	15.05640	0.920	-38.7529	57.6789
	Winter	17.3237	15.05640	0.671	-30.8922	65.5396
Winter	Autumn	-13.0643	15.05640	0.821	-61.2802	35.1516
	Spring	-7.8607	15.05640	0.951	-56.0766	40.3552
	Summer	-17.3237	15.05640	0.671	-65.5396	30.8922

Multiple comparisons, dependent variable: removal rate, Tukey honest significant difference.
Based on observed means. The error term is Mean Square (Error) = 340.043. Highlights show significant difference at the 0.05 level. std, standard; sig, significance.

Table B.22. Seasonal variations for the removal of *C. parvum* in SBR

(I) seasons		Mean Difference (I-J)	Std. Error	Sig.	95% Confidence Interval Lower Bound	95% Confidence Interval Upper Bound
Autumn	Spring	1.2430	5.28324	0.995	-15.6758	18.1618
	Summer	4.5750	5.28324	0.822	-12.3438	21.4938
	Winter	-3.9490	5.28324	0.875	-20.8678	12.9698
Spring	Autumn	-1.2430	5.28324	0.995	-18.1618	15.6758
	Summer	3.3320	5.28324	0.919	-13.5868	20.2508
	Winter	-5.1920	5.28324	0.763	-22.1108	11.7268
Summer	Autumn	-4.5750	5.28324	0.822	-21.4938	12.3438
	Spring	-3.3320	5.28324	0.919	-20.2508	13.5868
	Winter	-8.5240	5.28324	0.423	-25.4428	8.3948
Winter	Autumn	3.9490	5.28324	0.875	-12.9698	20.8678
	Spring	5.1920	5.28324	0.763	-11.7268	22.1108
	Summer	8.5240	5.28324	0.423	-8.3948	25.4428

Multiple comparisons, dependent variable: removal rate, Tukey honest significant difference.
Based on observed means. The error term is Mean Square (Error) = 41.869. Highlights show significant difference at the 0.05 level. std, standard; sig, significance.

Table B.23. Seasonal variations for the removal of *C. parvum* in CoFlUV

(I) seasons		Mean Difference (I-J)	Std. Error	Sig.	95% Confidence Interval Lower Bound	95% Confidence Interval Upper Bound
Autumn	Spring	22.2820	16.32314	0.552	-29.9905	74.5545
	Summer	-13.9500	16.32314	0.827	-66.2225	38.3225
	Winter	-14.7243	16.32314	0.804	-66.9968	37.5481
Spring	Autumn	-22.2820	16.32314	0.552	-74.5545	29.9905
	Summer	-36.2320	16.32314	0.197	-88.5045	16.0405
	Winter	-37.0063	16.32314	0.185	-89.2788	15.2661
Summer	Autumn	13.9500	16.32314	0.827	-38.3225	66.2225
	Spring	36.2320	16.32314	0.197	-16.0405	88.5045
	Winter	-0.7743	16.32314	1.000	-53.0468	51.4981
Winter	Autumn	14.7243	16.32314	0.804	-37.5481	66.9968
	Spring	37.0063	16.32314	0.185	-15.2661	89.2788
	Summer	0.7743	16.32314	1.000	-51.4981	53.0468

Multiple comparisons, dependent variable: removal rate, Tukey honest significant difference.
Based on observed means. The error term is Mean Square (Error) = 399.668. Highlights show significant difference at the 0.05 level. std, standard; sig, significance.

Table B.24. Seasonal variations for the removal of *C. parvum* in MBR

(I) seasons		Mean Difference (I-J)	Std. Error	Sig.	95% Confidence Interval Lower Bound	95% Confidence Interval Upper Bound
Autumn	Spring	1.1360	2.28749	0.958	-6.1893	8.4613
	Summer	0.3010	2.28749	0.999	-7.0243	7.6263
	Winter	3.0307	2.28749	0.574	-4.2947	10.3560
Spring	Autumn	-1.1360	2.28749	0.958	-8.4613	6.1893
	Summer	-0.8350	2.28749	0.982	-8.1603	6.4903
	Winter	1.8947	2.28749	0.840	-5.4307	9.2200
Summer	Autumn	-0.3010	2.28749	0.999	-7.6263	7.0243
	Spring	0.8350	2.28749	0.982	-6.4903	8.1603
	Winter	2.7297	2.28749	0.647	-4.5957	10.0550
Winter	Autumn	-3.0307	2.28749	0.574	-10.3560	4.2947
	Spring	-1.8947	2.28749	0.840	-9.2200	5.4307
	Summer	-2.7297	2.28749	0.647	-10.0550	4.5957

Multiple comparisons, dependent variable: removal rate, Tukey honest significant difference.
Based on observed means. The error term is Mean Square (Error) = 7.849. Highlights show significant difference at the 0.05 level. std, standard; sig, significance.